

TESTING OF METHANE DETECTION SYSTEMS – PHASE 2

FINAL REPORT

SwRI® Project No. 18.21160

Prepared for:

Environmental Defense Fund
1875 Connecticut Ave., NW
Washington, DC 20009

September 18, 2015



SOUTHWEST RESEARCH INSTITUTE®

TESTING OF METHANE DETECTION SYSTEMS – PHASE 2

FINAL REPORT

SwRI® Project No. 18.21160

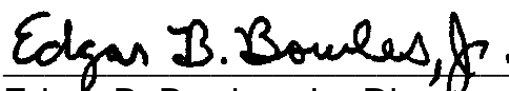
Prepared for:

Environmental Defense Fund
1875 Connecticut Ave., NW
Washington, DC 20009

Prepared by:

Adam Janka
John Edlebeck
Shane Siebenaler

Approved:



Edgar B. Bowles, Jr., Director
Fluid and Machinery Engineering Department

ADVERTISING, CONFIDENTIALITY, AND RECORD RETENTION POLICY

All work related to this project is subject to the Southwest Research Institute[®] Advertising, Confidentiality, and Record Retention Policy. This policy specifically addresses the distribution of abridged versions of SwRI[®] reports (including excerpts) and also restricts the use of the SwRI name, logo, and test results for advertising purposes. SwRI policies specifically prohibit the use in advertising of its name, logo, and results provided by our studies. The following paragraph, extracted verbatim from SwRI contractual documents clarifies this point:

“SwRI shall not publish or make known to others the subject matter or results of the Project or any information obtained in connection therewith which is proprietary and confidential to Client without Client’s written approval. No advertising or publicity containing any reference to SwRI, or any of their employees, either directly or by implication shall be made use of by Client or on Client’s behalf without SwRI’s written approval. In the event Client distributes any report issued by SwRI on this Project outside its own organization, such report shall be used in its entirety, unless SwRI approves a summary of abridgment for distribution.”

SwRI will retain a record copy of the report for a period of five (5) years. This permits us to answer questions that may be raised after a report has been mailed and provides a basis for additional work, if required. The contents of the report and any information that comes into our possession during the course of a study are held confidential to the company conducting the study and are not disclosed to anyone without client’s prior permission.

TABLE OF CONTENTS

<u>Section</u>	<u>Page</u>
TABLE OF CONTENTS	iii
LIST OF FIGURES	v
LIST OF TABLES	vii
EXECUTIVE SUMMARY	viii
1. INTRODUCTION	1-1
1.1 Applications for Phase 2.....	1-1
1.2 Phase 2 Objectives and Approach.....	1-3
1.3 Report Organization	1-3
2. TECHNOLOGIES.....	2-1
2.1 Technology Developer Requirements.....	2-1
2.2 Nomenclature	2-1
2.3 Developer A	2-1
2.4 Developer B	2-2
2.5 Developer C	2-3
2.6 Developer D	2-3
3. TEST APPROACH.....	3-1
3.1 Overview	3-1
3.2 Reference Instruments	3-1
3.3 Initial Concentration Monitoring	3-1
3.3.1 Instances of Systems Tested.....	3-2
3.3.2 Methodology and Test Setup.....	3-2
3.3.3 Methane Testing.....	3-3
3.3.4 Contaminant Testing	3-3
3.4 Outdoor Testing.....	3-4
3.4.1 Methodology for Performing Outdoor Releases	3-4
3.4.2 Test Setup at Location #1	3-4
3.4.3 Test Setup at Location #2.....	3-7
4. RESULTS	4-1
4.1 Initial Concentration Monitoring	4-1
4.1.1 Methane Testing.....	4-1
4.1.2 Contaminant Testing	4-4
4.1.1 Summary	4-6
4.2 Controlled Outdoor Releases	4-6
4.2.1 Test Matrix	4-6

TABLE OF CONTENTS (cont'd)

<u>Section</u>	<u>Page</u>
4.2.2 Overall Detection Comparison	4-7
4.2.3 Time-Resolved Analysis Methodology	4-8
4.2.4 The Use and Selection of Detection Thresholds.....	4-9
4.3 Developer B Results	4-11
4.4 Developer C Results	4-16
4.5 Developer D Results	4-20
4.5.1 Developer D Temperature Sensitivity	4-26
4.6 Developer A Results	4-30
4.7 System Robustness	4-33
5. CONCLUSIONS	5-1
APPENDIX A – Outdoor Testing Graphs – Developer A	A-1
APPENDIX B – Outdoor Testing Graphs – Developer B	B-1
APPENDIX C – Outdoor Testing Graphs – Developer C.....	C-1
APPENDIX D – Outdoor Testing Graphs – Developer D.....	D-1

LIST OF FIGURES

<u>Section</u>	<u>Page</u>
Figure 1.1. Example of Sensors being used to Monitor Thief Hatches on a Tank Battery ..	1-2
Figure 1.2. Example of Sensors being used to Monitor an Entire Site.....	1-2
Figure 2.1. Developer A System	2-2
Figure 2.2. Developer B System	2-2
Figure 2.3. Developer C System	2-3
Figure 2.4. “Two-Gun” System Provided by Developer D.....	2-4
Figure 3.1. Concentration Monitoring Setup.....	3-3
Figure 3.2. General Test Approach for Outdoor Testing.....	3-4
Figure 3.3. Test Setup for Outdoor Testing at Location #1	3-5
Figure 3.4. Outdoor Testing co-location Point with Reference Instruments at Location #1 .	3-6
Figure 4.1. Results from the 2-ppmv Increment Methane Test for the Systems of Developer C and Developer D	4-1
Figure 4.2. Results from the 2-ppmv Increment Methane Test for Systems of Developer A and Developer B.....	4-2
Figure 4.3. Results from the 10-ppmv Increment, 10-Minute Hold Methane Test for the Systems of Developer C and D	4-2
Figure 4.4. Results from the 10-ppmv Increment, 10-Minute Hold Methane Test for the Systems of Developer A and B	4-3
Figure 4.5. Results from the 10-ppmv increment, Four-Minute Hold Methane Test for All Developers.....	4-3
Figure 4.6. Results from the Carbon Monoxide Background Contamination Test.....	4-4
Figure 4.7. Results from Ethane Background Contamination Test	4-5
Figure 4.8. Results from the 5-ppmv Increment Ethane Contamination Test.....	4-6
Figure 4.9. Conceptual Illustration of the Agreement Rate Metric	4-9
Figure 4.10. Comparison Between Standard and Custom Thresholds for Developers B and D for a Common Trial (2.5 scfm from 70 ft)	4-11
Figure 4.11. Raw Signals from the Reference Instrument and Developer B’s System	4-11
Figure 4.12. Illustration of the High-Pass Filtering Process for Developer B’s System	4-12
Figure 4.13. Illustration of the Time Alignment Process for Developer B’s System.....	4-13
Figure 4.14. Illustration of the Baseline Truncation Process for Developer B’s System.....	4-13
Figure 4.15. Plot Showing Agreement between Developer B’s System and the Reference Measurement.....	4-14
Figure 4.16. Agreement Rate Bar Chart for Developer B’s System.....	4-14
Figure 4.17. Agreement Rate Chart for 130-ft Point for Developer B’s System	4-15
Figure 4.18. Methane Agreement Rate for Developer B’s System	4-15
Figure 4.19. Methane Agreement Rate Chart for 130-ft Point for Developer B’s System....	4-16
Figure 4.20. Raw signals from the Reference Instrument and Developer C’s System.....	4-17
Figure 4.21. Illustration of the Time Alignment Process for Developer C’s System	4-17
Figure 4.22. Illustration of the Truncation Process for Developer C’s System	4-18

LIST OF FIGURES (cont'd)

<u>Section</u>	<u>Page</u>
Figure 4.23. Plot Showing Agreement between Developer C's System and the Reference Instrument	4-18
Figure 4.24. Agreement Rate Bar Chart for Developer C's System.....	4-19
Figure 4.25. Agreement Rate Chart for 130-ft Point for Developer C's System	4-19
Figure 4.26. Methane Agreement Rate for Developer C's System	4-20
Figure 4.27. Methane Agreement Rate Chart for 130-ft Point for Developer C's System ...	4-20
Figure 4.28. Raw data for Developer D (System #1) and the Reference Instrument	4-21
Figure 4.29. Illustration of the Time Alignment Process for Developer D's System	4-22
Figure 4.30. Illustration of the Baseline Truncation Process for Developer D's System.....	4-22
Figure 4.31. Plot Showing Agreement between Developer D's System and the Reference Instrument	4-23
Figure 4.32. Agreement Rate Bar Chart for Developer D's System.....	4-23
Figure 4.33. Agreement Rate Chart for 130-ft Point for Developer D's System	4-24
Figure 4.34. Methane Agreement Rate for Developer D's System	4-24
Figure 4.35. Methane Agreement Rate Chart for 130-ft Point for Developer D's System ...	4-25
Figure 4.36. Data from Developer D's System at 5-m Path Length for 5 scfm at a 40-ft Distance.....	4-25
Figure 4.37. Data from Developer D's System at 20-m Path Length for 5 scfm at a 40-ft Distance.....	4-26
Figure 4.38. Early Morning Trial (Temperature around 80°F) of Develop D System.....	4-26
Figure 4.39. Identical Test Run to Previous Figure at Higher Temperatures (>100°F)	4-27
Figure 4.40. Developer D, Systems #2 and #3 Concentration Traces during the 72-Hour Trial.....	4-27
Figure 4.41. Concentration Traces from all Developer D Systems after Solar Shielding is Installed	4-28
Figure 4.42. Results from the 2-ppmv Increment Methane Test for Developer D's Systems at Ambient Temperature.....	4-29
Figure 4.43. Results from the 2-ppmv Increment Methane Test for Developer D's Systems at Elevated Temperature	4-29
Figure 4.44. Results from the 10-ppmv Increment Methane Test for Developer D's Systems at Ambient Temperature.....	4-30
Figure 4.45. Results from the 2-ppmv increment Methane Test for Developer D's Systems at Elevated Temperature	4-30
Figure 4.46. Example Data from 1 scfm at 130 ft	4-31
Figure 4.47. Example Data from 2.5 scfm at 82 ft	4-32

LIST OF TABLES

<u>Section</u>	<u>Page</u>
Table 3.1. Methane Concentration Monitoring Tests.....	3-3
Table 3.2. Contaminant Concentration Monitoring Tests	3-4
Table 3.3. Instruments Used During Outdoor Release Testing	3-6
Table 4.1. Test Matrix for Controlled Release Testing	4-7
Table 4.2. Leak Detection Capability Demonstrated for Tests for 5-scfm Leaks.....	4-7
Table 4.3. Leak Detection Capability Demonstrated for Tests for 2.5-scfm Leaks.....	4-8
Table 4.4. Leak Detection Capability Demonstrated for Tests for 1-scfm Leaks.....	4-8
Table 4.5. Leak Detection Capability Demonstrated for Tests for 0.5-scfm Leaks.....	4-8
Table 4.6. Agreement State Decision Table.....	4-9
Table 4.7. Summary of Detection Limit Threshold Deviation, δi , Above Baseline Mean .	4-10
Table 4.8. Detection Rate Using 99.9% Confidence Interval.....	4-32
Table 4.9. Detection Rate Using 95% Confidence Interval.....	4-32
Table 4.10. Detection Rate Using 90% Confidence Interval.....	4-32
Table 4.11. Detection Rate Using the Detection Limit of Three Standard Deviations	4-33
Table 4.12. Developer A Event Log	4-33
Table 4.13. Developer B Event Log	4-33
Table 4.14. Developer C Event Log.....	4-34
Table 4.15. Developer D Event Log.....	4-34
Table 5.1. Leak Detection Capability Demonstrated for Tests for 5-scfm Leaks.....	5-1
Table 5.2. Leak Detection Capability Demonstrated for Tests for 2.5-scfm Leaks.....	5-1
Table 5.3. Leak Detection Capability Demonstrated for Tests for 1-scfm Leaks.....	5-1
Table 5.4. Leak Detection Capability Demonstrated for Tests for 0.5-scfm Leaks.....	5-2
Table 5.5. Comparison of System Performance for Various Parameters Defined in RFP .	5-2
Table 5.6. Gaps for Each Developer's System	5-3

EXECUTIVE SUMMARY

The Methane Detectors Challenge (MDC) was initiated to expedite development and commercialization of low-cost methane detection technologies. MDC is a collaborative, multi-stakeholder partnership to improve the speed and cut the costs associated with methane detection from natural gas facilities, such as well pads and compressor stations, in order to reduce overall methane emissions. The MDC commenced with a set of laboratory tests (“Phase 1”) of five different sensor technologies in 2014. Four of these five technologies were selected for further development (by the suppliers) and assessment in a follow-up effort deemed “Phase 2.”

The Phase 1 testing evaluated the sensors from each of the technology developers. Other “system” components, such as power supplies, pumps, data acquisition, etc. were not considered part of the test, even if they were needed in order to allow the sensors to work for that phase of the testing. In contrast, Phase 2 tested each technology developer’s entire system in controlled laboratory and outdoor settings in order to ensure that the systems performed as required prior to moving into industry pilots. The systems were treated as “end-to-end” units whereby all components (e.g., sensor, data acquisition, enclosures, etc.) needed to perform according to the provided specifications. While cost is expected to be a key parameter influencing industry adoption at scale, it was not evaluated as part of Phase 2.

The primary objectives of the Phase 2 testing were to determine the readiness of the technologies for pilot testing in the field and identify continuous improvement opportunities. The primary means of this evaluation was to determine if the systems could detect leaks in a dynamic environment with minimal false alarms and little to no maintenance or user interaction. Some additional objectives were:

- Evaluate peripheral equipment (pumps, fans, data acquisition systems (DAQs), etc.) to identify any deficiencies.
- Close any developer-specific technology gaps identified during Phase 1 testing.
- Provide feedback to technology developers to spur further technology improvement.

There were four technologies tested as part of this program:

- Developer A utilized an array of off-the-shelf gas, humidity, and temperature sensors integrated into a circuit board.
- Developer B utilized a non-dispersive infrared sensor coupled with a long path length platform.
- Developer C utilized laser absorption spectroscopy as the sensor approach.
- Developer D utilized tunable diode laser absorption spectroscopy.

Testing was performed in both indoor and outdoor environments. The systems were placed in an outdoor setting during a central Texas summer for over eight weeks. Controlled releases were performed for leak rates of 0.5 scfm to 5 scfm at distances up to 130 ft away from the sensors.

The primary application for technology that is part of the MDC is the binary leak or no leak status akin to a “smoke alarm” for methane. While the ability to accurately quantify the methane concentration allows for a system to be more robust, it was not a requirement of this program. During the testing in this project, Developer C’s system was able to detect all leaks, while the other developers were able to detect each leak at distances up to 82 ft for leak rates

ranging from 1 scfm to 5 scfm. While each of the sensors has the ability to detect these leaks, Developer A’s and Developer B’s systems, in their current form, generated less-consistent data and more point-to-point variability than Developer C and Developer D. Both Developer A and Developer B require some manner of manual processing in order to determine the leak state. It is important to recognize that during periods in which there were no leaks, there were no measurements from the systems that would indicate a false positive.

In reviewing the performance of the various systems, a baseline can be made by comparing the performance of each technology relative to the Phase 2 requirements outlined in the original MDC request for proposal (RFP). The following table summarizes how each technology performed relative to the requirements of the RFP. It is important to note that “leak detection capability” is interpreted as meaning “capable of detecting such a leak.” While some of the technology developers had a simplified alarm threshold, none of the companies had initiated full alarm algorithms at the time of the Phase 2 testing.

Comparison of System Performance for Various Parameters Defined in RFP

The majority of the requirements were met by all developers.

Specification	RFP Requirement	Dev A	Dev B	Dev C	Dev D
		Was Requirement Met?			
Detection limit	5 ppm	Yes	Yes	Yes	Yes
Detection range	5 ppm to 250 ppm	Yes	Yes	Yes	Yes
Leak detection capability	5 scfm	Yes	Yes	Yes	Yes
Ability to measure methane	Binary (yes/no)	Yes	Yes	Yes	Yes
Ability to isolate on-site methane from off-site	Binary (yes/no)	Unknown ^a	Unknown ^a	Unknown ^a	Unknown ^a
Power requirements	Single solar panel with rechargeable battery	Yes	No	Yes	Yes
Protected from weather	Binary (yes/no)	Yes	Yes	Yes	Yes
Temperature range	-20°F to 120°F	Yes	Yes	Yes	Yes
Humidity	0 to 100% relative humidity	Yes	Yes	Yes	Yes
Unaffected by poisons	Binary (yes/no)	No ^b	No ^c	Yes	Yes

^aWhile most developers had anemometers, none fully leveraged such information to determine the source of gas.

^bPerformance impacted by presence of various contaminants.

^cPerformance impacted by presence of ethane.

Two RFP requirements for the pilot phase that are currently not met by any of the systems are:

- Certification for use in a hazardous gas environment (e.g., Class 1, Division 1 or 2).
- Ability to estimate the leak size.

The following table provides remaining gaps that may need to be closed prior to each technology being deployed for a pilot trial. It is anticipated that pilot testing could occur in waves, allowing more time for technologies at lower levels of readiness to mature before field deployment.

Gaps for Each Developer's System

It will be up to pilot sponsors and technology developers to determine together which gaps must be closed prior to pilot testing. Developer C's and Developer D's systems would not require further laboratory confirmation prior to deployment in the field. Developer A's and Developer B's systems require further work to improve the reliability of their leak detection capabilities before field deployment.

Technology Developer	Remaining Gaps
Developer A	Does not have a robust algorithm for automated leak detection. Does not have a Class 1, Division 1 or 2 certification. Ensure the robustness of the systems over extended operation. Determine a means of detecting methane in the presence of contaminants.
Developer B	Does not have a robust algorithm for automated leak detection. Does not have a Class 1, Division 1 or 2 certification. Stabilize the drifting/offsetting signals. Integrate a solar panel into the assemblies. Ensure robustness of hardware over extended operation.
Developer C	Does not have a robust algorithm for automated leak detection. Does not have a Class 1, Division 1 or 2 certification.
Developer D	Does not have a robust algorithm for automated leak detection. Does not have a Class 1, Division 1 or 2 certification. Consider modifying the resolution to <1 ppm.

1. INTRODUCTION

The Methane Detectors Challenge (MDC) was initiated to expedite development and commercialization of low-cost methane detection technologies. The intended application of the MDC is to improve the speed and cut the costs associated with methane detection from natural gas facilities, such as well pads and compressor stations, in order to reduce overall methane emissions. The MDC commenced with a set of laboratory tests (“Phase 1”) of five different sensor technologies in 2014. Four of these five technologies were selected for further development (by the suppliers) and assessment in a follow-up effort deemed “Phase 2.”

The Phase 1 testing evaluated the sensors from each of the technology developers. Other “system” components, such as power supplies, pumps, data acquisition, etc. were not considered part of the test, even if they were needed in order to allow the sensors to work for that phase of the testing. In contrast, Phase 2 tested each technology developer’s entire system in controlled laboratory and outdoor settings in order to ensure that the systems performed as required prior to moving into industry pilots. The systems were treated as “end-to-end” units whereby all components (e.g., sensor, data acquisition, enclosures, etc.) needed to perform according to the provided specifications. This report details the findings from the Phase 2 testing.

1.1 Applications for Phase 2

There are two general categories of applications that were identified as input for Phase 2:

Targeted – In this scenario, a fixed piece of equipment, such as a battery of tanks (with focus on the thief hatches), would be the application. Instead of the systems being deployed to have coverage over an entire well pad or compressor station, the systems would focus only on a key asset or limited set of assets. This approach could lead to more localization of the systems and potentially remove the need for any meteorological data to be integrated into the output of the systems, as the concentrations would be high enough to rule out other sources. This concept is conceptualized in Figure 1.1, in which an open-path sensor and a point sensor are used to monitor the thief hatches on a tank battery.

Broad – In this scenario, it is desired to have coverage over a wider area, such as all major leak sources “inside the fence” at a multi-well well pad or compressor station. This application would require either fence-line monitoring or, perhaps, the installation of multiple systems at the site. Meteorological data may be critical as general changes in background level induced at the monitored site would need to be differentiated from releases at nearby locations. This scenario is illustrated in Figure 1.2, which shows an example of a point sensor and an open-path sensor monitoring a broad area for leaks.

The testing in Phase 2 was designed to evaluate both scenarios by looking at both close up, high leak rate scenarios and further away, lower leak rate scenarios.

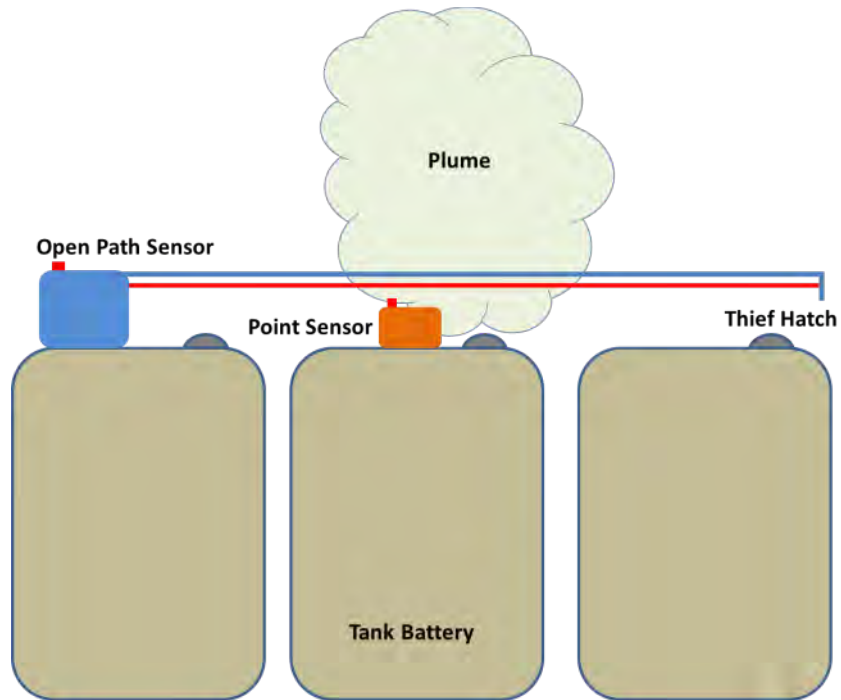


Figure 1.1. Example of Sensors being used to Monitor Thief Hatches on a Tank Battery
Such a configuration represents a targeted application in which specific assets are monitored, as opposed to an entire area.

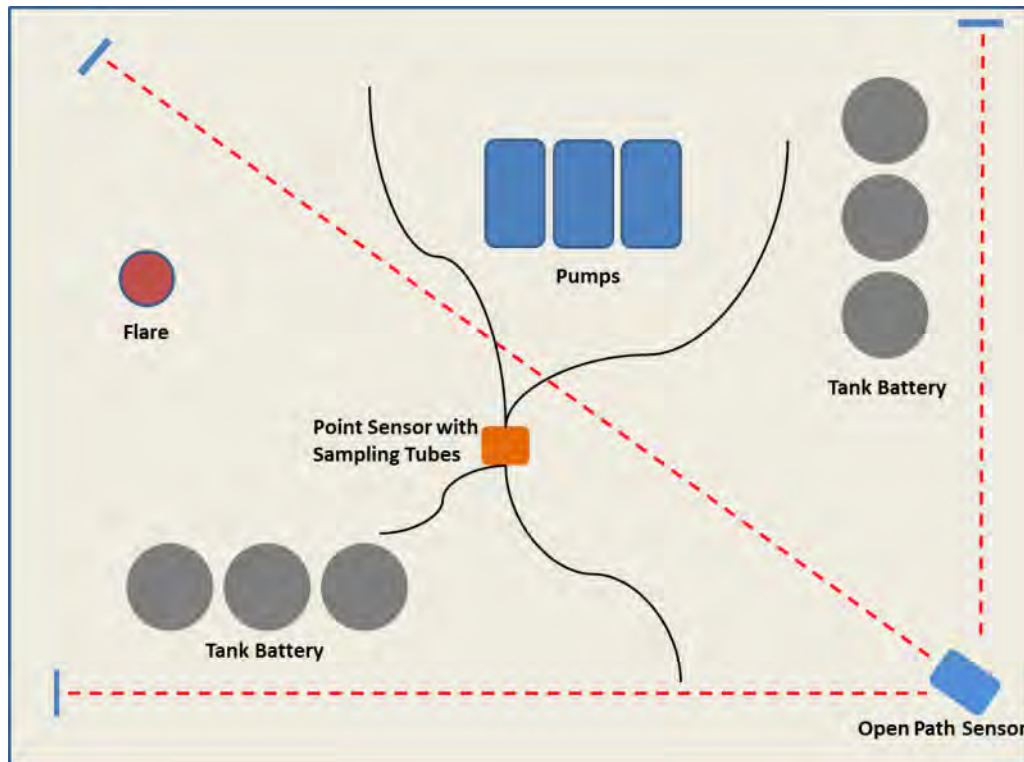


Figure 1.2. Example of Sensors being used to Monitor an Entire Site
Distributed sensors and/or open-path technologies are required for such an application.

1.2 Phase 2 Objectives and Approach

The primary objectives of the Phase 2 testing were to determine the readiness of the technologies for pilot testing in the field and identify continuous improvement opportunities. The primary means of this evaluation was to determine if the systems could detect leaks in a dynamic environment with minimal false alarms and little to no maintenance or user interaction. Some additional objectives were:

- Evaluate peripheral equipment (pumps, fans, DAQs, etc.) to identify any deficiencies.
- Close any developer-specific technology gaps identified during Phase 1 testing.
- Provide feedback to technology developers to spur further technology improvement.

1.3 Report Organization

The report is divided into the following sections:

Section	Title	Contents
1	Introduction	Background information and objectives of the project
2	Technologies	Description of the four technologies tested
3	Test Approach	Outline of the test setup and protocol
4	Results	Results from testing
5	Conclusions	Overall conclusions from Phase 2
Appendices	Time-Resolved Charts	Charts for each of the test points outlined in Section 3

2. TECHNOLOGIES

2.1 Technology Developer Requirements

The technology developers were requested to supply full systems that should be capable of operating as standalone “plug and play” units. The following list highlights key required features of the technologies that were submitted to the technology developers as input to Phase 2:

- *Detection Algorithm* – The system must be able to detect a leak on its own. The recommended method is to use a trinary alarm indicating the severity of a possible event (e.g., “no leak, small leak, large leak” or “no probability of leak, some probability of leak, high probability of leak”). Additional outputs that may assist operators in identifying the leak size and location, such as concentration in ppm, hourly average concentration, wind speed, wind direction, etc. can also be implemented by the technology developers. It should be noted that while several of the technology developers supplied rudimentary alarms (e.g., alarms when the system is above a concentration threshold), algorithms that could perform in transient conditions were not supplied with any of the systems.
- *Power* – The system must be “self-powered.” Three of the four technology developers supplied solar panels with battery packs for this testing. One of the technology developers utilized AC power for this phase of testing.
- *Components* – All peripheral components (e.g., fans, pumps, DAQ, tubes, clock, heat tracing, etc.) required for the sensor to operate in the field must be incorporated into the system.
- *Weatherization* – The system must be able to be placed in an outdoor environment for an extended period of time, so it must be fully weatherized (e.g., NEMA 4X enclosure classification).
- *Communication* – It was recommended that the technology developers provide a 4-20 mA signal proportional to the real-time concentration of methane and another 4-20 mA signal that provides alarm information. Two technology developers provided 4-20 mA signals: one used a USB signal, and one used a wireless signal.

2.2 Nomenclature

The data provided in this report blind the names of the technology developers. Thus, the four providers of technology are referred to as Developer A, Developer B, Developer C, and Developer D.

2.3 Developer A

Developer A provided three independent devices for testing. These systems integrate an array of off-the-shelf gas (including methane), humidity, and temperature sensors onto a single integrated circuit board. Specially-developed, post-processing algorithms (developed in MatLab) are used to combine the individual measurements from these sensors to generate a single concentration reading. The working principle behind these sensors is that the resistivities of the sensing elements change in the presence of a given species, such as methane, carbon monoxide, carbon dioxide, or non-methane hydrocarbons. All units had a stated detection range of zero to 30 ppmv, though they were able to provide readings at levels orders of magnitude higher.



Figure 2.1. Developer A System

System was powered by solar panel and communicated via a 4-20 mA signal.

2.4 Developer B

Developer B's device uses a non-dispersive infrared (NDIR) sensor coupled with a long path length (LPL) platform. The LPL platform provides a 1.3-m optical length that is contained in an 8-cm long package. This system measures infrared absorption through a sample gas (methane-air) and compares it against the absorption through a zero gas (ambient air). The tested prototype calibrates on a regular basis through a process noted as "zero calibration." This feature is controlled autonomously through software. Zero calibration performed at regular intervals minimizes the thermal sensitivity of the NDIR measurement technique. The concentration reading is updated after every zero calibration at a range of zero to 32,000 ppmv. A program developed in-house was used for the data acquisition and control of the Develop B system. The program allowed for the adjustment of settings, such as the zero calibration period and sample gas period. The units provided for testing were not integrated with a solar panel. Instead, AC power was supplied to these devices via an extension cord.



Figure 2.2. Developer B System

This technology developer provided two units, each powered by AC power and communicating through a USB connection.

2.5 Developer C

The Developer C technology is a sensor that uses a laser absorption spectroscopy measurement technique. The laser path line is contained within the device's housing. As such, this system uses small fans to advect methane-air into the housing through the laser path line. The Developer C system also allows for time-resolved measurements at 1 Hz over a range of zero to 5,000 ppmv. The system was calibrated prior to its arrival at SwRI, but was not calibrated during the testing period. Developer C specifies that the system does not need to be calibrated frequently, but may require maintenance, such as the replacement of air filters. During testing, methane concentration measurements were gathered via a mobile router.



Figure 2.3. Developer C System

This system was powered by a solar panel and communicated wirelessly.

2.6 Developer D

The Developer D system uses a tunable diode laser absorption spectroscopy (TDLAS) measurement technique to quantify methane concentration integrated over a path length in units such as ppm-m. With knowledge of the laser's total path length, an absolute methane concentration can be directly calculated. In general, laser absorption-based measurement techniques measure the amount of laser light that is absorbed by the species of interest. The Developer D system is open path, meaning it does not require a fan or pump to advect the methane-air mixture through the laser's path line. The system's laser path length is variable, ranging anywhere from 0.5 to 10 m. Two different systems were used for most of the testing: a single-gun system and a two-gun system. The tested prototypes allowed for time-resolved measurements at 1 Hz over a range of one to 3,000 ppm-m. Methane concentrations were provided through 4-20 mA outputs in ppmv, which is the average concentration over the sensor path length. The data logging rate, sensor rate, sensor path length, and laser settings could be manually adjusted within the system's software.

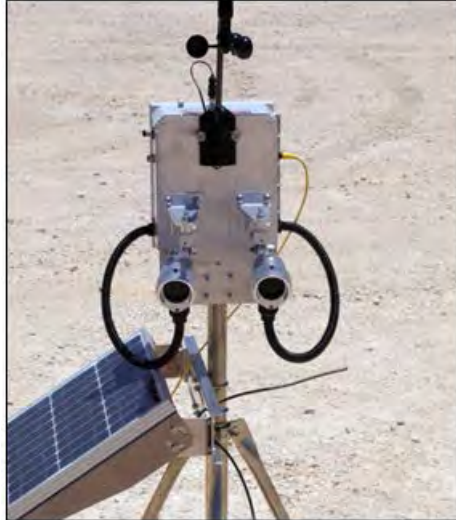


Figure 2.4. “Two-Gun” System Provided by Developer D

This technology developer also provided a single-gun system. Each system was powered by a solar panel and communicated through a 4-20 mA line (with available digital signal).

3. TEST APPROACH

3.1 Overview

The testing was organized into the following three stages:

1. Initial “concentration monitoring” testing to provide baseline performance data. This testing was similar to the testing in Phase 1.
2. Outdoor testing over several months to evaluate the technologies’ abilities to detect transient events and operate for an extended period of time in an outdoor setting.

3.2 Reference Instruments

Two types of instruments were used to take reference measurements of methane concentration during testing. A Picarro Cavity Ring-Down Spectroscopy (CRDS) gas analyzer was used to take measurements during concentration monitoring testing and a Boreal Laser GasFinder2 gas analyzer was used as a reference during controlled release testing.

A Picarro G2204 analyzer was used for the initial concentration monitoring testing and for other testing conducted indoors. The Picarro uses a vacuum pump to continuously draw in and analyze sample gas. Ports for the Picarro inlet and outlet sampling lines were installed at various locations on the testing chamber in order to allow for verifying that the contents of the chamber were well mixed. Although the accuracy specified by the manufacturer (≤ 2.0 ppbv) is only guaranteed for the specified operating range of zero to 20 ppmv, the instrument is capable of taking measurements at much higher concentrations. During Phase 1 testing, the accuracy of the Picarro, in the range of zero to 2,000 ppmv, was verified using a gas chromatograph flame ionization detector (FID). The Picarro and FID measurements agreed within 1% at a concentration of 2,000 ppmv. For Phase 2 concentration monitoring testing, methane concentrations in the range of zero to 100 ppmv were tested. Within this range, the Picarro analyzer is an accurate reference instrument. Near its specified operating range, the Picarro updated readings on the order of 1 Hz. However, at higher concentrations, the Picarro updated less frequently, on the order of 0.3 Hz.

The Boreal Laser GasFinder2 gas analyzer is an open-path gas detector, which uses tunable diode laser absorption spectroscopy (TDLAS) to integrate methane concentration over its path length. Laser light emitted from the transceiver travels through the air to the reflector and back to a photo-diode. Methane concentration is determined based on the absorption of near infrared laser light by methane along the path length. The analyzer can be used to measure concentration along path lengths up to 750 m. For the majority of the outdoor release testing, the Boreal Laser was positioned such that its path length was approximately 10 m long and directed through the center of the co-location point. Developer D’s systems were positioned directly next to the Boreal Laser in order to directly compare their measurements. In addition to being a direct reference measurement for Developer D, the Boreal Laser also served well as an overall reference. All systems compared favorably against the Boreal Laser, despite expected differences in an open path versus point measurement.

3.3 Initial Concentration Monitoring

Phase 2 of the Methane Detector Challenger (MDC) began with a series of concentration monitoring tests that were conceptually identical to the testing previously conducted in Phase 1.

The purpose of this testing was to provide baseline data for the performance of the new systems and to identify any issues with the systems prior to setting them up for outdoor testing. The data collected by each system were provided to the respective technology developer in order to allow for continual improvement opportunities.

3.3.1 Instances of Systems Tested

Due to the timing and the findings of the initial concentration monitoring testing, the systems used for the initial concentration monitoring testing had changes made to them or, in some cases, were replaced entirely by different systems prior to outdoor testing.

- Developer A supplied three systems with only one analog output signal for the initial concentration monitoring. It was not entirely clear to SwRI how the single analog output signal was generated from the measurements taken by the three systems. During outdoor testing, two output signals were supplied for two of the three individual units.
- Developer B supplied two systems for the initial concentration monitoring testing. One system used nitrogen as a calibration gas and one system used air as a calibration gas. Based on the results of the testing, Developer B decided to provide two new systems for outdoor testing, both of which used air as a calibration gas.
- Due to time constraints, Developer C provided the same system that was tested in Phase 1 for the initial concentration monitoring. A new system was provided for outdoor testing.
- Developer D provided one system for the initial concentration monitoring testing. This system was also used for outdoor testing in addition to two other systems that were not present for the initial concentration monitoring.

3.3.2 Methodology and Test Setup

The concentration monitoring tests consisted of fully immersing the systems into a quiescent environment of constant methane concentration. The containment chamber shown in Figure 3.1 was constructed and equipped with an explosion-proof stirring fan. Pure methane was injected into the chamber using a mass flow controller and then stirred with the fan to achieve a given concentration of methane. A Picarro CRDS was used as a reference instrument and logged chamber concentration in real time at approximately 0.3 Hz. A variety of contaminants were also injected into the chamber in order to investigate the effects on the systems.

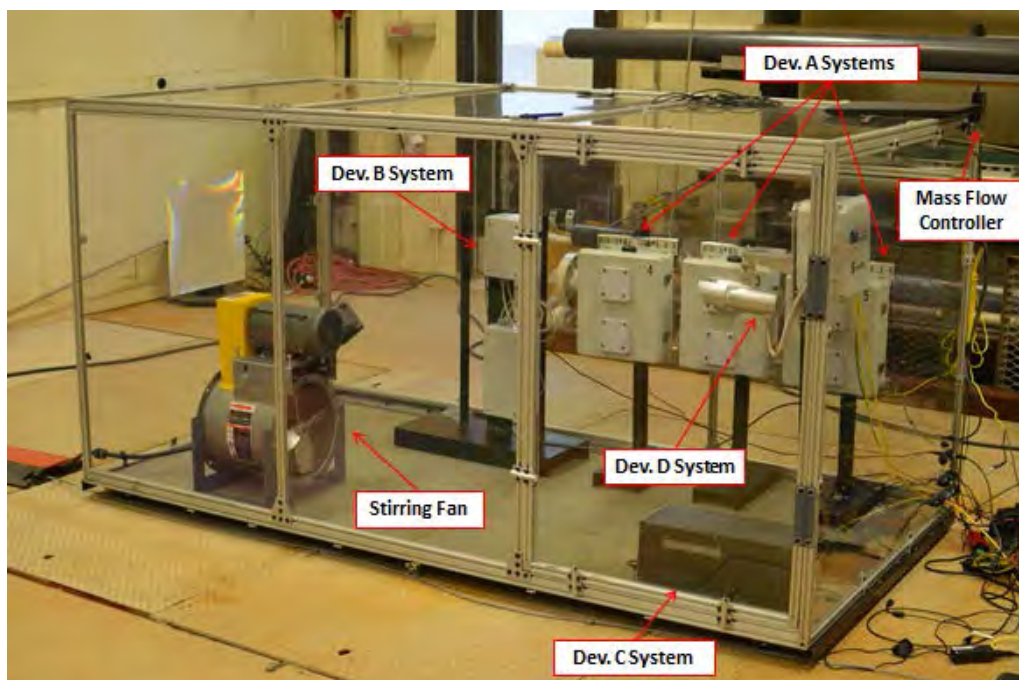


Figure 3.1. Concentration Monitoring Setup

Test configuration allowed for tight control of methane concentrations. The test systems were removed from their tripods and powered via local power supply for this portion of testing.

3.3.3 Methane Testing

The concentration monitoring testing that was performed at the beginning of Phase 2 can be broken up into two parts: methane testing and contaminant testing. Table 3.1 summarizes the methane testing that was performed. Each test consisted of increasing the methane concentration in the containment chamber by a specified increment and maintaining each concentration for a specified holding time.

Table 3.1. Methane Concentration Monitoring Tests

These tests were conducted as stepped ramps.

Test	Hold Time (min.)	Methane Concentrations (ppmv)
1	10	Amb., 5, 7, 9, 11, 13, 15, 17, 19
2	10	Amb., 13, 23, 33, 43, 53
3	4	Amb., 13, 23, 33, 43, 53

3.3.4 Contaminant Testing

The systems were also exposed to carbon monoxide and ethane, which are contaminants that could be present at an oil and gas facility. Table 3.2 summarizes the contaminant testing that was performed. Two types of tests were performed: incremental increases in methane concentration with a background contaminant concentration and incremental increases in contaminant concentration.

Table 3.2. Contaminant Concentration Monitoring Tests

Each test was conducted as a stepped ramp.

Test	Hold Time (min.)	Contaminant	Contaminant Conc. (ppmv)	Methane Conc. (ppmv)
4	10	Carbon Monoxide (CO)	50, Background	Amb., 5, 7, 9, 11, 13, 15, 17, 19
5	10	Ethane (C ₂ H ₆)	50, Background	Amb., 8, 13, 18, 23
6	4	Ethane (C ₂ H ₆)	Amb., 8, 13, 18, 23, 28, 33, 38, 43, 48, 53	-

3.4 Outdoor Testing

Outdoor testing was performed over the course of approximately 75 days at two outdoor testing facilities at SwRI. The purpose of the testing was to evaluate the systems' responses to transient methane plumes in realistic weather conditions and to determine the durability of the systems when exposed to outdoor conditions for an extended time period. The results of this testing are useful for evaluating each system's ability to detect leaks in both broad and targeted scenarios (see Section 1.1).

3.4.1 Methodology for Performing Outdoor Releases

The methodology for performing outdoor release testing at both outdoor testing locations involved co-locating the systems and reference instruments and moving a point leak source around this co-location point. The leak source was placed at an upwind location from the systems. This general test approach is shown in Figure 3.2. Distance between the leak source and the co-location point, leak rate, leak duration, and leak apparatus were varied throughout testing.

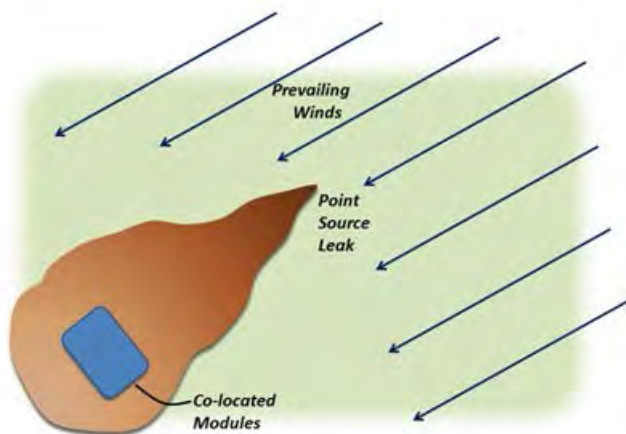


Figure 3.2. General Test Approach for Outdoor Testing

Test modules are located downwind of the release point.

3.4.2 Test Setup at Location #1

Location #1 is a turbomachinery testing facility at SwRI with a large (approximate 150-ft by 150-ft) outdoor testing area. At the time that the outdoor release testing was performed, there

was no other testing in progress and no additional sources of methane present in the outdoor testing area. A diagram of the general test setup that was used for outdoor testing at Location #1 is shown in Figure 3.3. All of the systems and reference instruments were placed in an area near the center of the outdoor testing area. The general locations of each developer's systems at the co-location points are shown in Figure 3.3. However, various adjustments were made to the arrangement of the systems throughout testing. For the majority of the outdoor release testing, the path lengths of the open-path systems and the Boreal Laser analyzer were directed across the center of the co-location point in order to measure the average concentration within the co-location point. Additional tests were performed with the open-path systems and the Boreal Laser analyzer at longer path lengths. In addition to the Picarro and Boreal Laser analyzers, the temperature, relative humidity, and wind speed and direction were measured at the co-location point using a thermocouple, a relative humidity sensor, and an anemometer, respectively. The co-location point without reference instrumentation at Location #1 is shown in Figure 3.4.

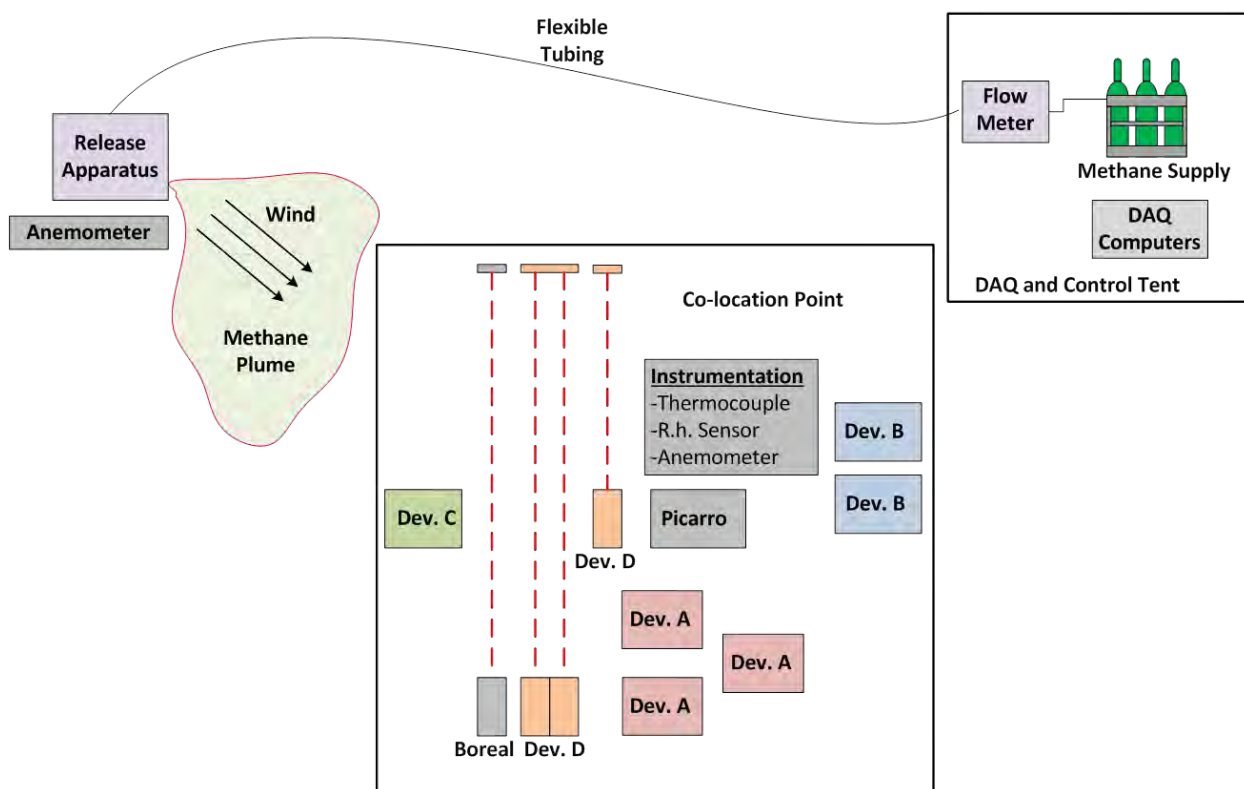


Figure 3.3. Test Setup for Outdoor Testing at Location #1
This configuration was in an open, gravel-surfaced field.

The data acquisition and control computers and the methane supply system were stored in the DAQ and Control Tent. A flow meter was used to control the flow rate of methane from cylinders of compressed methane gas through flexible tubing to the release apparatus. Three types of release apparatuses were used for testing – a bucket containing coiled perforated tubing to simulate a highly-dispersed plume, a flange with a defective gasket to simulate a leaking flange connection, and single 0.25-inch diameter tube to simulate a point leak. Two flow meters were used during testing – a mass flow controller for flow rates below 2 scfm and an orifice flow meter for flow rates above 2 scfm. An anemometer was used to measure the wind speed and direction at the location of the release apparatus. Table 3.3 shows the instruments that were used for outdoor release testing at Location #1. This table does not include the Boreal Laser and

Picarro analyzers, which will be discussed in the following sections. The analog outputs of all instruments, with the exception of the Picarro analyzer and Developer B’s systems, were fed into National Instruments cDAQ modules and logged using a custom program written in LabVIEW. Data from the Picarro analyzer were logged on the Picarro computer itself, and data from Developer B’s systems were logged on a separate computer with custom software provided by Developer B.

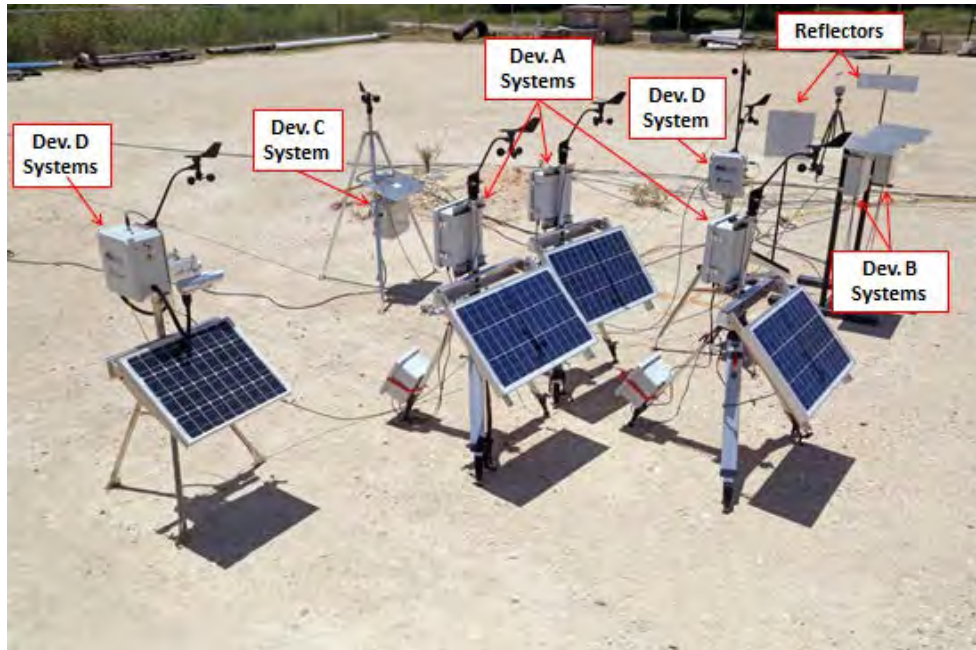


Figure 3.4. Outdoor Testing co-location Point with Reference Instruments at Location #1
This testing was conducted in an open, gravel-packed field.

Table 3.3. Instruments Used During Outdoor Release Testing

Description	Make/Model	Range	Accuracy
Co-location point thermocouple	Type K Thermocouple	N/A	+/- 2°C
Co-location point relative humidity sensor	Omega HX71-V1	0-100% relative humidity	+/- 4% relative humidity
Co-location point wind speed/direction	Novalynx 200-WS-23	0-100 mph 0-360°	+/- 3% full scale +/- 3°
Release apparatus location wind speed/direction	Novalynx 200-WS-23	0-100 mph 0-360°	+/- 3% full scale +/- 3°
Low flow mass flow controller	Sierra Smart-Trak 100M Series	0-200 slpm	+/-1% full scale
Orifice meter static pressure transmitter	Rosemount 3051	0-4,000 psig	+/- 0.075% full scale
Orifice meter temperature transmitter	Rosemount 3144P	0-100°C	+/- 0.55°C
Orifice meter differential pressure transmitter	Rosemount 3051	0-1,000 inH ₂ O	+/- 0.075% full scale

3.4.3 Test Setup at Location #2

After approximately seven weeks of outdoor testing at Location #1, the systems were moved to Location #2, which is a natural gas testing facility at SwRI. The technologies ran for several weeks at this location. The reasons for re-locating the systems to Location #2 included additional exposure of the systems to outdoor weather conditions, exposure of the systems to leaking valves and fittings at a natural gas facility, and exposure of the systems to natural gas that contains additional hydrocarbons such as ethane and propane. Although it was not the primary focus of the testing at Location #2, a number of intentional natural gas releases were performed. The performance of the technologies at this location mirrored that at the first location. Thus, except where noted, all data are from Location #1.

4. RESULTS

4.1 Initial Concentration Monitoring

4.1.1 Methane Testing

Figure 4.1 and Figure 4.2 show concentration histories from the 2-ppm methane ramp. In both, the Picarro reference trace is shown in black. In general, all systems were able to detect changes in methane with varying degrees of accuracy. Figure 4.1 compares Developer C and Developer D measurements against those of the Picarro analyzer. Both of these systems were highly accurate. Figure 4.2 compares Developer A and Developer B measurements against those of the Picarro analyzer. Developer B's systems exhibited fair accuracy compared to the Picarro analyzer, but also exhibited periods of erroneous readings during calibration periods. Developer A's system indicated sensitivity to the elevating methane levels, but with a lesser degree of accuracy than the other systems. It also exhibited large measurement spikes when the methane concentration in the containment chamber was adjusted.

For the 10-ppm increment, 10-minute hold methane test shown in Figure 4.3 and Figure 4.4, the systems of Developer C, Developer D, and Developer B showed good stability and accuracy when exposed to the elevated methane levels. Developer A's system, however, was extremely reactive – a 50-ppmv methane level resulted in a 120-ppmv reading.

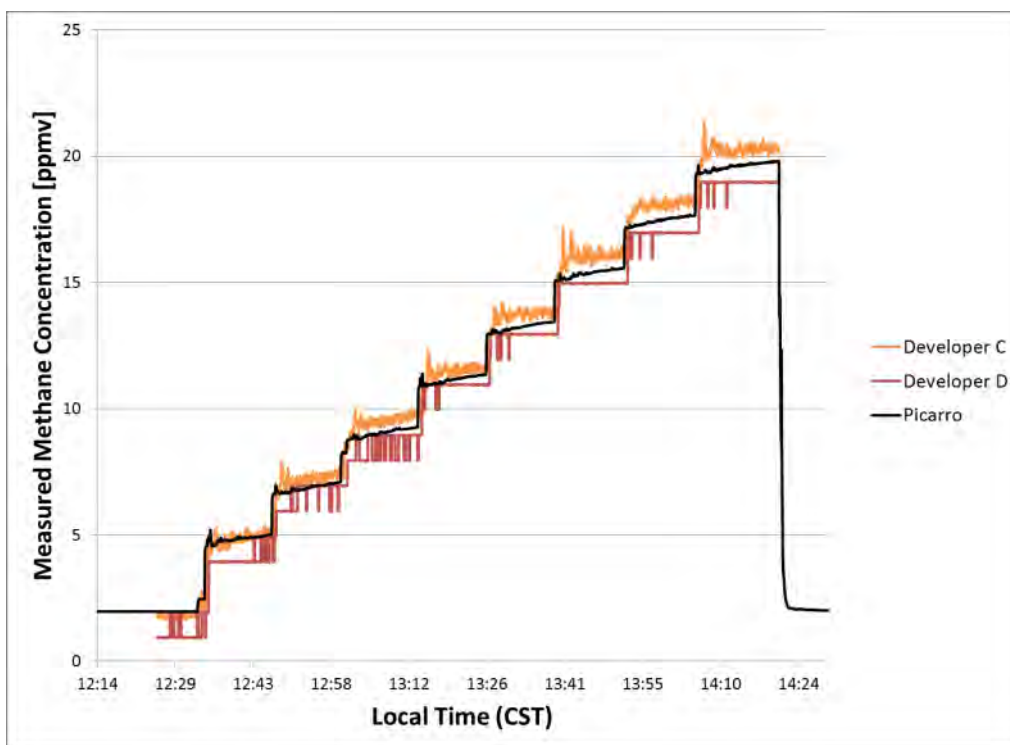


Figure 4.1. Results from the 2-ppmv Increment Methane Test for the Systems of Developer C and Developer D
Systems show accurate levels of responsiveness.

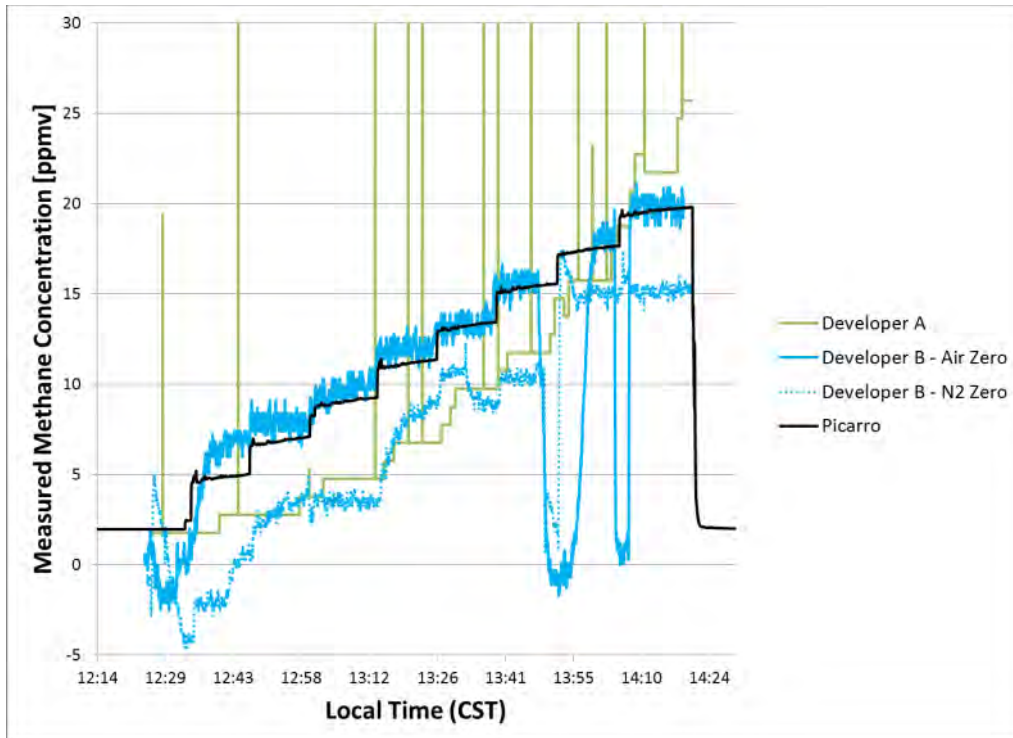


Figure 4.2. Results from the 2-ppmv Increment Methane Test for Systems of Developer A and Developer B

Developer A was able to detect changes in background, though not able to provide accurate quantification. The “nitrogen-zeroed” system provided by Developer B incurred an offset.

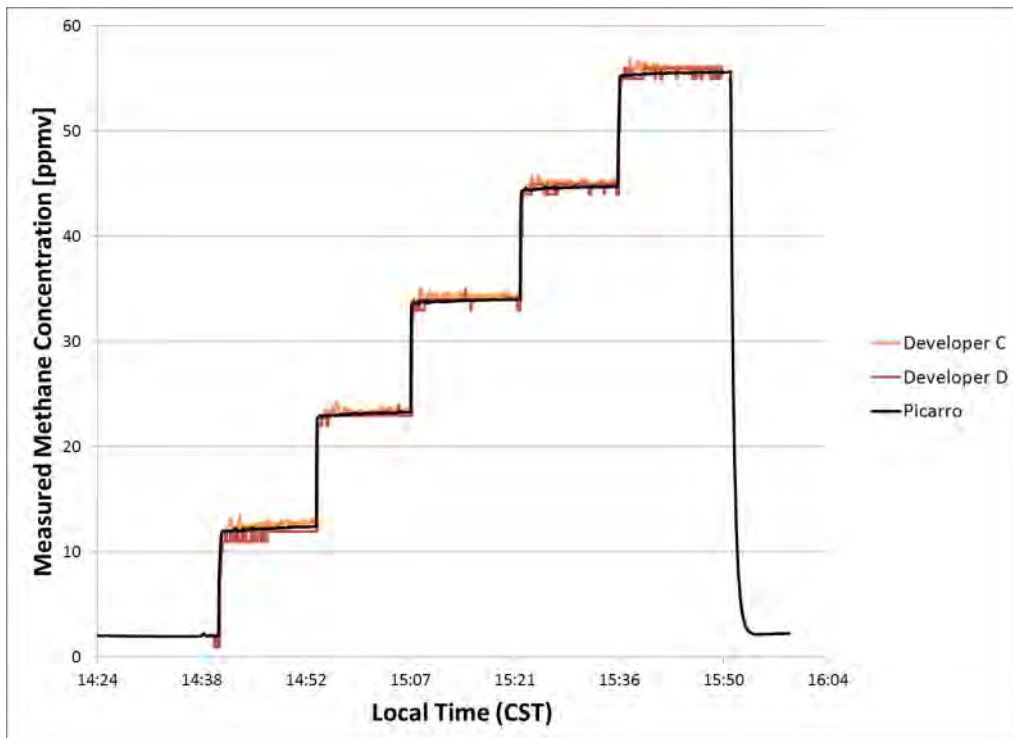


Figure 4.3. Results from the 10-ppmv Increment, 10-Minute Hold Methane Test for the Systems of Developer C and D

These systems again exhibited very accurate performance.

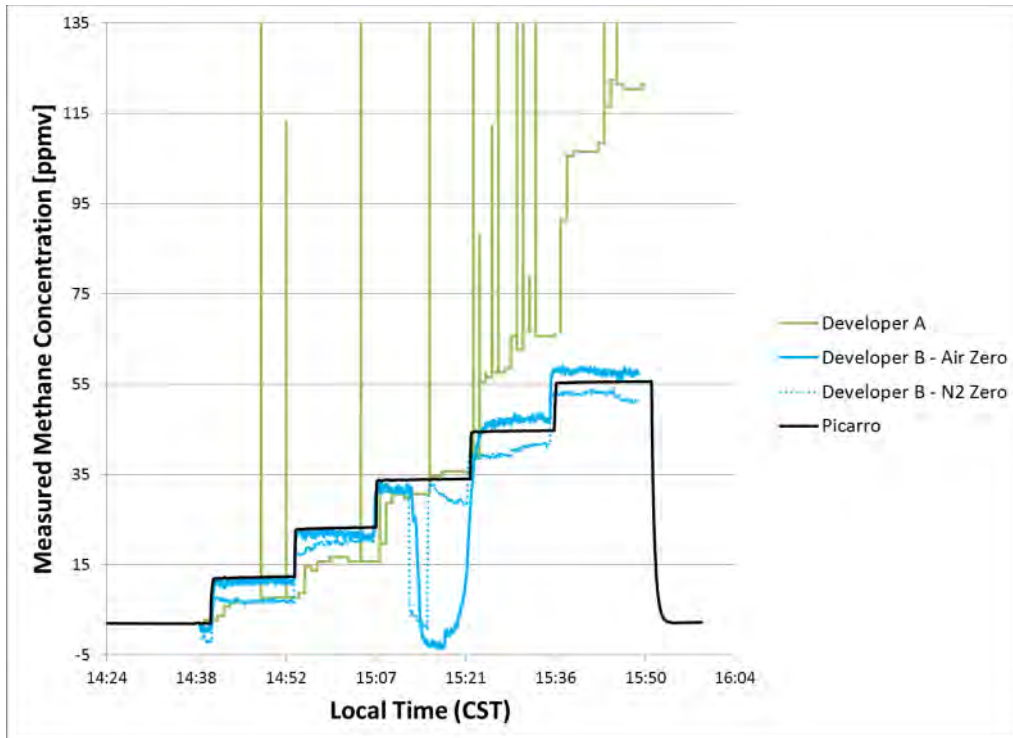


Figure 4.4. Results from the 10-ppmv Increment, 10-Minute Hold Methane Test for the Systems of Developer A and B
Developer A's system demonstrated less accuracy at higher methane concentrations.

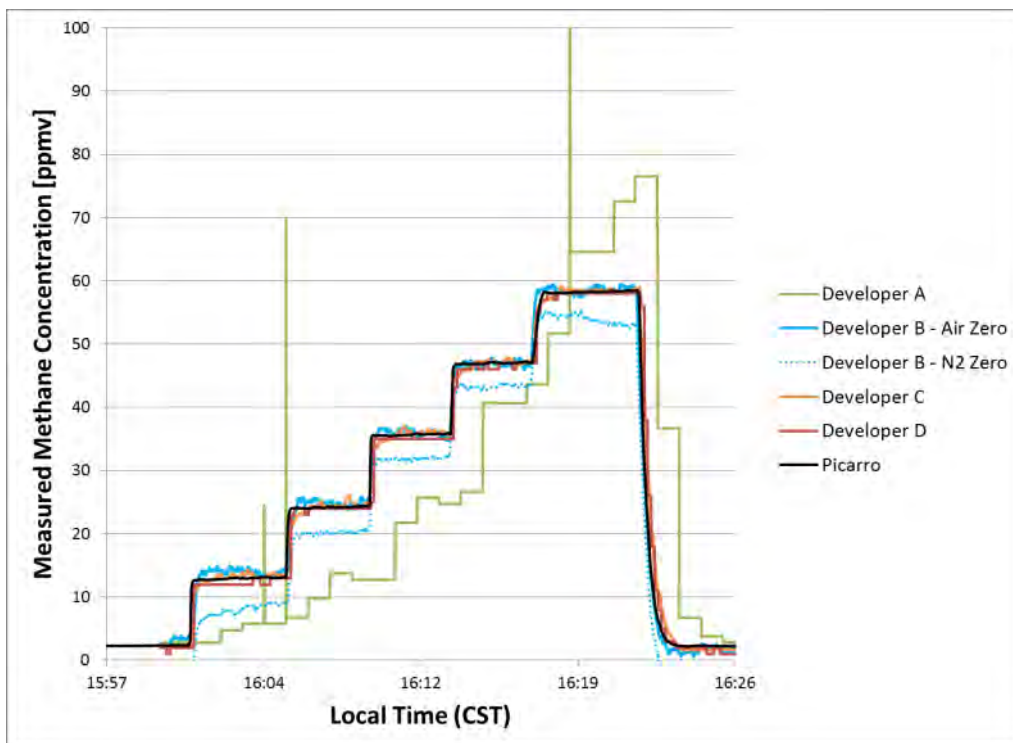


Figure 4.5. Results from the 10-ppmv increment, Four-Minute Hold Methane Test for All Developers
While Developer A's system had an offset, it was responsive to changes in background level.

Figure 4.5 shows the results from the 10-ppmv increment, four-minute hold methane test for all developers. As in the previous tests, the systems of Developer C, Developer D, and Developer B showed high accuracy and stability when compared with the Picarro analyzer. It should be noted that Developer B's air-calibrated system showed higher accuracy than its nitrogen-calibrated system. Developer A's system had inconsistent accuracy, but it was able to measure changes in methane concentration. It is also interesting to note that the large spikes that were seen in Developer A's measurements during longer hold times in previous tests are less common during shorter holds.

4.1.2 Contaminant Testing

The results from the carbon monoxide background contamination test are shown in Figure 4.6. Developer C's and Developer D's systems showed no sensitivity to the contaminant. At the beginning of the test, Developer A's system stopped transmitting data and temporarily shut down. The cause of this behavior was unknown at the time, but was believed to be related to the system's software. This shutdown also occurred in a separate test, the results of which are not shown here. Although it appears that Developer B's air-calibrated system was affected by the presence of the background contaminant, the lack of accuracy was likely associated with a need for self-calibration. This behavior happened periodically, but corrected itself after sufficient self-calibration.

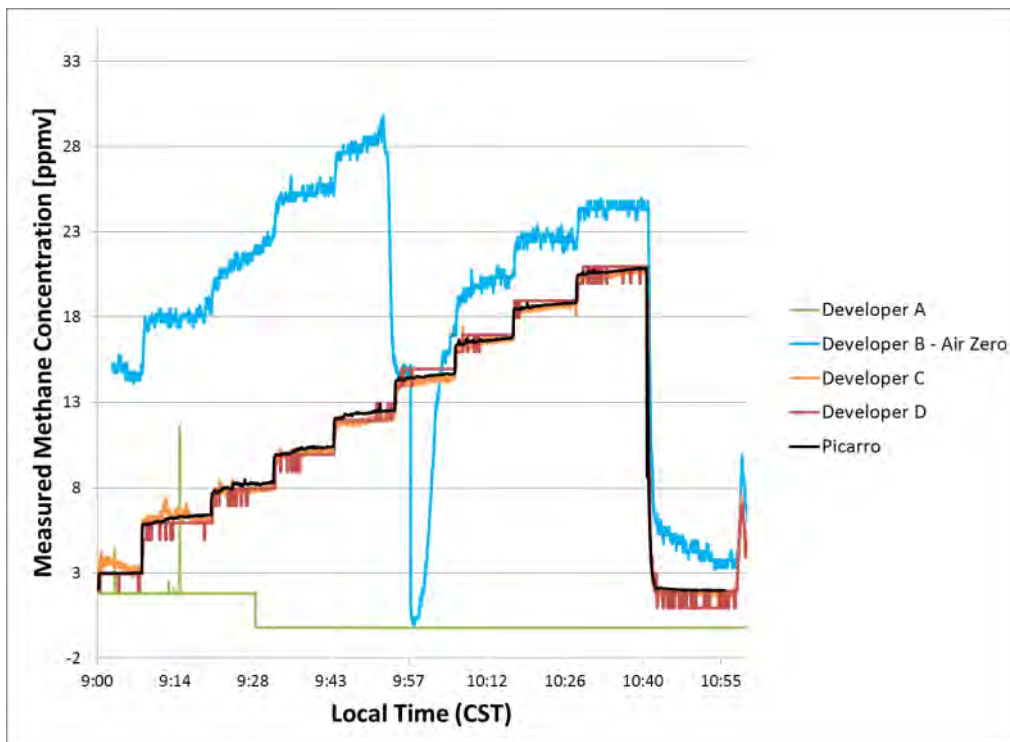


Figure 4.6. Results from the Carbon Monoxide Background Contamination Test
 Developer A's and Developer B's systems were impacted by the contaminant. Developer A's system did not provide valid readings when exposed to carbon monoxide.

Figure 4.7 shows the results from the ethane background test. Developer A's and Developer B's systems were unable to distinguish between the ethane and methane. Both of these systems showed elevated sensitivity to the presence of ethane, reporting methane concentration readings on the order of 100 ppmv or more for actual methane concentrations

between zero and 20 ppmv. Developer C's and Developer D's systems showed no sensitivity to the ethane and were able to accurately measure methane concentration.

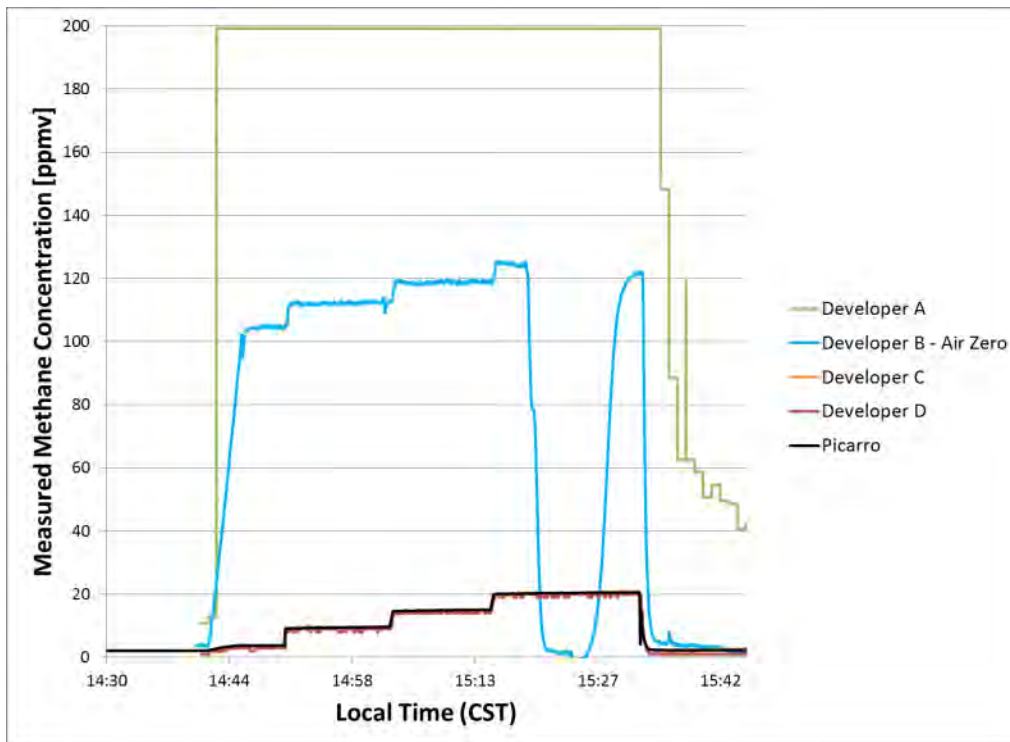


Figure 4.7. Results from Ethane Background Contamination Test

Developer A's and Developer B's systems were impacted by the contaminant. Developer A's system did not provide valid readings when exposed to ethane.

Figure 4.8 shows the results from the test in which the ethane concentration in the containment chamber was increased in 5-ppmv increments with a 10-minute holding time. It is important to note that methane was injected into the containment chamber during this test. Developer A's and Developer B's systems mistook the ethane for methane. Both of these systems reported elevated concentrations (as high as 100 ppmv and 200 ppmv) of methane in the presence of ethane. Developer C's and Developer D's systems showed no sensitivity to the elevated levels of ethane.

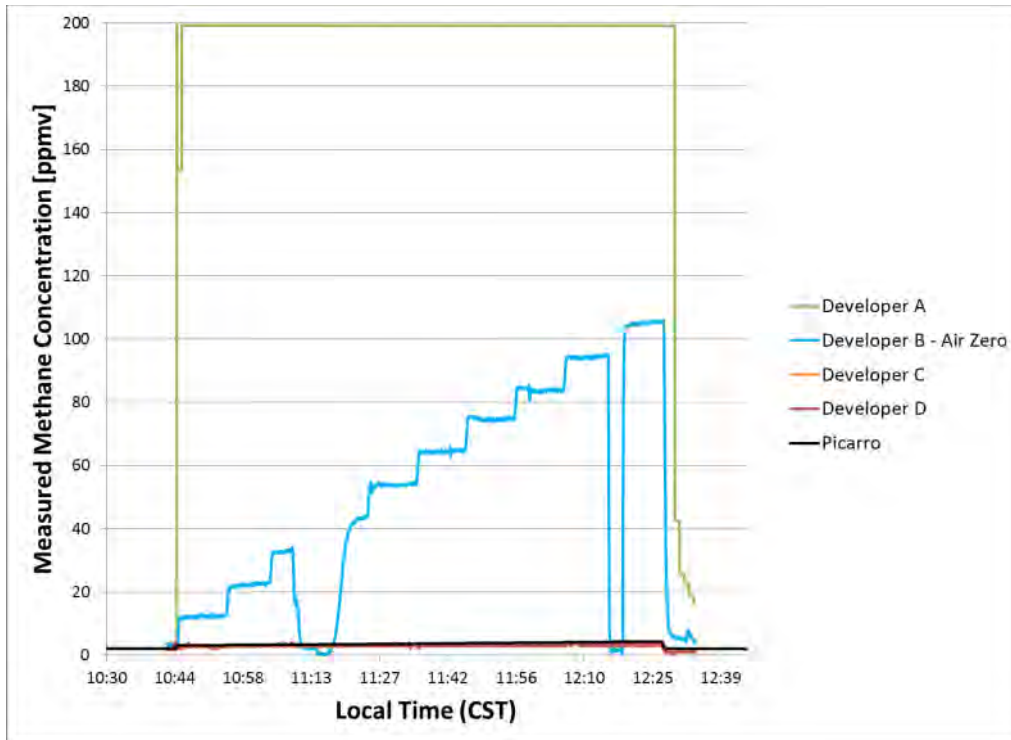


Figure 4.8. Results from the 5-ppmv Increment Ethane Contamination Test
 Developer A's and Developer B's systems were impacted by the contaminant. Developer A's system did not provide valid readings when exposed to ethane.

4.1.1 Summary

Results and conclusions from the initial concentration monitoring tests are summarized below. In general, all systems indicated the same behaviors shown from Phase 1 testing.

- Developer C's and Developer D's systems demonstrated consistent accuracy and no sensitivity to the selected contaminants.
- Developer B's systems (one using nitrogen as a calibration gas, the other using scrubbed air) were also responsive to small changes in methane concentration, despite exhibiting periods of drift. This drift was believed to be caused by sensor exposure to excess water vapor. These systems also reported periodically-erroneous measurements during self-calibration.
- Developer A's systems (three were used in total) exhibited sensitivity to changing methane levels, but with limited accuracy. These units also showed susceptibility to contamination. Exposure to ethane led to exaggerated and erroneous readings. Exposure to carbon monoxide led to a temporary system shut-down due to a bug in system processing.

4.2 Controlled Outdoor Releases

4.2.1 Test Matrix

The controlled releases covered a range of leak flow rates and ranges to simulate a wide variety of detection scenarios. In general, methane leaks ranging from 0.5 to 5 scfm were placed upwind from the co-location grouping at ranges varying from 30 to 130 ft. A full test matrix is

listed below in Table 4.1 where “X” indicates a test point. Longer release ranges (82 and 130 ft) were used due to the physical constraints of the Location #1 area – 82 ft is the distance from the co-location to the back fence and 130 ft is the distance from the co-location to the corner of the yard. Valid data were acquired at most test points for each device, with only a few extenuating omissions. The intent of this approach was to determine the functional detection limits with respect to flow rate and range for each test system. Reference instrumentation detected the methane plume at all points listed below. It is important to note that for a given combination of range and leak rate, the datasets for each system do not necessarily correspond to the same actual test point. As an example, the 2.5-scfm, 30-ft test for Developer B might have been a different 2.5-scfm, 30-ft test used for Developer C. This arrangement was due to the fact that several technology developers’ systems stopped functioning at various points of the outdoor testing.

Table 4.1. Test Matrix for Controlled Release Testing

		Leak Rate [scfm]			
		0.5	1	2.5	5
Range [ft]	30	--	X	X	X
	50	--	X	X	X
	70	--	X	X	X
	82	--	X	X	X
	130	X	X	X	X

4.2.2 Overall Detection Comparison

The subsequent sections will detail how each system was mathematically analyzed and provide some metrics, such as an “agreement rate.” However, it is first useful to assess for which releases a particular system would have detected the leak. The transient nature of the open-air releases results in a number of spikes of methane. It is not a requirement that a system detects every spike or even accurately quantifies the spike. The key parameter is whether or not the system detects spikes that are clearly outside the noise of the system signal. The following tables present the overall ability of the systems to detect various releases. The raw data traces used to establish these findings are located in the appendices to this report. It is important to recognize that during periods in which there were no leaks, there were no measurements from the systems that would indicate a false positive.

Table 4.2. Leak Detection Capability Demonstrated for Tests for 5-scfm Leaks

Some systems were not operational for some tests, hence the “unknown” designation for some points.

		Developer			
		A	B	C	D
Range [ft]	30	Yes	Yes	Yes	Yes
	50	Yes	Yes	Yes	Unknown
	70	Yes	Yes	Yes	Yes
	82	Yes	Yes	Yes	Yes
	130	No	Yes	Yes	Yes

Table 4.3. Leak Detection Capability Demonstrated for Tests for 2.5-scfm Leaks

Some systems were not operational for some tests, hence the “unknown” designation for some points.

		Developer			
		A	B	C	D
Range [ft]	30	Yes	Yes	Yes	Yes
	50	Yes	Yes	Yes	Yes
	70	Yes	Yes	Yes	Yes
	82	Yes	Yes	Yes	Yes
	130	No	Unknown	Yes	Yes

Table 4.4. Leak Detection Capability Demonstrated for Tests for 1-scfm Leaks

Some systems were not operational for some tests, hence the “unknown” designation for some points.

		Developer			
		A	B	C	D
Range [ft]	30	Yes	Yes	Yes	Yes
	50	Yes	Unknown	Yes	Yes
	70	Yes	Yes	Yes	Yes
	82	Yes	Yes	Yes	Yes
	130	Yes	Yes	Yes	No

Table 4.5. Leak Detection Capability Demonstrated for Tests for 0.5-scfm Leaks

This leak rate was only tested at a distance of 130 ft.

		Developer			
		A	B	C	D
Range [ft]	130	No	No	Yes	No

4.2.3 Time-Resolved Analysis Methodology

For systems with time-resolution (Developer B, Developer C, and Developer D), agreement rate metrics were used to quantitatively assess a system’s performance. Agreement rate metrics can be utilized to summarize the performance of a test system against a reference measurement for a certain leak flow rate and range. In general, this metric involves comparing the methane detection state of a test system against the detection state of the reference measurement.

For the present analysis, two types of agreement rates were computed:

1. Overall Agreement, where the agreement between test system and reference instrument is determined at all points.
2. Methane Agreement, where the agreement between test system and reference instrument is determined only during periods of elevated methane levels.

To compute an agreement rate, the concentration time series is decomposed into windows and the concentration reading in that window is compared against the system’s baseline readings. The detection state of a test system or a reference instrument is determined by comparing the mean concentration measurement in a window against a threshold derived from baseline levels. A system is said to detect methane if the mean measurement exceeds some threshold above baseline levels. A system agrees with the reference measurement if the system detection state matches the detection state of the reference instrument. This process is repeated for each window over the duration of the methane exposure interval.

The figure below illustrates the time-resolved comparison. Baseline magnitude and noise levels are calculated from data taken at the beginning of a trial prior to methane exposure. The exposure interval starts and ends when the reference measurement first and last detects methane. For time-resolved comparison, overlapping windows are used to minimize sampling error incurred by window termination in the middle of a detection event.

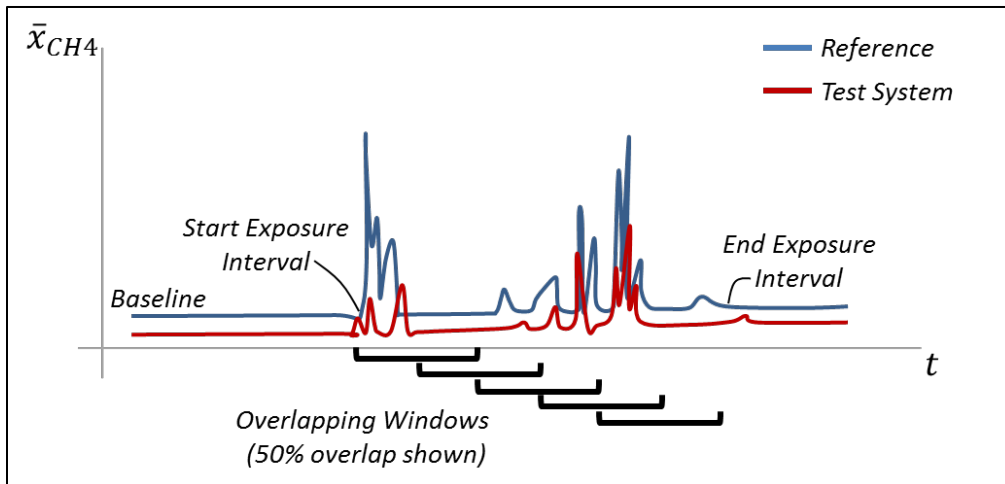


Figure 4.9. Conceptual Illustration of the Agreement Rate Metric
Overlapping windows are used for analysis.

In terms of formally defining detection states, if the mean concentration during a window exceeds the threshold level, then the system has detected methane (if $\bar{X}_{window} > x_{thresh}$, then state = “detect”). Conversely, if the mean concentration during a window remains below the threshold, then the system has not detected methane (if $\bar{X} \leq x_{thresh}$, then state = “no detect”). Table 4.6 lists the possible agreement outcomes given the detection states of a test system and reference instrument. If the test system and reference instrument states match, then the systems agree. If they do not match, then the systems disagree. The overall agreement rate is calculated at *all reference instrument detection states*, regardless of methane levels. The methane agreement rate is calculated *only when the reference measurement indicates a positive detection state*. This latter case removes any data skew resulting from long periods of the absence of methane.

Table 4.6. Agreement State Decision Table

Test System State	Reference State	Agreement State
<i>Detect</i>	<i>Detect</i>	Agree
No Detect	<i>Detect</i>	Disagree
<i>Detect</i>	No Detect	Disagree
No Detect	No Detect	Agree

4.2.4 The Use and Selection of Detection Thresholds

The practice of determining a detection state by using a baseline-derived threshold is common in measurement techniques. The detection limit threshold used in this report is derived from mean baseline readings and noise levels (variance), where the baseline measurement is the signal in the absence of excess methane. The detection limit threshold can be generally defined as:

$$x_{thresh} = \bar{X}_{BL} + \delta$$

where \bar{X}_{BL} is the mean concentration measurement during a baseline period and δ is some deviation above this baseline mean. It is common to define the deviation, δ , based on measured baseline noise levels so that the deviation is a scaled multiple of the noise levels. This can be algebraically described as:

$$\delta = a * \sigma_{BL}$$

where σ_{BL} is the standard deviation of the baseline signal and a is some multiplier. A multiplier of $a = 3$ is common practice and its use results in strong confidence of the detection status.

Instead of using a standard noise multiplier of $a = 3$ for all devices, tailored thresholds specific to each device were selected for the agreement rate analysis to help improve agreement rate results for a given test system. Table 4.7 summarizes the selections of δ_i for all test systems and the reference measurement. This more subjective threshold selection leverages the clear coherence between the test systems and the reference and takes into account the signal quality and type. For all of the trials considered in the agreement rate analysis, the Boreal Laser was used exclusively as the reference methane measurement. A noise multiplier of $a = 10$ was used for the Boreal Laser, since a higher multiplier ensures reference accuracy and prevents false positives and false negatives in detection status. Some commentary on the specific thresholds chosen for each developer includes:

- The deviation used for Developer B features a relaxed noise multiplier of 2 so that $\delta_B = 2 * \sigma_{BL,B}$. This relaxed multiplier was used since a low-pass filter applied to Developer B's signal had a tendency to minimize observable coherent methane spikes.
- Unlike for Developers B and D, the threshold used for Developer C used the standard noise multiplier so $\delta_C = 3 * \sigma_{BL,C}$. This threshold was selected since Developer C's readings were precise and featured low noise and high resolution.
- The test system from Developer D's signal featured a zero noise, ppmv-only resolution. Anytime this system's reading exceeded one ppmv, the signal was relevant and indicated elevated methane levels. As such, a constant, non-noise-based deviation was used to reflect these signal characteristics, meaning $\delta_D = 1$ [ppmv].

Table 4.7. Summary of Detection Limit Threshold Deviation, δ_i , Above Baseline Mean
Different thresholds (function of standard deviation of baseline) used for each developer due to differences in resolution and system noise are shown.

System	δ_i
Developer B	$2 * \sigma_{BL,B}$
Developer C	$3 * \sigma_{BL,C}$
Developer D	1 [ppmv]
Boreal Laser (reference)	$10 * \sigma_{BL,ref}$

To help illustrate the benefit of using custom thresholds, Figure 4.10 compares the agreement rates computed with a standardized threshold of $x_{thresh} = \bar{X}_{BL} + 3 * \sigma_{BL}$ against the agreement rates computed with the customized thresholds listed in Table 4.7. These particular results are for a trial with a leak rate of 2.5 scfm placed at a range of 70 ft. The customized thresholds improve agreement for Developers B and D and this is typical for all trials. The graph shows slight improvement for Developer B, but more dramatic improvement for Developer D.

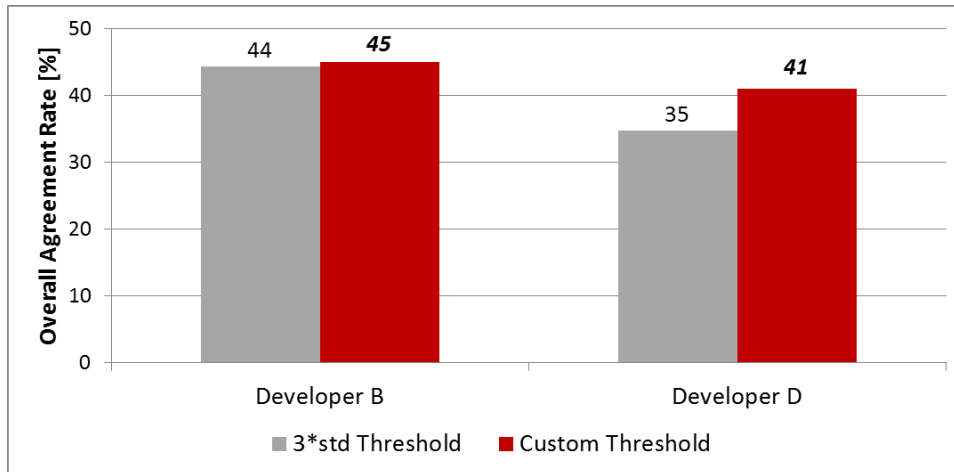


Figure 4.10. Comparison Between Standard and Custom Thresholds for Developers B and D for a Common Trial (2.5 scfm from 70 ft)
Customized thresholds provide better agreement results for Developers B and D.

4.3 Developer B Results

The following details a sample agreement rate calculation performed with the data taken with Developer B’s system. Figure 4.11 shows the raw data (as collected) with the reference signal (Boreal Laser) shown in black and the signal from Developer B, System #1 shown in blue. This particular trial featured a 1-scfm leak from a 70-ft range for a duration of 20 minutes. Immediately noticeable is the significant baseline offset and drift exhibited by Developer B’s system. This behavior was typical of Developer B’s system, despite timed calibrations every six hours.

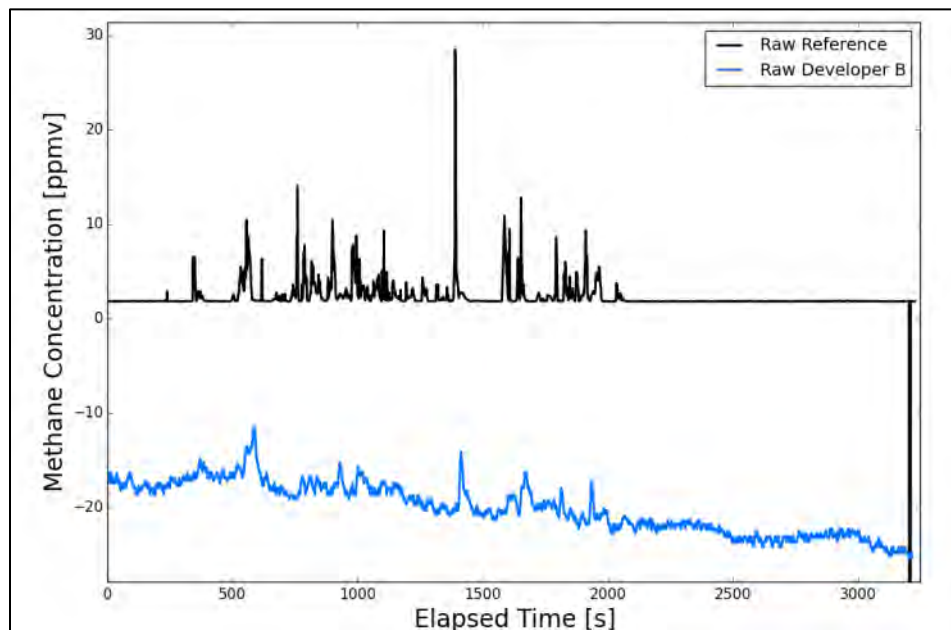


Figure 4.11. Raw Signals from the Reference Instrument and Developer B’s System
Since event detection focuses on a change in signal, the offset is not critical.

To correct this baseline drift, a centered, moving average, high-pass filter was applied to Developer B’s signal. This process is illustrated in Figure 4.12. The low-pass component (gray,

dotted) is computed and then subtracted from the raw signal to yield a filtered signal. The filtered signal is then used in the remaining agreement rate analysis.

A typical feature seen in all of the concentration series data is an evident time lag between test system and the reference instrument. In general, test system measurements and reference measurements showed a very strong coherence in which similar methane peaks or “structures” are seen in all measurements. This time lag has physical (delay in methane plume advection between measurement locations) and non-physical (DAQ latency, lag between separate DAQ computers) causes. To account for this, test system and reference time series are programmatically aligned using cross-correlation. This process is shown in Figure 4.13. In addition to cross-correlation alignment, the process of using windows of data also remedies lag seen between coherent structures.

At this point, test system and reference baseline characteristics are computed (mean and standard deviation) and used to build the threshold value described above. In most cases, a kernel of 100 points was taken from the front end of the data file to determine baseline characteristics for the test system and reference instrument. The detection threshold for Developer B’s system is defined as $x_{thresh} = \bar{X}_{BL} + 2 * \sigma_{BL}$. A noise multiplier of three is often considered an industry standard when determining minimum detection limits. However, a relaxed multiplier of two was used in the present case due to the filtering process, which had a tendency to bury obviously coherent structures and in effect act as a penalty.

Baseline truncation is the last step prior to computing the agreement rate, shown in Figure 4.14. Baseline removal is done so that agreement during inactive periods does not skew the agreement rate upward. The files truncated according to the first and last times the reference measurement detected methane.

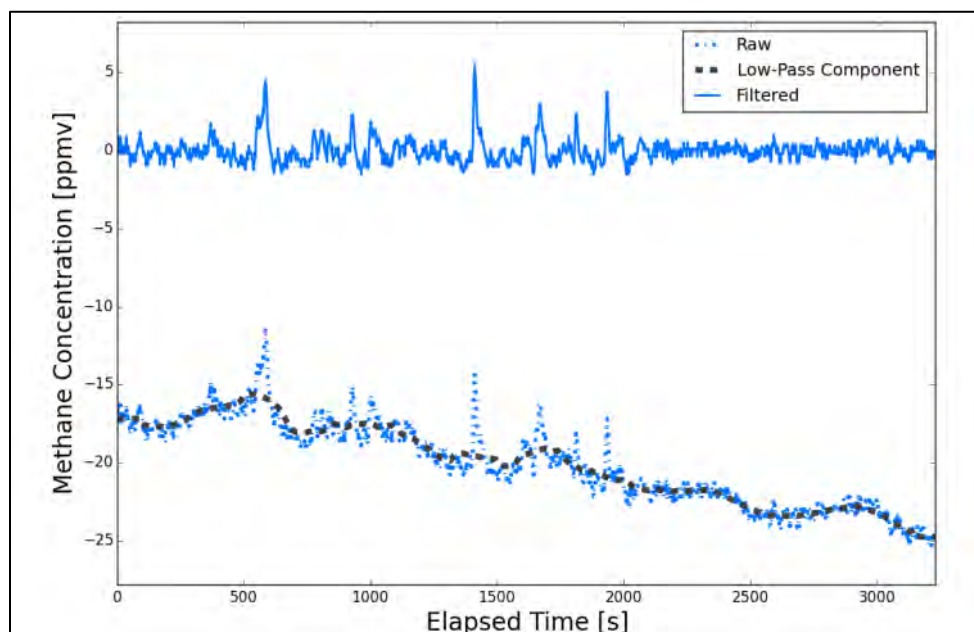


Figure 4.12. Illustration of the High-Pass Filtering Process for Developer B’s System
Filtering is required due to drifting of the baseline signal.

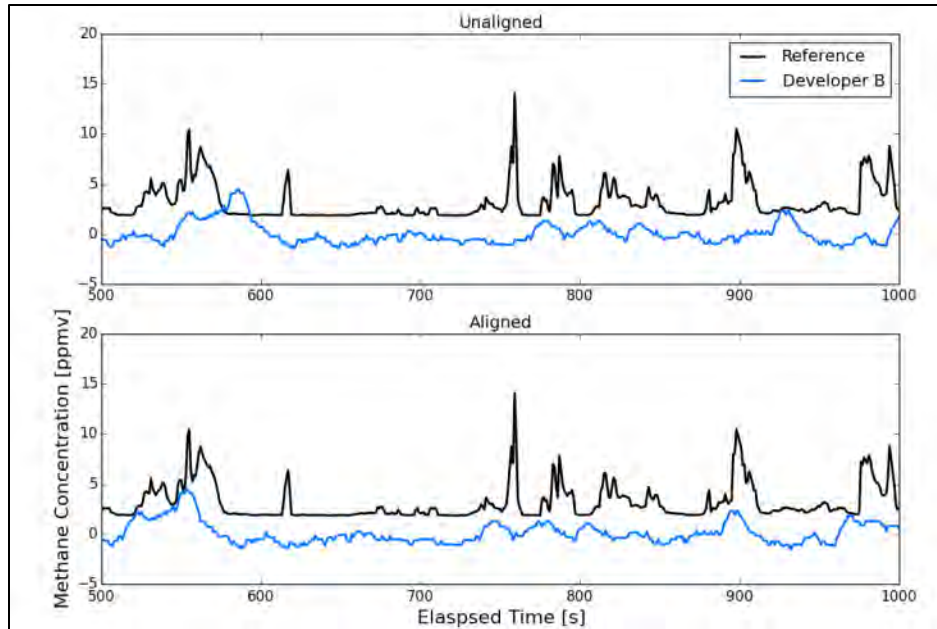


Figure 4.13. Illustration of the Time Alignment Process for Developer B's System
This process corrects for synchronization offset with the reference instrument.

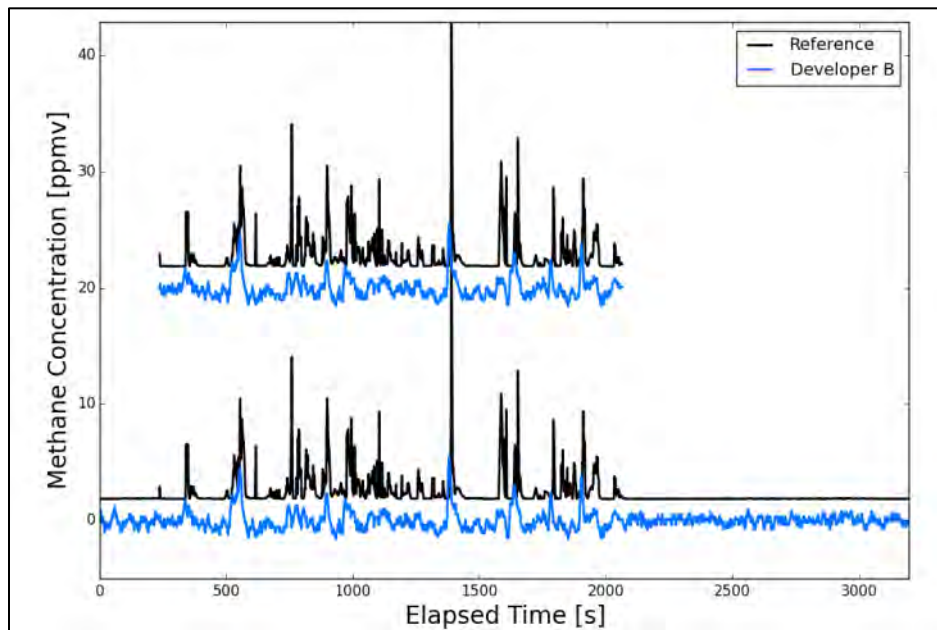


Figure 4.14. Illustration of the Baseline Truncation Process for Developer B's System
Long periods of background before or after leaks are removed in order to not skew data.

Figure 4.15 is a plot which highlights all of the windows in which Developer B's system agreed with the reference measurement. Times of agreement are shaded green. This particular trial resulted in an overall agreement of 45.3% and a methane agreement rate of 15.2%. The signal from Developer B's system shows strong coherence with the reference measurement, especially with the larger methane peaks. However, many smaller peaks are subjectively identifiable, but do not exceed the minimum detection threshold.

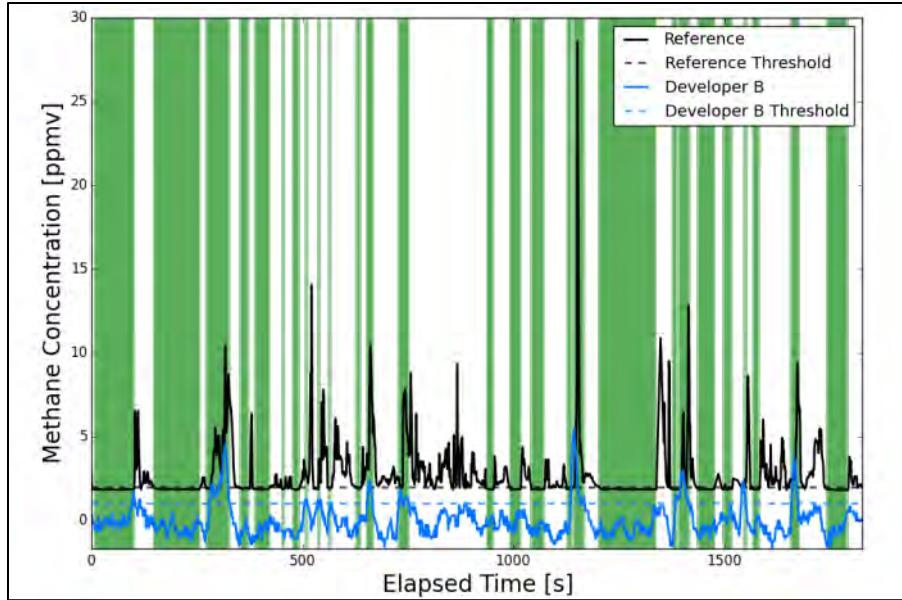


Figure 4.15. Plot Showing Agreement between Developer B’s System and the Reference Measurement

Green bars represent periods in which the developer system agreed with the reference instrument as to the state of the presence of methane.

Both overall agreement and methane agreement (defined in Section 4.2.3) between Developer B’s system and the reference instrument were calculated for all data points. The results are summarized in the following figures. Agreement rate results vary significantly from trial to trial, due to data quality issues associated with the persistent baseline drift. Trials that featured less significant drift generally resulted in stronger agreement, since the filtering process tended to artificially bury smaller methane peaks.

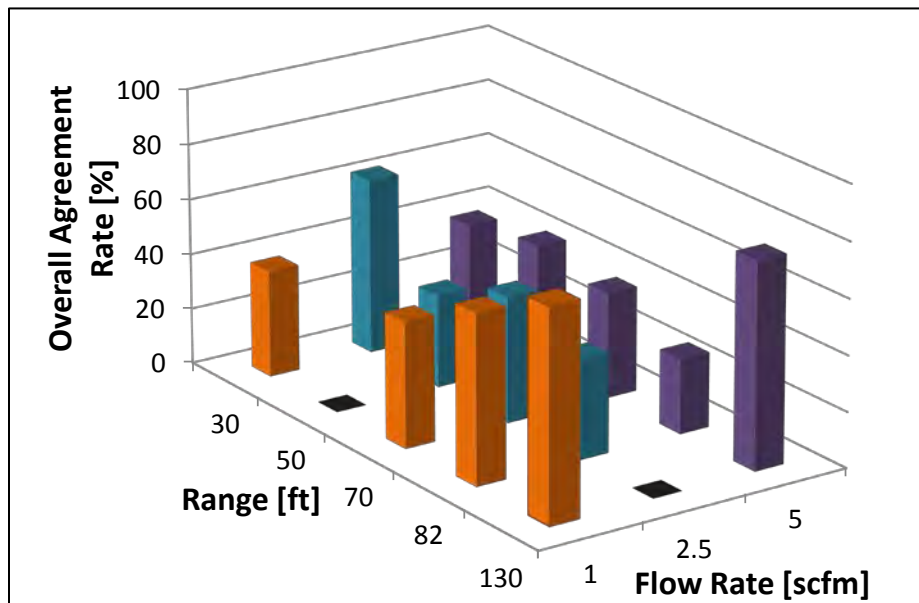


Figure 4.16. Agreement Rate Bar Chart for Developer B’s System

The chart shows the percentage of time that the developer system agreed with the reference instrument, regardless of state. The surfaces in black denote points for which the developer system was not online during testing and no data are available.

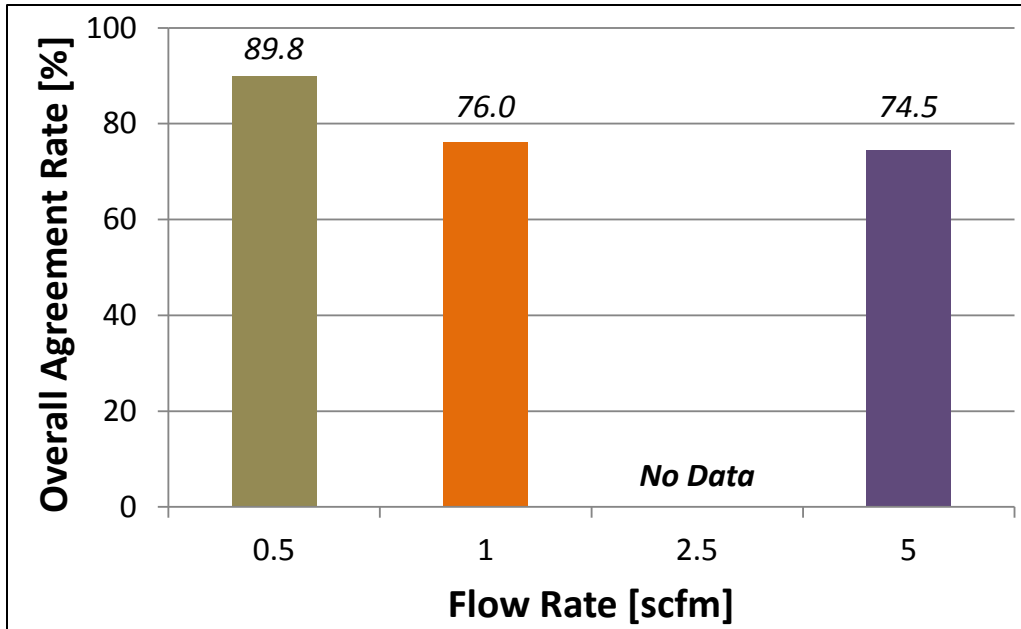


Figure 4.17. Agreement Rate Chart for 130-ft Point for Developer B's System
Data at every point, other than 0.5 scfm, are included in a prior chart.

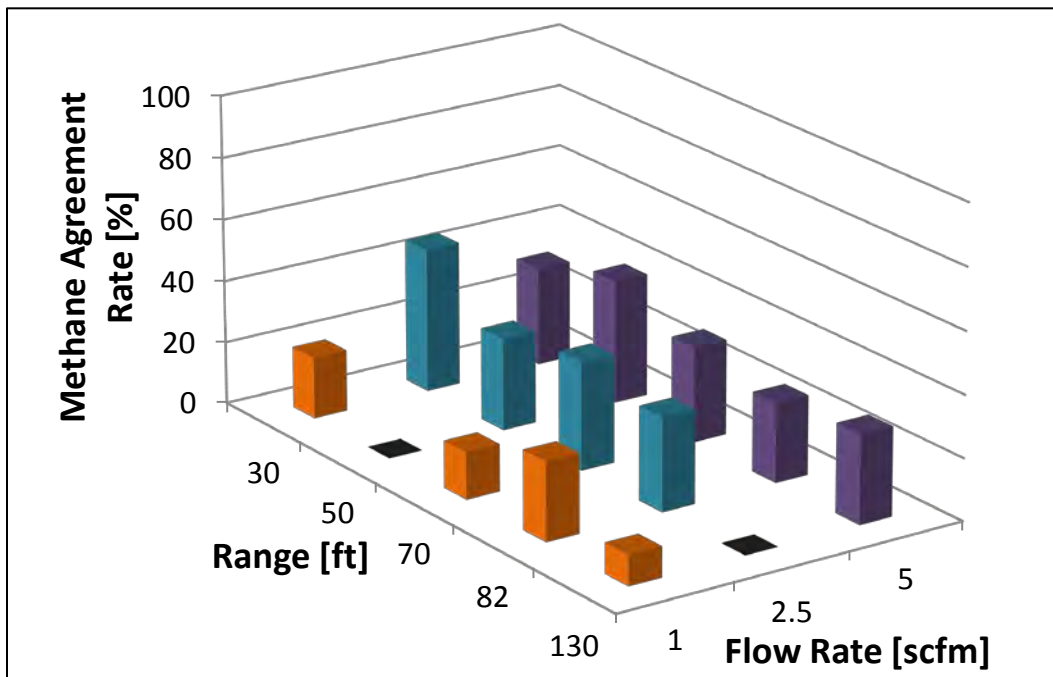


Figure 4.18. Methane Agreement Rate for Developer B's System
These percentages are the agreement rates only during periods in which the reference instrument measured methane concentrations in excess of background. The surfaces in black denote points for which the developer system was not online during testing and no data are available.

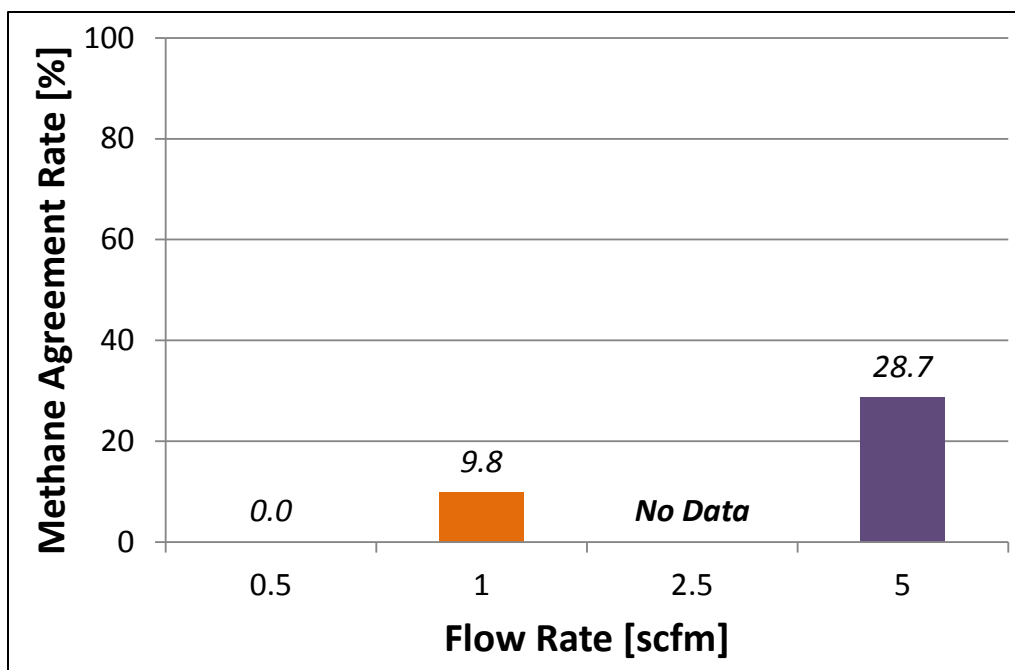


Figure 4.19. Methane Agreement Rate Chart for 130-ft Point for Developer B's System
Data at every point, other than 0.5 scfm, are included in a prior chart. The system would not have detected a leak at the 0.5-scfm, 130-ft range.

4.4 Developer C Results

The following details a sample agreement rate calculation performed with the data taken with Developer C's system. Figure 4.20 shows the raw data (as collected) with the reference signal (Boreal Laser) shown in black and the signal from Developer C's system shown in purple. This particular trial featured a 1-scfm leak from an 80-ft range for a duration of 20 minutes. Note the occasional dropout in signal from Developer C's system. These features are artifacts of SwRI's data acquisition and are not found in the signal provided Developer C's system. These dropouts were not removed in post-processing since they were found to have minimal effect on the agreement rate calculation.

A typical feature seen in all of the concentration series data is an evident time lag between the test system and the reference instrument. In general, test system measurements and reference measurements showed a very strong coherence in which similar methane peaks or "structures" are seen in all measurements. This time lag has physical (delay in methane plume advection between measurement locations) and non-physical (DAQ latency, lag between separate DAQ computers) causes. To account for this, test system and reference time series are programmatically aligned using cross-correlation. This process is shown in Figure 4.21. In addition to cross-correlation alignment, the process of using windows of data also remedies lag seen between coherent structures.

At this point, test system and reference baseline characteristics are computed (mean and standard deviation) and used to build the threshold value described above. In most cases, a kernel of 100 points was taken from the front end of the data file to determine baseline characteristics for the test system and reference instrument. The detection threshold for

Developer C's system is defined as $x_{thresh} = \bar{X}_{BL} + 3 * \sigma_{BL}$. A noise multiplier of three is often considered an industry standard when determining minimum detection limits.

Baseline truncation is the last step prior to computing the agreement rate, shown in Figure 4.22. Baseline removal is done so that agreement during inactive periods does not skew the agreement rate upward. The files truncated according to the first and last times the reference measurement detected methane.

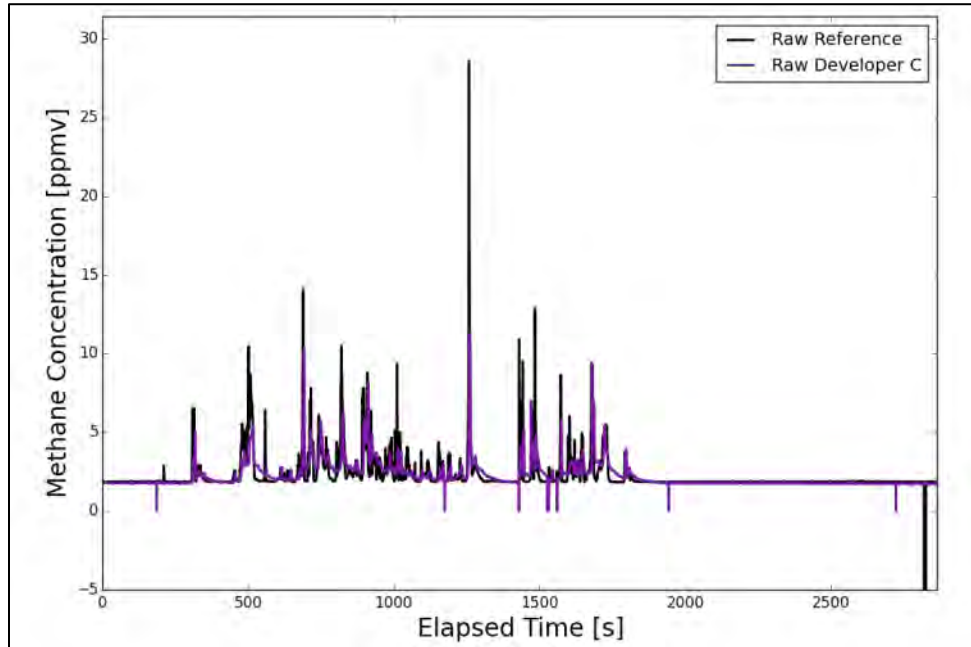


Figure 4.20. Raw signals from the Reference Instrument and Developer C's System

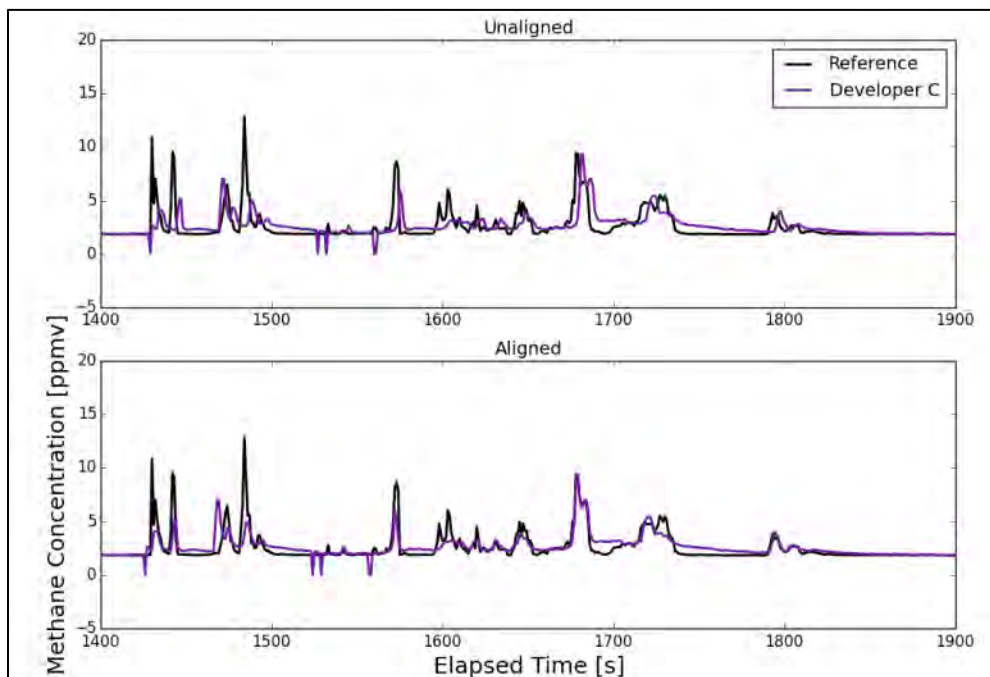


Figure 4.21. Illustration of the Time Alignment Process for Developer C's System

This process corrects for synchronization offset with the reference instrument.

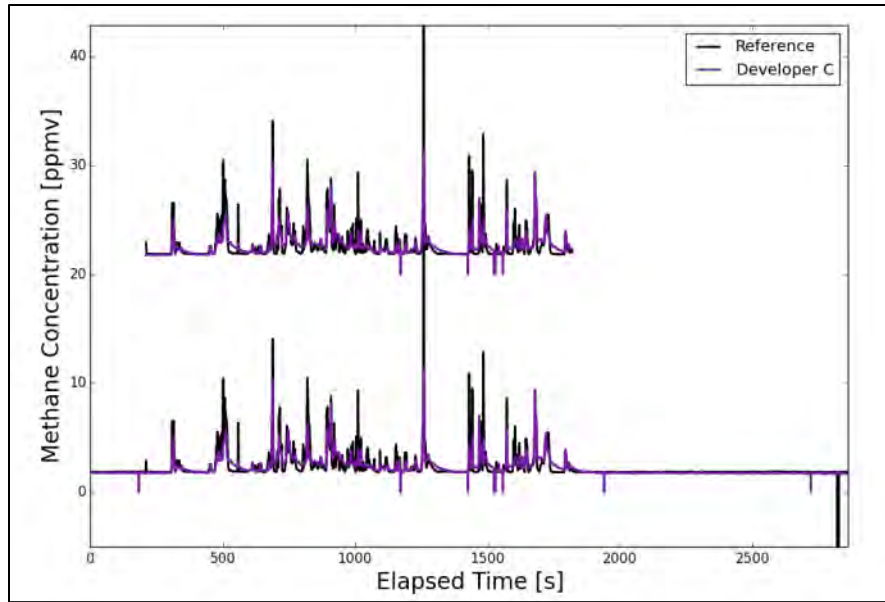


Figure 4.22. Illustration of the Truncation Process for Developer C’s System
 Long periods of background before or after leaks are removed in order to not skew data.

Figure 4.22 is a plot that highlights all of the windows in which Developer C’s system agreed with the reference measurement. Times of agreement are shaded green. This particular trial resulted in an overall agreement of 62.9% and a methane agreement rate of 100%. The signal from Developer C’s system shows strong coherence with the reference measurement with nearly all peaks/structures. Most areas of disagreement come during the brief moments between peaks when the test system measurement is decaying. This decay is characteristic of the circulation and residence time associated with the system design. The sensor is contained within an enclosure that ingests and expels sample gas using small blower fans.

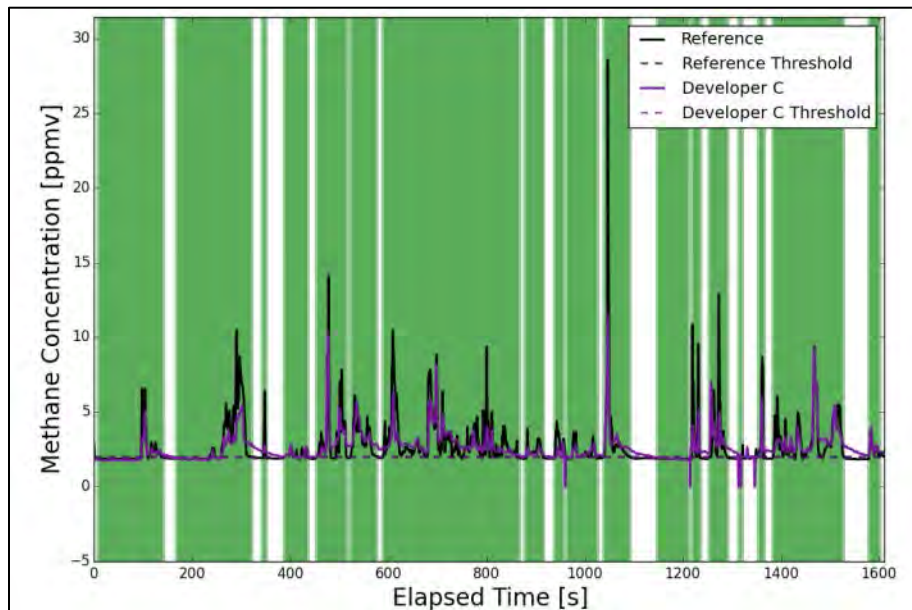


Figure 4.23. Plot Showing Agreement between Developer C’s System and the Reference Instrument

Green bars represent periods in which the developer system agreed with the reference instrument as to the state of the presence of methane.

Both overall agreement and methane agreement (defined in Section 4.2.3) between Developer C’s system and the reference instrument were calculated for all data points. The results are summarized in the following figures.

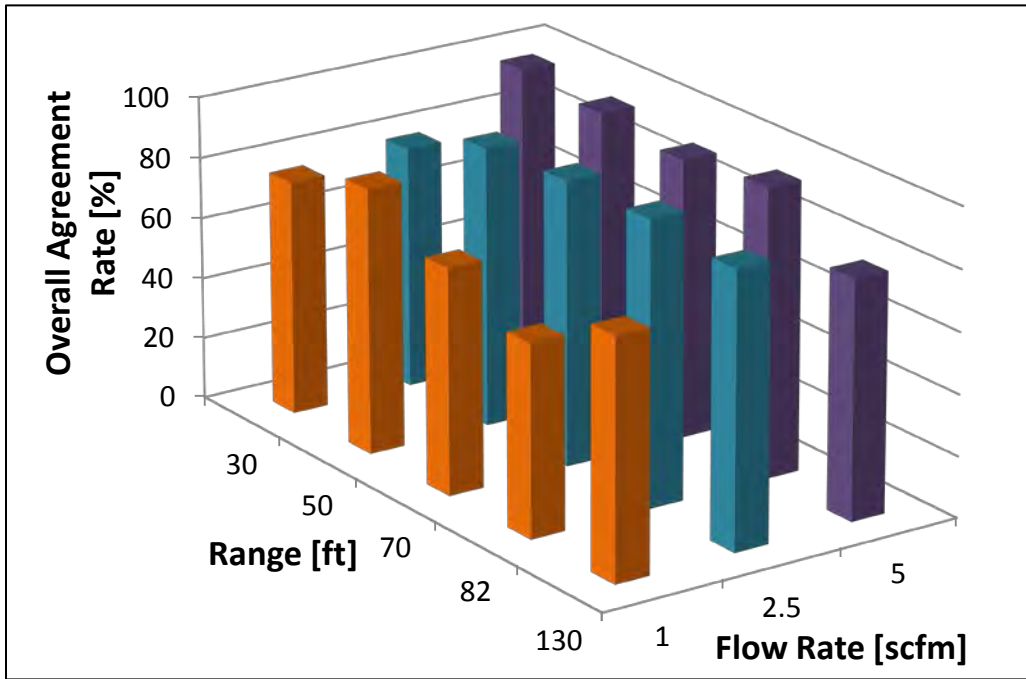


Figure 4.24. Agreement Rate Bar Chart for Developer C’s System

The chart shows the percentage of time that the developer system agreed with the reference instrument, regardless of state.

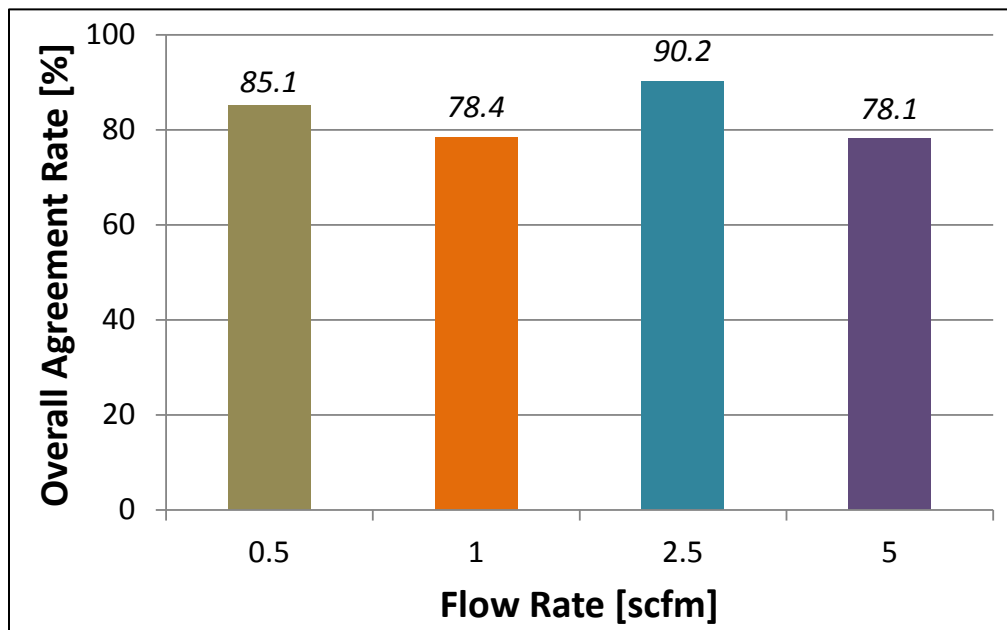


Figure 4.25. Agreement Rate Chart for 130-ft Point for Developer C’s System

Data at every point, other than 0.5 scfm, are included in a prior chart.

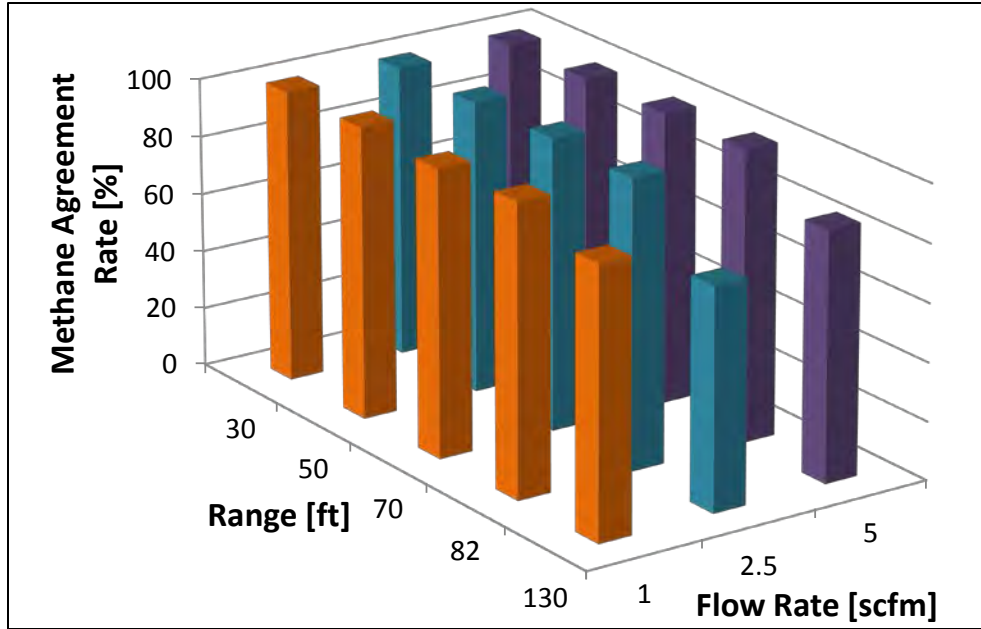


Figure 4.26. Methane Agreement Rate for Developer C's System

These percentages are the agreement rates only during periods in which the reference instrument measured methane concentrations in excess of background. This system positively detected all leaks.

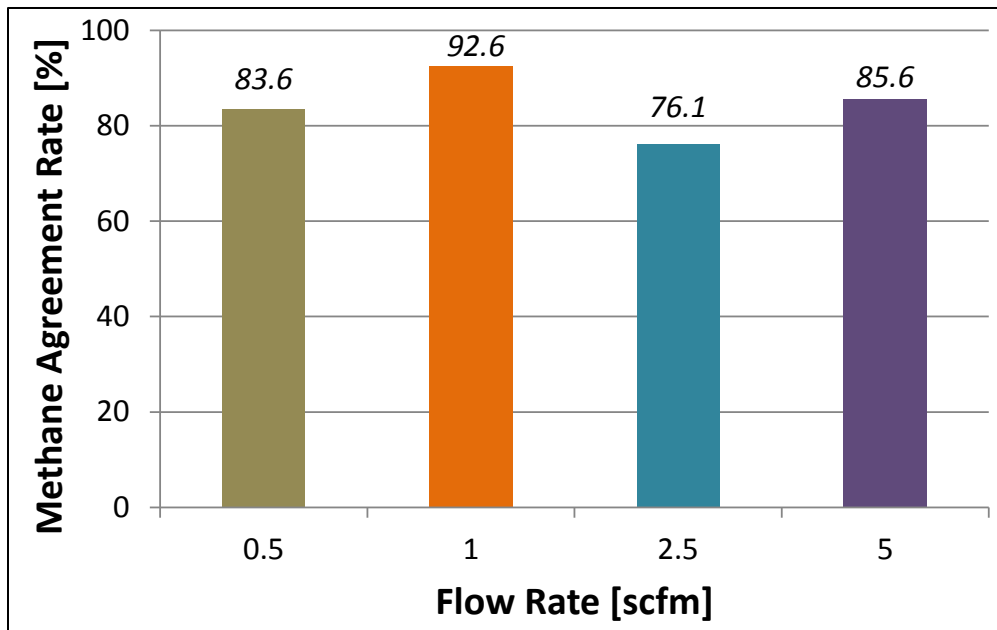


Figure 4.27. Methane Agreement Rate Chart for 130-ft Point for Developer C's System

Data at every point, other than 0.5 scfm, are included in a prior chart.

4.5 Developer D Results

The following details a sample agreement rate calculation performed with the data taken with System #1 from Developer D. This particular system was configured for a short, open-path measurement (path length = 2 m). Figure 4.28 shows the raw data (as collected) with the reference signal (Boreal Laser) shown in black and the signal from Developer D's system shown in red. This particular trial featured a 2.5-scfm leak from an 80-ft range for a duration of

20 minutes. The signal provided to SwRI by Developer D’s system was pre-processed. This pre-processing averaged (filtered) the raw signal and truncated the result to the nearest integer value. This means that this particular instance of Developer D’s technology does not provide any sub-ppm resolution.

A typical feature seen in all of the concentration series data is an evident time lag between test system and the reference instrument. In general, test system measurements and reference measurements showed a very strong coherence in which similar methane peaks or “structures” are seen in all measurements. This time lag has physical (delay in methane plume advection between measurement locations) and non-physical (DAQ latency, lag between separate DAQ computers) causes. To account for this, test system and reference time series are programmatically aligned using cross-correlation. This process is shown in Figure 4.29. In addition to cross-correlation alignment, the process of using windows of data also remedies lag seen between coherent structures.

At this point, test system and reference baseline characteristics are computed (mean and standard deviation) and used to build the threshold value described above. In most cases, a kernel of 100 points was taken from the front end of the data file to determine baseline characteristics for the test system and reference instrument. The detection threshold for Developer D’s system is defined as $x_{thresh} = \bar{X}_{BL} + 1$. The detection threshold for Developer D, System #1 is not based on noise levels like the other systems. As mentioned before, the pre-processing truncates the signal to integer values and does not feature any sub-ppm resolution. However, by comparing to the reference signal, it is evident that anytime the system registered above 1 ppmv, the system was experiencing elevated methane levels. A mean baseline signal of 0 ppmv to 1 ppmv was typical.

Baseline truncation is the last step prior to computing the agreement rate, shown in Figure 4.30. Baseline removal is done so that agreement during inactive periods does not skew the agreement rate upward. The files truncated according to the first and last times the reference measurement detected methane.

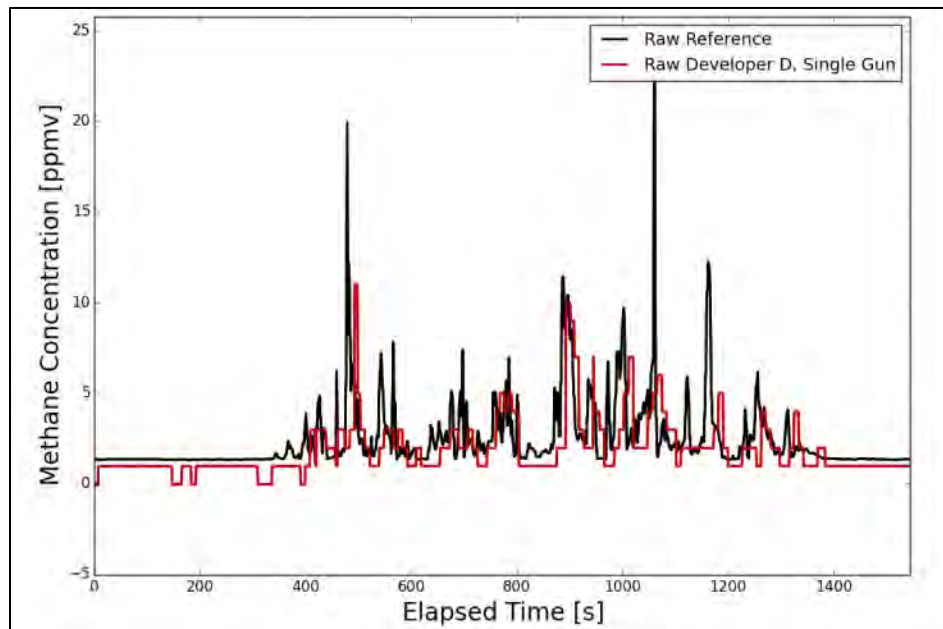


Figure 4.28. Raw data for Developer D (System #1) and the Reference Instrument

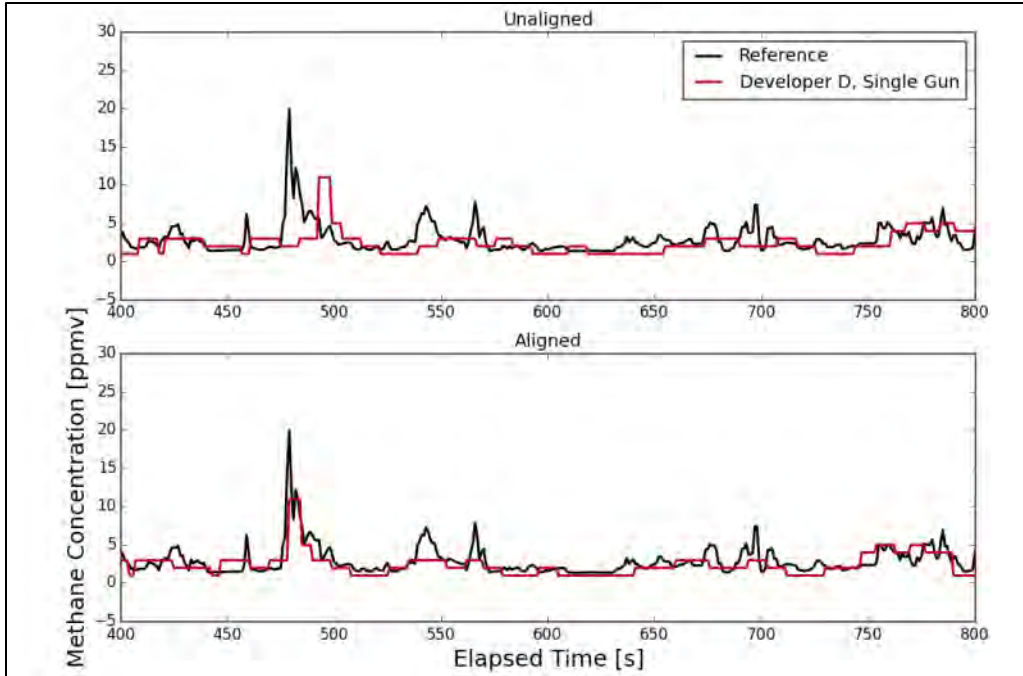


Figure 4.29. Illustration of the Time Alignment Process for Developer D's System
This process corrects for synchronization offset with the reference instrument.

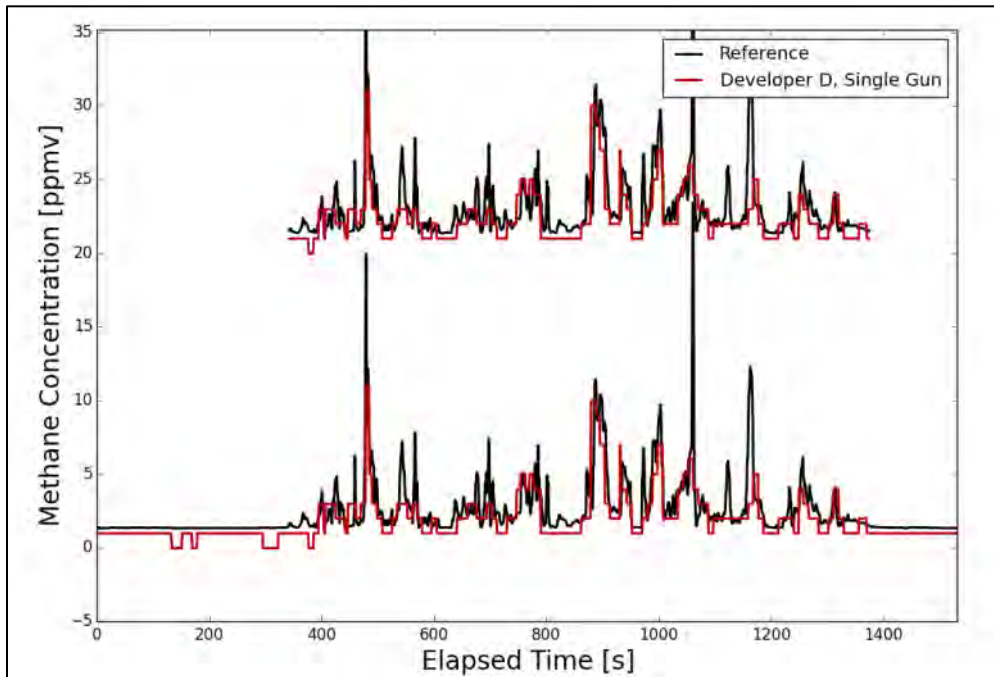


Figure 4.30. Illustration of the Baseline Truncation Process for Developer D's System
Long periods of background before or after leaks are removed in order to not skew data.

Figure 4.31 is a plot that highlights all of the windows in which Developer D's system agreed with the reference measurement. Times of agreement are shaded green. This particular trial resulted in an overall agreement of 66.8% and a methane agreement rate of 64.9%. The signal from Developer D's system shows strong coherence with the reference measurement with many of the large methane peaks, but cannot resolve the smaller ones.

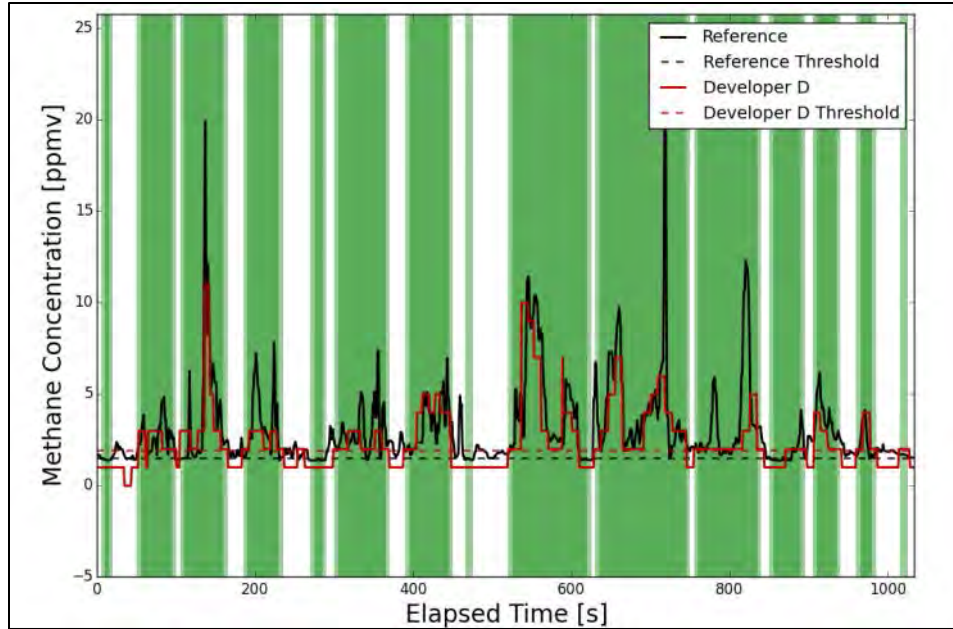


Figure 4.31. Plot Showing Agreement between Developer D's System and the Reference Instrument

Green bars represent periods in which the developer system agreed with the reference instrument as to the state of the presence of methane.

Both overall agreement and methane agreement (defined in Section 4.2.3) between Developer D's system and the reference instrument were calculated for all data points. The results are summarized in the following figures. Agreement rate results varied greatly from trial to trial, due to temperature sensitivity in Developer D's system (described in detail below). This sensitivity greatly decreased system sensitivity and was noticed in many trials conducted in the afternoon.

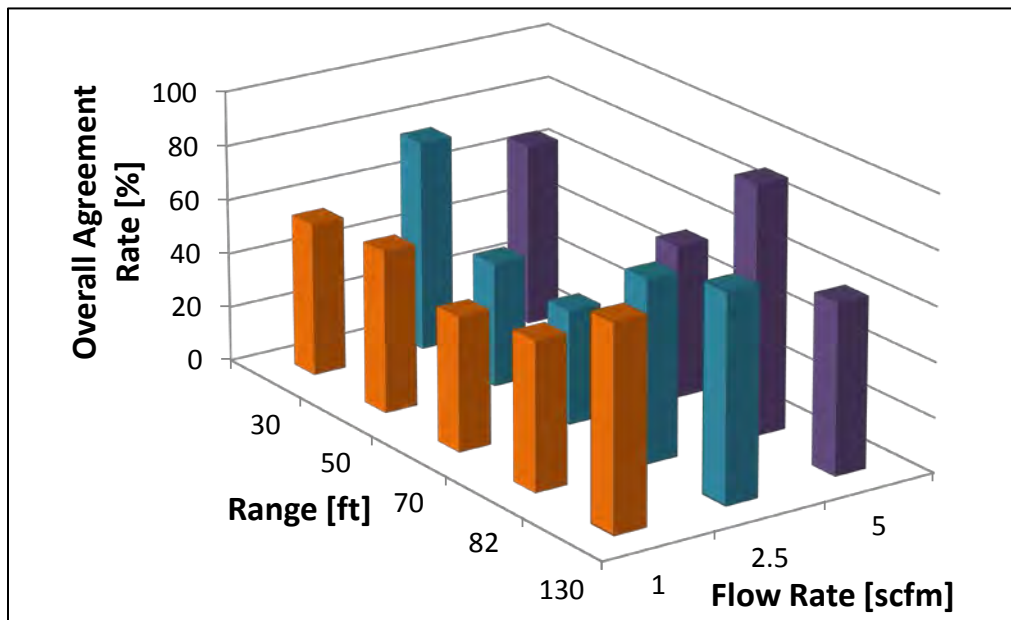


Figure 4.32. Agreement Rate Bar Chart for Developer D's System

The chart shows the percentage of time that the developer system agreed with the reference instrument, regardless of state.

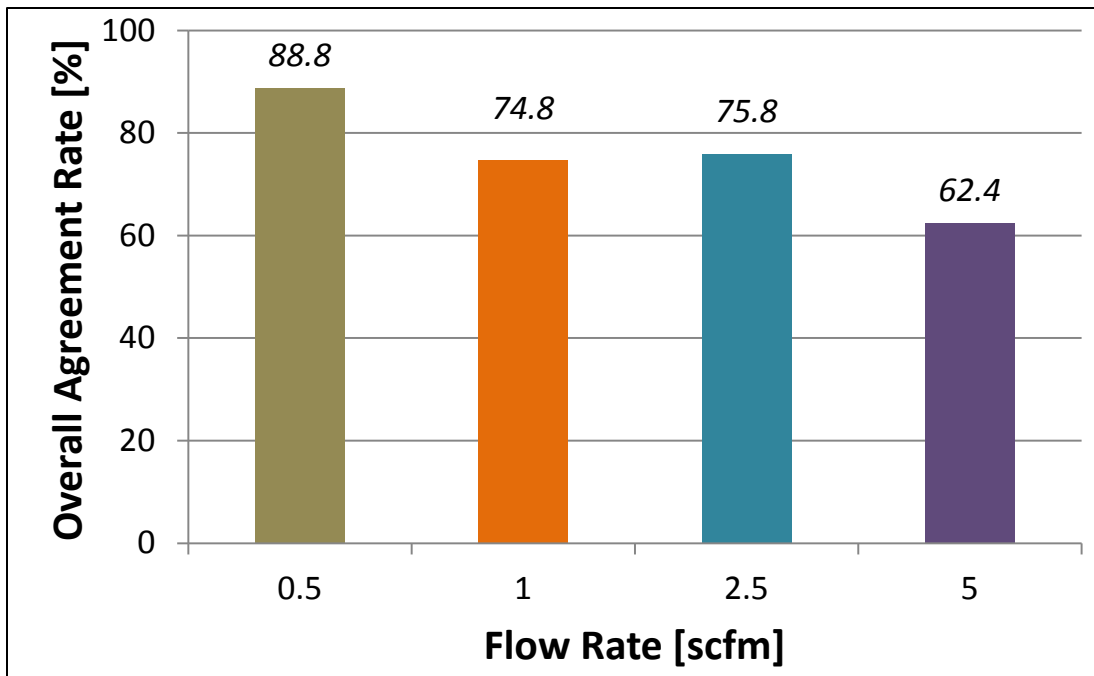


Figure 4.33. Agreement Rate Chart for 130-ft Point for Developer D's System
Data at every point, other than 0.5 scfm, are included in a prior chart.

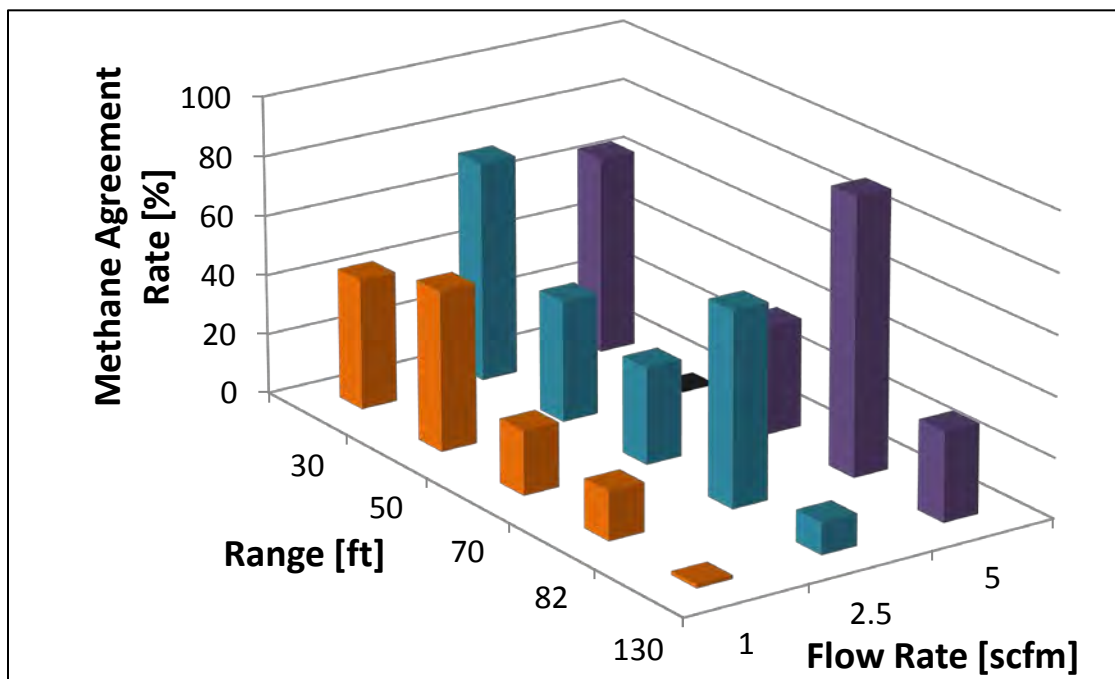


Figure 4.34. Methane Agreement Rate for Developer D's System
These percentages are the agreement rates only during periods in which the reference instrument measured methane concentrations in excess of background. The surfaces in black denote points for which the developer system was not online during testing and no data are available.

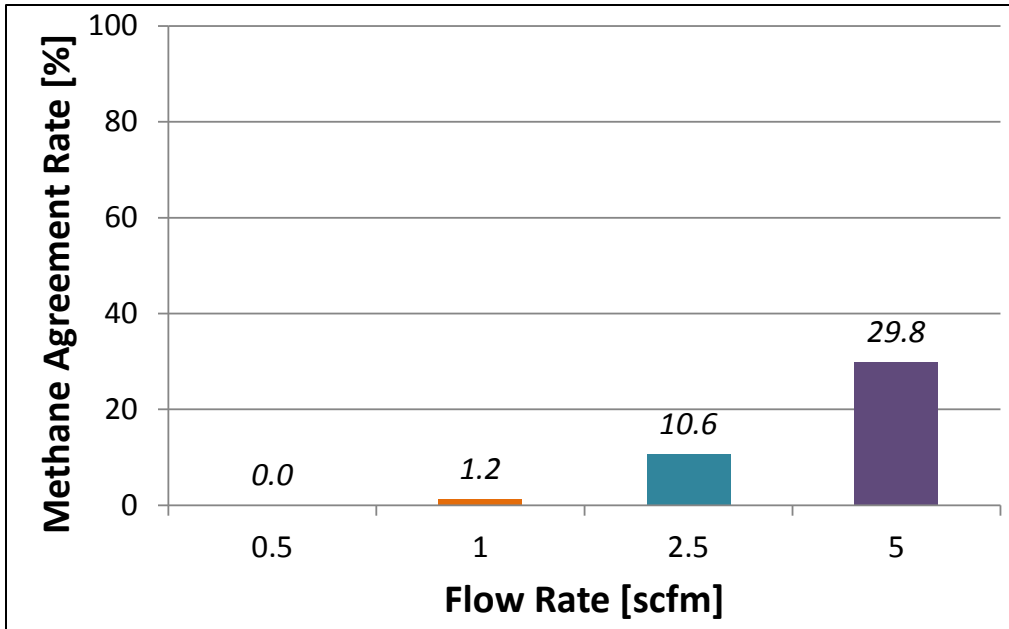


Figure 4.35. Methane Agreement Rate Chart for 130-ft Point for Developer D’s System
Data at every point, other than 0.5 scfm, are included in a prior chart. The system would not have detected a leak at the 0.5-scfm, 130-ft range.

The path length of Developer D’s system was configurable. The following plots show identical test points for two different path lengths. The plots show that Developer D’s system is more sensitive to elevated methane levels at shorter path lengths than at longer path lengths. However, even with decreased sensitivity, the system is capable of detecting leaks at longer path lengths.

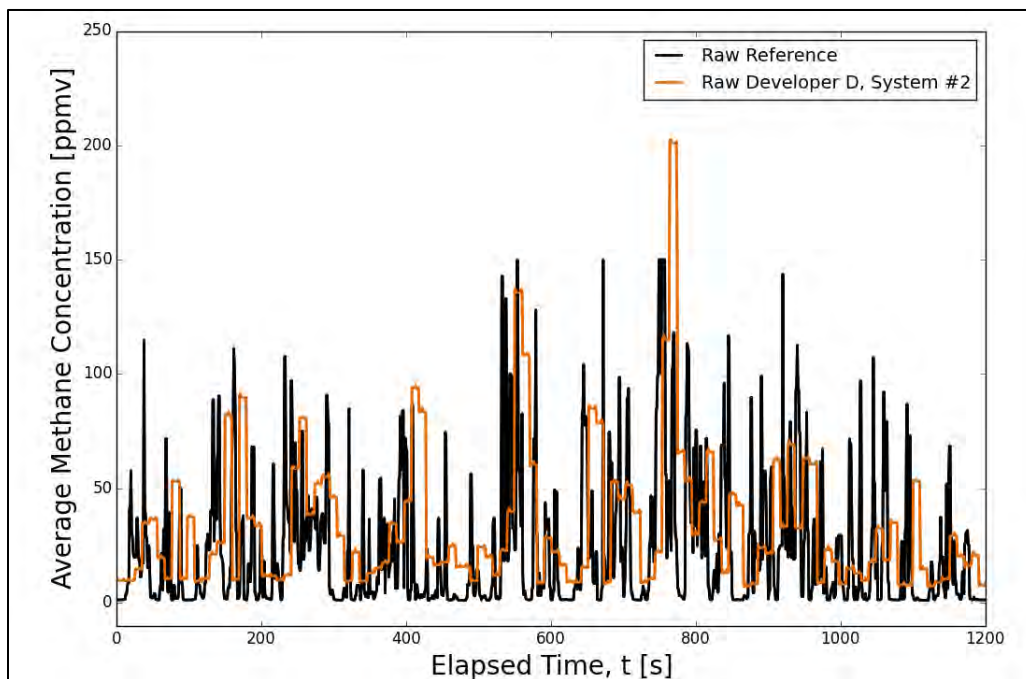


Figure 4.36. Data from Developer D’s System at 5-m Path Length for 5 scfm at a 40-ft Distance
Performance is favorable to that at the 1-m path length.

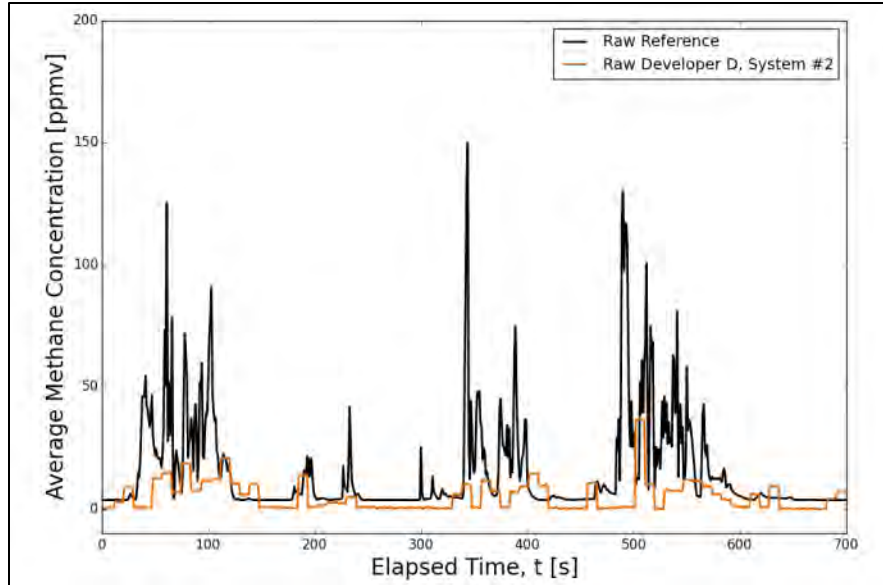


Figure 4.37. Data from Developer D’s System at 20-m Path Length for 5 scfm at a 40-ft Distance
While not as sensitive as the system at shorter path lengths, this configuration would also have resulted in positive detection of the leak.

4.5.1 Developer D Temperature Sensitivity

An important effect that was discovered during the outdoor testing was Developer D’s sensitivity to high temperatures. The following two plots (Figure 4.38 and Figure 4.39) illustrate this effect. Each of these concentration traces are from tests with the same release rate and range. However, the first trial was performed in the early morning and the second was performed in late afternoon. At the time of the outdoor testing, it was unknown if this loss in sensitivity was from a sensor/associated hardware deficiency or from an analog signal generator deficiency. This analog signal generator was used to supply the independent signal monitored by SwRI.

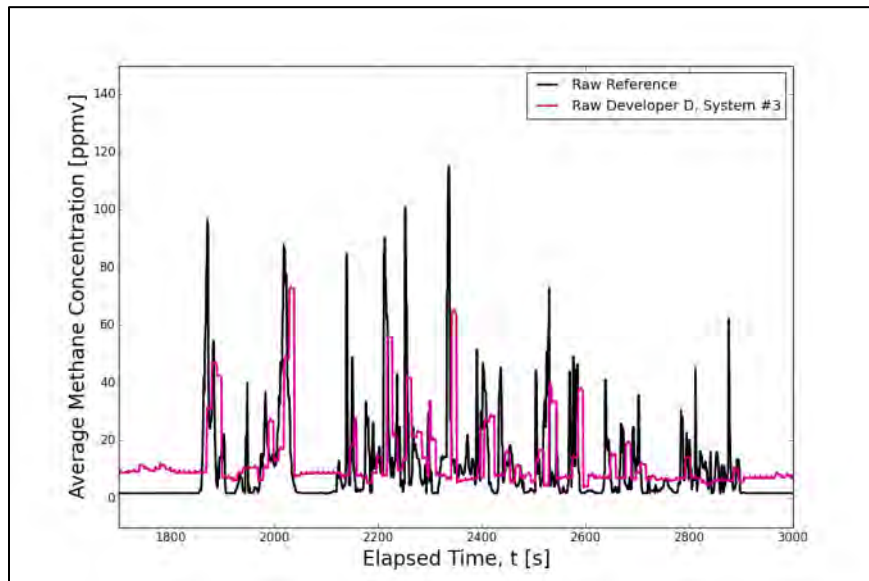


Figure 4.38. Early Morning Trial (Temperature around 80°F) of Develop D System
System demonstrated high sensitivity.

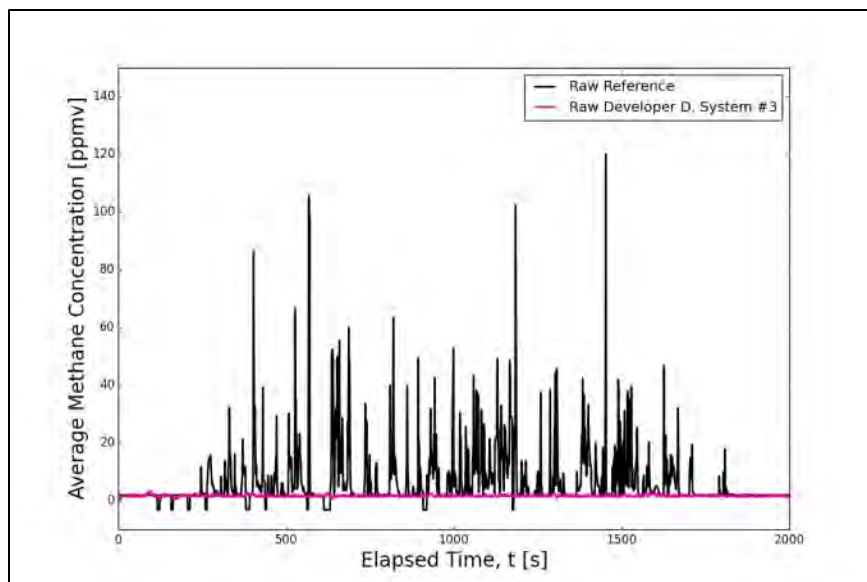


Figure 4.39. Identical Test Run to Previous Figure at Higher Temperatures (>100°F)
Developer D system stops producing valid reading at elevated temperatures.

Developer D’s sensitivity to high temperatures was also observed during outdoor testing at Location #2. Figure 4.40 shows ambient temperature and concentration data for Developer D’s systems over a period of 72 hours at Location #2. The sensitivity of Developer D’s systems to temperature is apparent in this figure, as the concentrations fluctuate with ambient temperature.

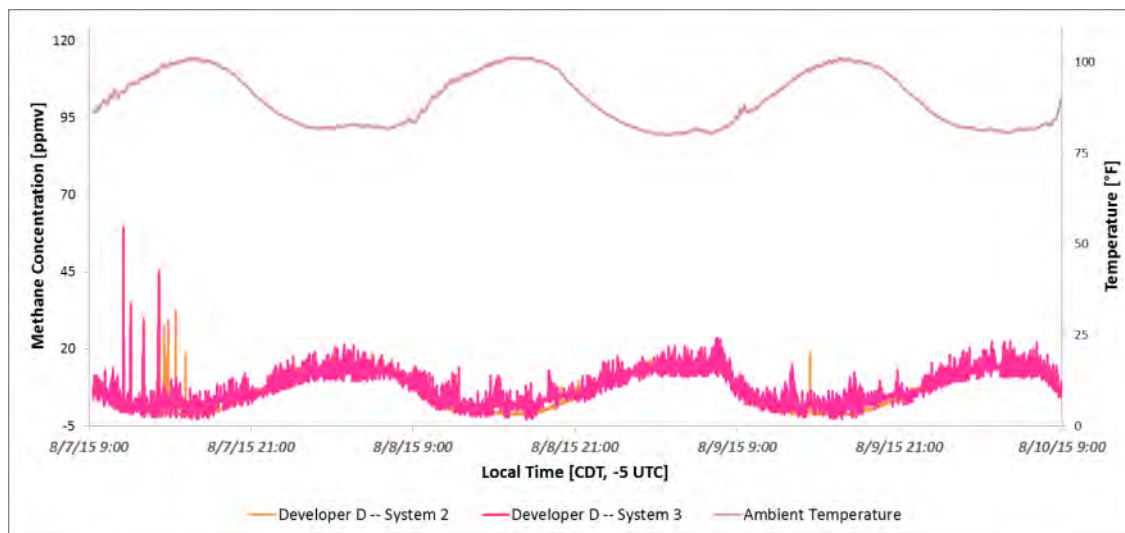


Figure 4.40. Developer D, Systems #2 and #3 Concentration Traces during the 72-Hour Trial
This plot helps to highlight the temperature sensitivity of Developer D’s technology. Drift in baseline correlates strongly with diurnal temperature change.

To address the observed sensitivity to temperature exhibited by Developer D’s systems, SwRI began troubleshooting during outdoor testing by shielding different portions of the system to prevent solar exposure. Applying a simple solar shield to the control boxes of Systems #1, #2, and #3 proved to be an effective solution to this sensitivity. Figure 4.41 represents a concentration trace that shows the signals from each of Developer D’s systems. Although the

time window is short, this graph and additional user experience demonstrate significantly improved performance after the shield was applied. System #2 and #3 traces have been vertically shifted to show the coherence between signals. Sensitivity, accuracy, and repeatability all improve with this shielding.

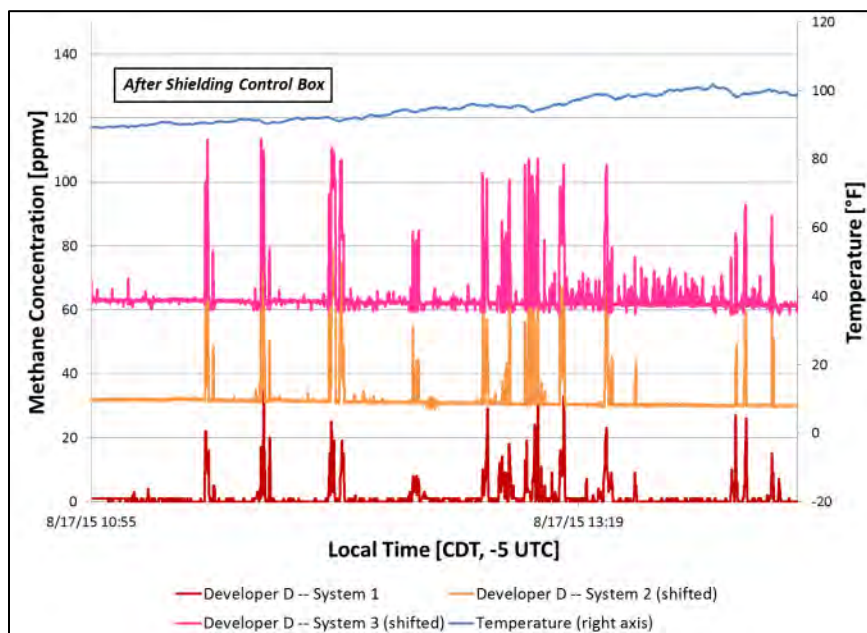


Figure 4.41. Concentration Traces from all Developer D Systems after Solar Shielding is Installed
Performance drastically improves after the installation of the shield.

After being informed by SwRI that its systems were observed to be sensitive to temperature, Developer D diagnosed the issue and fabricated a new system for comparison testing with the temperature sensitive systems. Upon receiving the new system from Developer D, SwRI performed concentration monitoring tests at ambient temperatures and elevated temperatures (120°F) with all of Developer D’s systems. The procedure and test setup for concentration monitoring testing is described in detail in Section 3.3. For this set of tests, a ThermoTron temperature conditioner was used to maintain the air-methane mixture in the testing chamber at 120°F for elevated temperature testing. Two tests were performed at both ambient and elevated temperatures. During the first test, the methane concentration in the chamber was increased in 2-ppmv increments to 12 ppmv with 10-minute holds at each concentration. During the second test, the methane concentration in the chamber was increased in 10-ppmv increments to 60 ppmv with 10-minute holds at each concentration.

The results of the testing for System #1 (original unit) and System #4 (modified unit) are shown in the following figures. The results from System #2 and System #3 are omitted, since they were nearly identical to those of System #1. The results show that Developer D was successful in addressing the temperature sensitivity of its systems. At ambient temperature, both versions of the system are sensitive to changes in methane concentration. At elevated temperatures, the original systems lose sensitivity, while the new system maintains its sensitivity to changes in methane concentration.

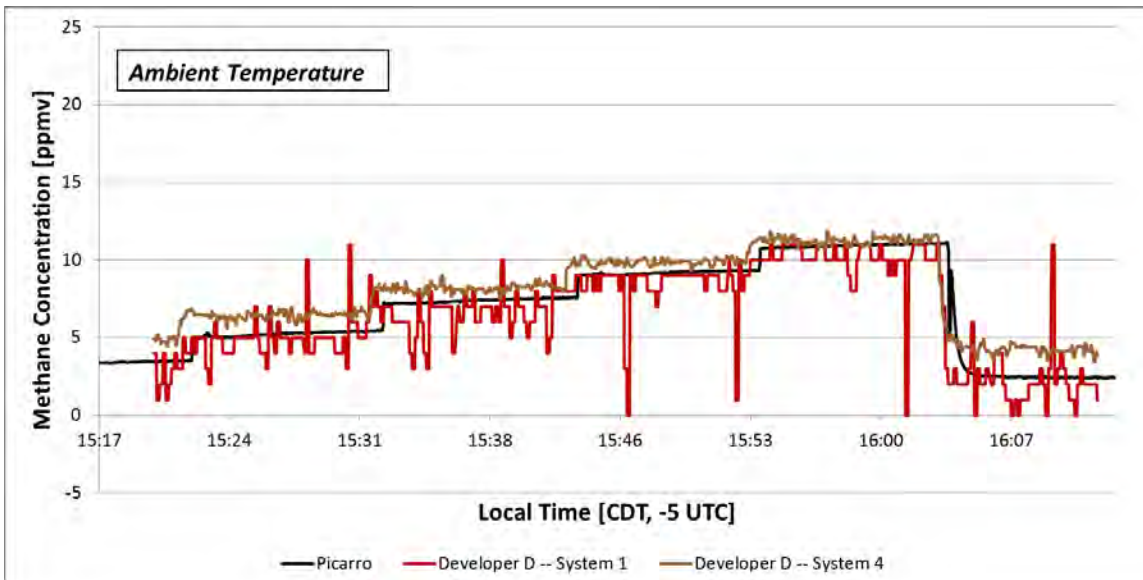


Figure 4.42. Results from the 2-ppmv Increment Methane Test for Developer D's Systems at Ambient Temperature
System #4 and System #1 are both sensitive to changes in methane concentration.

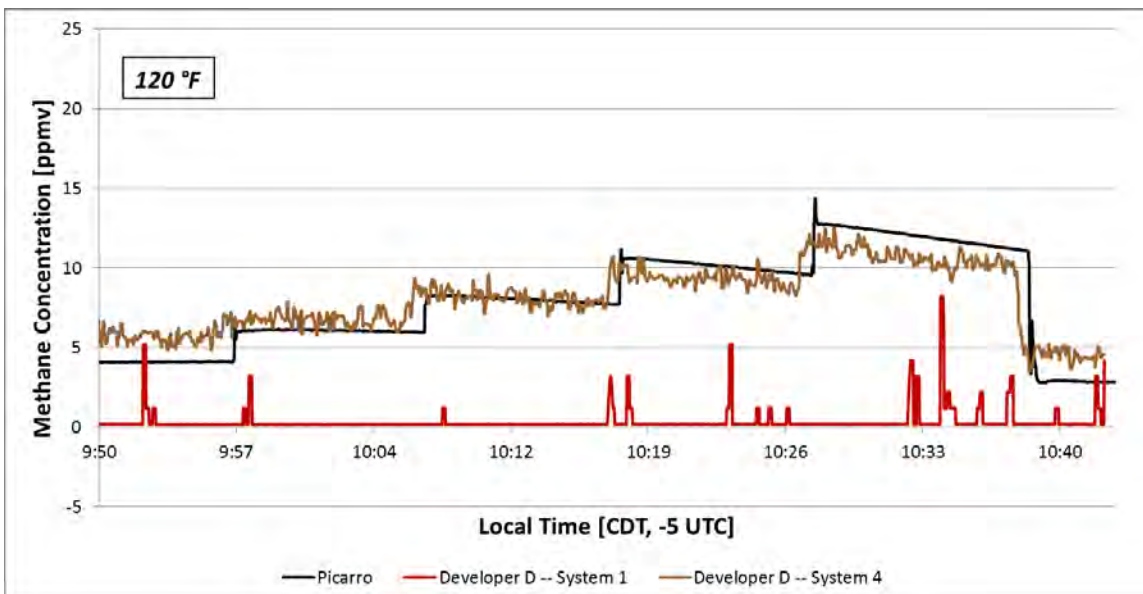


Figure 4.43. Results from the 2-ppmv Increment Methane Test for Developer D's Systems at Elevated Temperature
At elevated temperatures, System #4 (the newer, modified unit) was sensitive to changes in methane concentration.

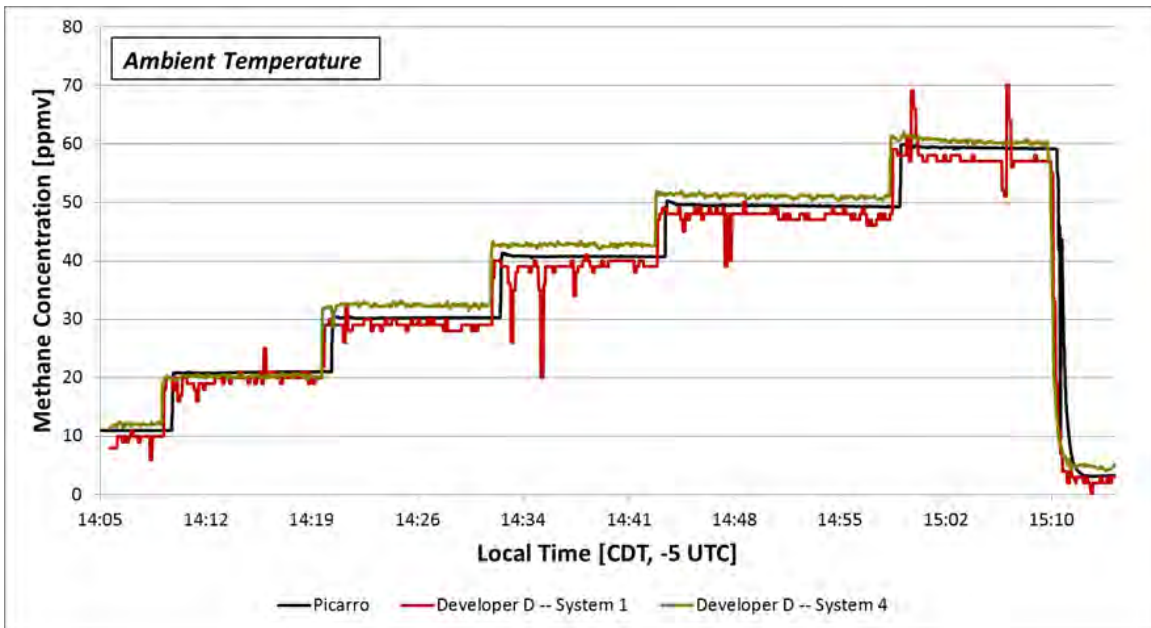


Figure 4.44. Results from the 10-ppmv Increment Methane Test for Developer D’s Systems at Ambient Temperature
System #4 and System #1 were both sensitive to changes in methane concentration.

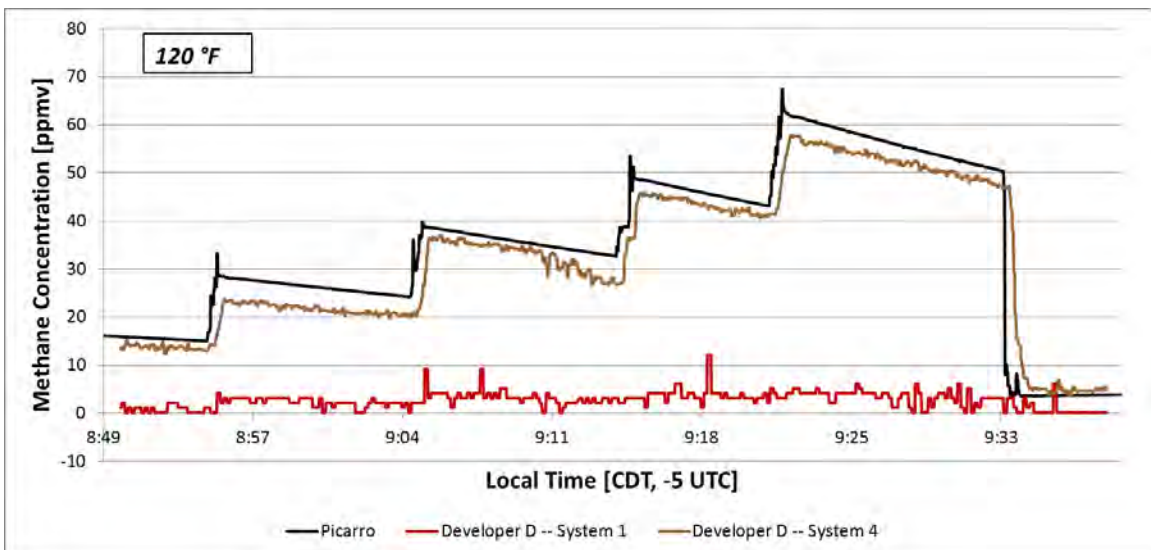


Figure 4.45. Results from the 2-ppmv increment Methane Test for Developer D’s Systems at Elevated Temperature
At elevated temperatures, System #4 was sensitive to changes in methane concentration..

4.6 Developer A Results

Analysis of Developer A’s controlled release data required a different treatment compared to other developers due to the low sampling rate (one sample/minute) and relatively small number of points for a given trial (typically less than 50 measurements total). Thus, the detection state of Developer A’s system at a given flow rate and range was treated as a binary value.

To determine the binary detection state, concentration measurements taken during methane exposure (excited state data) were compared against concentration measurements taken at baseline levels (baseline data). This comparison was made using a statistical tool known as Welch’s t-test. This type of test is useful in determining if two sets of small data are significantly different from one another. In this case, Welch’s t-test was used to see if the excited state measurements are greater than baseline measurements.

A test statistic, t , and the degrees of freedom, df , are computed and used with a t-distribution to determine a confidence that the excited state exceeds the baseline state. The statistic t is defined by the following:

$$t = \frac{\bar{X}_{ex} - \bar{X}_{BL}}{\sqrt{\frac{\sigma_{ex}^2}{N_{ex}} + \frac{\sigma_{BL}^2}{N_{BL}}}}$$

where \bar{X} represents the sample mean, σ^2 represents sample variance, and N represents the sample size. The subscripts “ex” and “BL” indicate excited and baseline measurements, respectively. The degrees of freedom, df , are estimated using the following:

$$df \approx \frac{\left(\frac{\sigma_{ex}^2}{N_{ex}} + \frac{\sigma_{BL}^2}{N_{BL}}\right)^2}{\frac{\sigma_{ex}^4}{N_{ex}^2 * df_{ex}} + \frac{\sigma_{BL}^4}{N_{BL}^2 * df_{BL}}}$$

where $df_{BL} = N_{BL} - 1$ and $df_{ex} = N_{ex} - 1$. Using the computed values of t and df , a confidence level that the test system detected methane during the excitation period can be determined. Figure 4.46 and Figure 4.47 provide examples of this arrangement. The subsequent tables provide results for various confidence intervals.

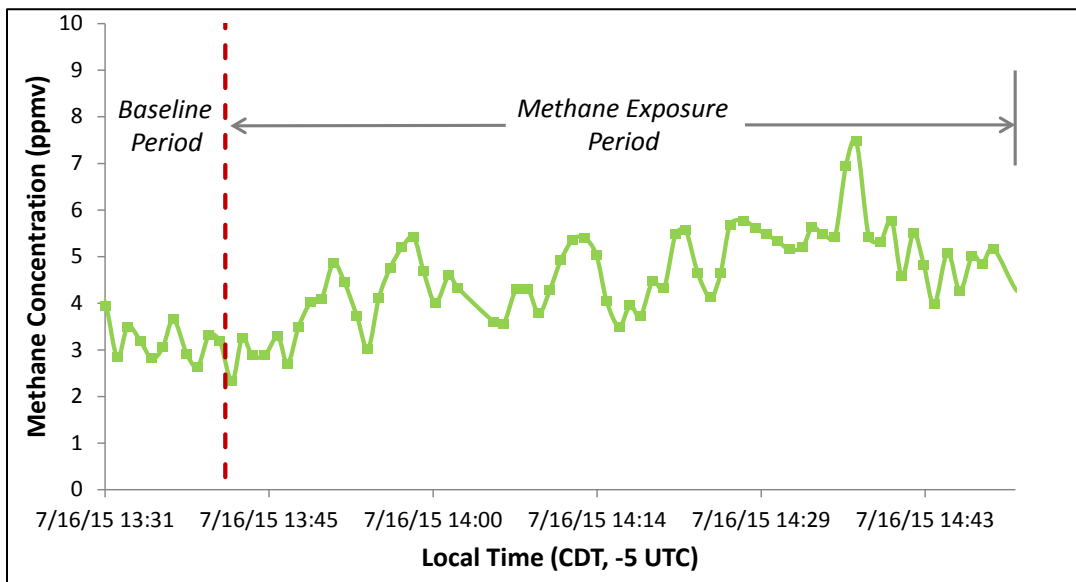


Figure 4.46. Example Data from 1 scfm at 130 ft
The red line denotes demarcation between the background level and elevated exposure.

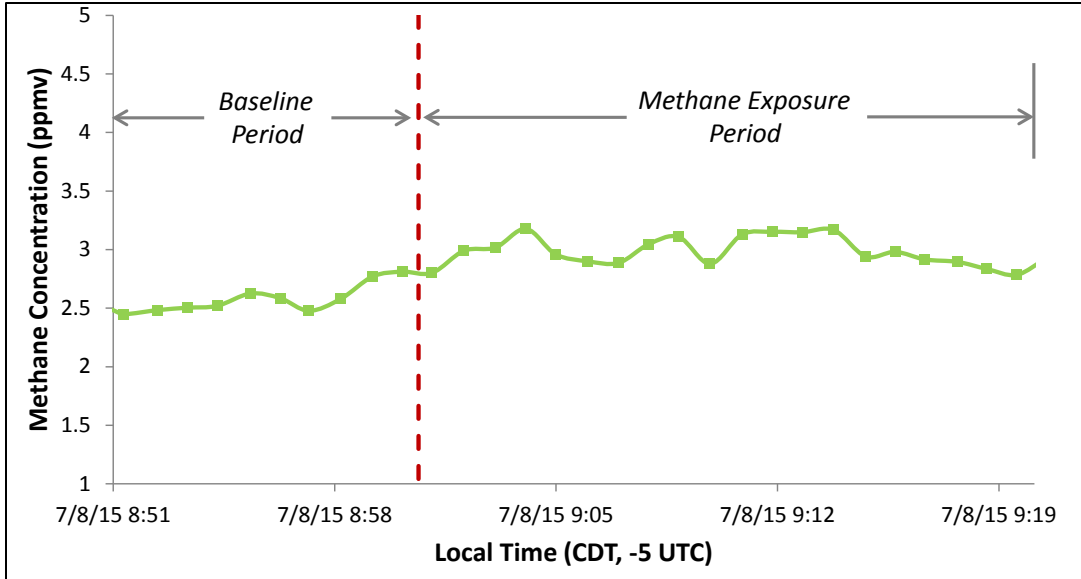


Figure 4.47. Example Data from 2.5 scfm at 82 ft
 The red line denotes demarcation between the background level and elevated exposure.

Table 4.8. Detection Rate Using 99.9% Confidence Interval
 Green cells represent positive detection and red cells equate to a missed leak.

		Leak Rate [scfm]			
		0.5	1	2.5	5
Range [ft]	30	N/A	Red	Green	Green
	50	N/A	Green	Red	Green
	70	N/A	Red	Green	Green
	82	N/A	Red	Green	Green
	130	Red	Green	Red	Red

Table 4.9. Detection Rate Using 95% Confidence Interval
 Green cells represent positive detection and red cells equate to a missed leak.

		Leak Rate [scfm]			
		0.5	1	2.5	5
Range [ft]	30	N/A	Green	Green	Green
	50	N/A	Green	Red	Green
	70	N/A	Green	Green	Green
	82	N/A	Red	Green	Green
	130	Red	Green	Red	Red

Table 4.10. Detection Rate Using 90% Confidence Interval
 Green cells represent positive detection and red cells equate to a missed leak.

		Leak Rate [scfm]			
		0.5	1	2.5	5
Range [ft]	30	N/A	Green	Green	Green
	50	N/A	Green	Green	Green
	70	N/A	Green	Green	Green
	82	N/A	Green	Green	Green
	130	Red	Green	Red	Red

Table 4.11. Detection Rate Using the Detection Limit of Three Standard Deviations
Green cells represent positive detection and red cells equate to a missed leak.

		Leak Rate [scfm]			
		0.5	1	2.5	5
Range [ft]	30	N/A			
	50	N/A			
	70	N/A			
	82	N/A			
	130				

4.7 System Robustness

Each of the four technologies needed some manner of servicing or repair during the course of this project. The following four tables provide an overview of the actions taken for each system during the course of the project.

Table 4.12. Developer A Event Log

This table shows any required servicing of the system during testing.

Date	Event
6/30/15	System #3 was no longer communicating wirelessly or through its analog output. SwRI swapped the antennae in System #2 and System #3. System #3 was still not communicating. The developer decided to ship a new system to replace System #3.
7/27/15	The replacement system (System #4) was received. System #4 was swapped for System #5.
8/3/15	The system was updated remotely and configured to communicate with System #4 by the developer.

Table 4.13. Developer B Event Log

This table shows any required servicing of the system during testing.

Date	Event
6/15/15	Severe drift in baseline concentration measurement of System #1 was observed. System #1 was not responding to elevated methane levels. Severe drift in baseline concentration measurement of System #2 was observed.
6/26/15	Based on recommendations from the developer, SwRI made changes to the system software. The change did not fix the issues with either system.
7/13/15	System #2 was not responding to elevated methane levels. At this point, both systems were unresponsive.
7/15/15	Based on recommendations from the developer, SwRI investigated and reconnected loose hoses in both systems. Both systems began responding to elevated methane levels again. However, both systems still had severe drift in their baseline concentrations.

Table 4.14. Developer C Event Log

This table shows any required servicing of the system during testing.

Date	Event
6/4/15	The system powered off unexpectedly and would not power back on. The system was shipped back to the developer for diagnosis.
6/5/15	The problem was identified as a defective power converter. The developer conferred with the manufacturer of the defective part (part of a defective batch), and a replacement part was selected.
6/16/15	The repaired system was shipped back to SwRI.
6/22/15	The repaired system was received by SwRI. Based on incorrect background concentration measurements, the developer determined that the laser was out of alignment.
6/25/15	A representative from the developer was on site at SwRI to perform alignment of the laser.
6/26/15	The system was successfully repaired and tested.
8/11/15	The system lost its connection to the wireless modem. In order to re-establish the connection, SwRI had to cycle the system power.

Table 4.15. Developer D Event Log

This table shows any required servicing of the system during testing.

Date	Event
6/5/15	A representative from the developer came to SwRI to set up System #2 and System #3.
6/15/15	SwRI made adjustments to System #2 (made a larger reflector and adjusted the gain settings) based on recommendations from the developer.
8/25/15	SwRI received a new system (System #4) with modifications to improve performance at elevated temperature.

5. CONCLUSIONS

The primary application for technology as part of the MDC is the binary leak or no leak status akin to a “smoke alarm” for methane. While the ability to accurately quantify the methane concentration allows for a system to be more robust, it is not a requirement of this program. A starting place in evaluating the overall ability of each system to detect leaks is to revisit the detection tables in Section 4.2.2. These four tables are shown following this paragraph. Developer C’s system was able to detect all leaks, while the other developers were able to detect each leak at distances up to 82 ft. While each of the sensors has the ability to detect these leaks, Developer A and Developer B have less consistent data and more point-to-point variability than Developer C and Developer D. Both Developer A and Developer B require some manner of manual processing in order to determine the leak state. The data from Developer A were more inconsistent than others, hence the reason for detecting a 1-scfm leak at 130 ft, but missing larger leaks. It is important to recognize that during periods in which there were no leaks, there were no measurements from the systems that would indicate a false positive.

Table 5.1. Leak Detection Capability Demonstrated for Tests for 5-scfm Leaks

Some systems were not operational for some tests, hence the “unknown” designation for some points.

		Developer			
		A	B	C	D
Range [ft]	30	Yes	Yes	Yes	Yes
	50	Yes	Yes	Yes	Unknown
	70	Yes	Yes	Yes	Yes
	82	Yes	Yes	Yes	Yes
	130	No	Yes	Yes	Yes

Table 5.2. Leak Detection Capability Demonstrated for Tests for 2.5-scfm Leaks

Some systems were not operational for some tests, hence the “unknown” designation for some points.

		Developer			
		A	B	C	D
Range [ft]	30	Yes	Yes	Yes	Yes
	50	Yes	Yes	Yes	Yes
	70	Yes	Yes	Yes	Yes
	82	Yes	Yes	Yes	Yes
	130	No	Unknown	Yes	Yes

Table 5.3. Leak Detection Capability Demonstrated for Tests for 1-scfm Leaks

Some systems were not operational for some tests, hence the “unknown” designation for some points.

		Developer			
		A	B	C	D
Range [ft]	30	Yes	Yes	Yes	Yes
	50	Yes	Unknown	Yes	Yes
	70	Yes	Yes	Yes	Yes
	82	Yes	Yes	Yes	Yes
	130	Yes	Yes	Yes	No

Table 5.4. Leak Detection Capability Demonstrated for Tests for 0.5-scfm Leaks

This leak rate was only tested at a distance of 130 ft.

		Developer			
		A	B	C	D
Range [ft]	130	No	No	Yes	No

In reviewing the performance of the various systems, a baseline can be made by comparing the performance of each technology relative to the Phase 2 requirements outlined in the original MDC RFP. Table 5.5 summarizes how each technology performed relative to the requirements of the RFP. It is important to note that “leak detection capability” is interpreted as meaning “capable of detecting such a leak.” While some of the technology developers had a simplified alarm threshold, none of the companies had initiated full alarm algorithms at the time of the Phase 2 testing.

Table 5.5. Comparison of System Performance for Various Parameters Defined in RFP

The majority of the requirements were met by all developers.

Specification	RFP Requirement	Dev A	Dev B	Dev C	Dev D
		Was Requirement Met?			
Detection limit	5 ppm	Yes	Yes	Yes	Yes
Detection range	5 ppm – 250 ppm	Yes	Yes	Yes	Yes
Leak detection capability	5 scfm	Yes	Yes	Yes	Yes
Ability to measure methane	Binary (yes/no)	Yes	Yes	Yes	Yes
Ability to isolate on-site methane from off-site	Binary (yes/no)	Unknown ^a	Unknown ^a	Unknown ^a	Unknown ^a
Power requirements	Single solar panel with rechargeable battery	Yes	No	Yes	Yes
Protected from weather	Binary (yes/no)	Yes	Yes	Yes	Yes
Temperature range	-20°F-120°F	Yes	Yes	Yes	Yes
Humidity	0-100% relative humidity	Yes	Yes	Yes	Yes
Unaffected by poisons	Binary (yes/no)	No ^b	No ^c	Yes	Yes

^aWhile most developers had anemometers, none fully leveraged such information to determine the source of gas.

^bPerformance impacted by the presence of various contaminants.

^cPerformance impacted by the presence of ethane.

Two RFP requirements for the pilot phase that are currently not met by any of the systems are:

- Certification for use in a hazardous gas environment (e.g., Class 1, Division 1 or 2).
- Ability to estimate the leak size.

As noted earlier in this report, the primary objective of the Phase 2 testing was to determine if the systems were at the technology readiness level suitable for deployment in a pilot trial at an operational gas facility, such as a well pad or compressor station, and, if not, what steps could be taken to bring them to the appropriate level of readiness. Table 5.6 provides remaining gaps that may need to be closed prior to each technology being deployed for a pilot trial. It will be up to each individual operating company to determine which gaps shall be closed prior to the trial.

Table 5.6. Gaps for Each Developer’s System

It will be up to each pilot sponsor to determine which gaps need to be closed prior to pilot testing. Developer C’s and Developer D’s systems would not require further laboratory confirmation prior to deployment in the field.

Technology Developer	Remaining Gaps
Developer A	Does not have a robust algorithm for automated leak detection. Does not have a Class 1, Division 1 or 2 certification. Ensure the robustness of the systems over extended operation. Determine a means of detecting methane in the presence of contaminants.
Developer B	Does not have a robust algorithm for automated leak detection. Does not have a Class 1, Division 1 or 2 certification. Stabilize the drifting/offsetting signals. Integrate a solar panel into the assemblies. Ensure robustness of hardware over extended operation.
Developer C	Does not have a robust algorithm for automated leak detection. Does not have a Class 1, Division 1 or 2 certification.
Developer D	Does not have a robust algorithm for automated leak detection. Does not have a Class 1, Division 1 or 2 certification. Consider modifying resolution to <1 ppm.

APPENDIX A

OUTDOOR TESTING GRAPHS – DEVELOPER A

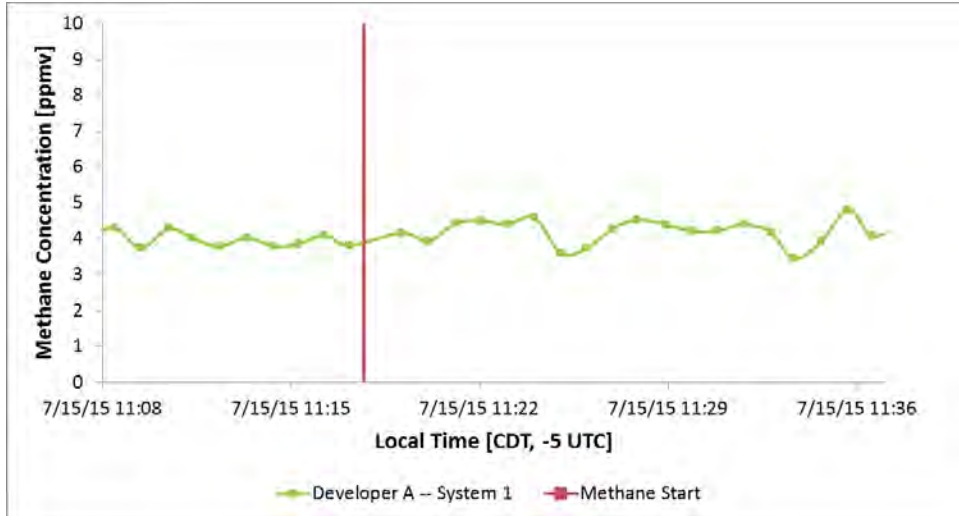


Figure A.1. Developer A Data Trace for a 1-scfm Leak from 30 ft of Distance



Figure A.2. Developer A Data Trace for a 1-scfm Leak from 50 ft of Distance



Figure A.3. Developer A Data Trace for a 1-scfm Leak from 70 ft of Distance

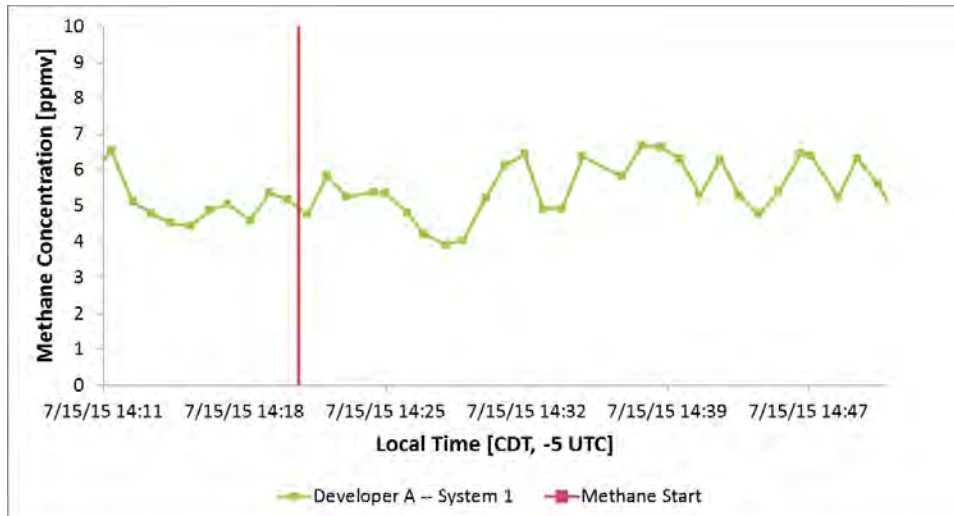


Figure A.4. Developer A Data Trace for a 1-scfm Leak from 82 ft of Distance

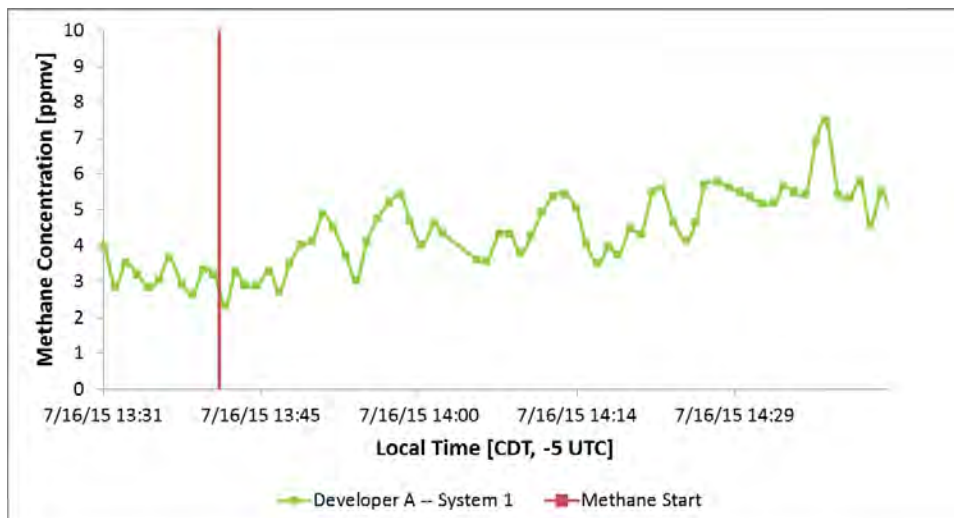


Figure A.5. Developer A Data Trace for a 1-scfm Leak from 130 ft of Distance



Figure A.6. Developer A Data Trace for a 2.5-scfm Leak from 30 ft of Distance



Figure A.7. Developer A Data Trace for a 2.5-scfm Leak from 50 ft of Distance

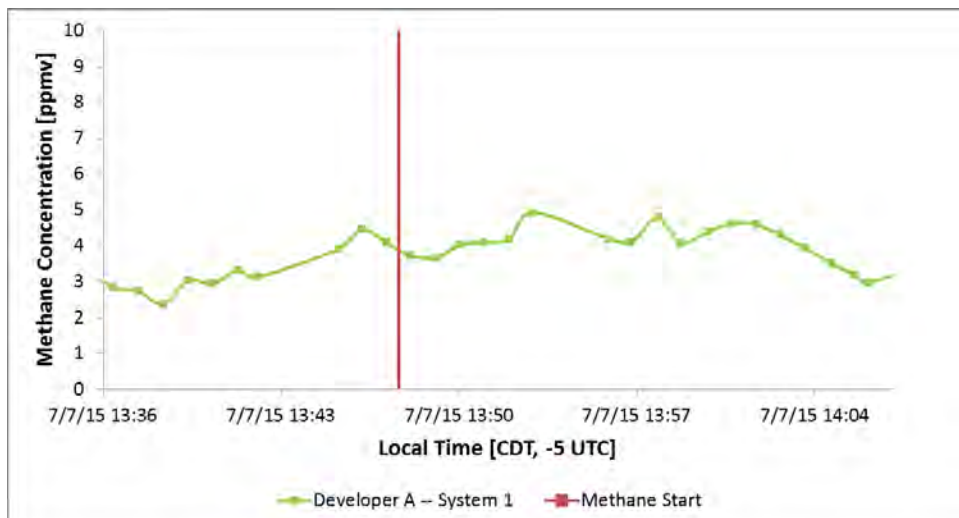


Figure A.8. Developer A Data Trace for a 2.5-scfm Leak from 70 ft of Distance



Figure A.9. Developer A Data Trace for a 2.5-scfm Leak from 82 ft of Distance

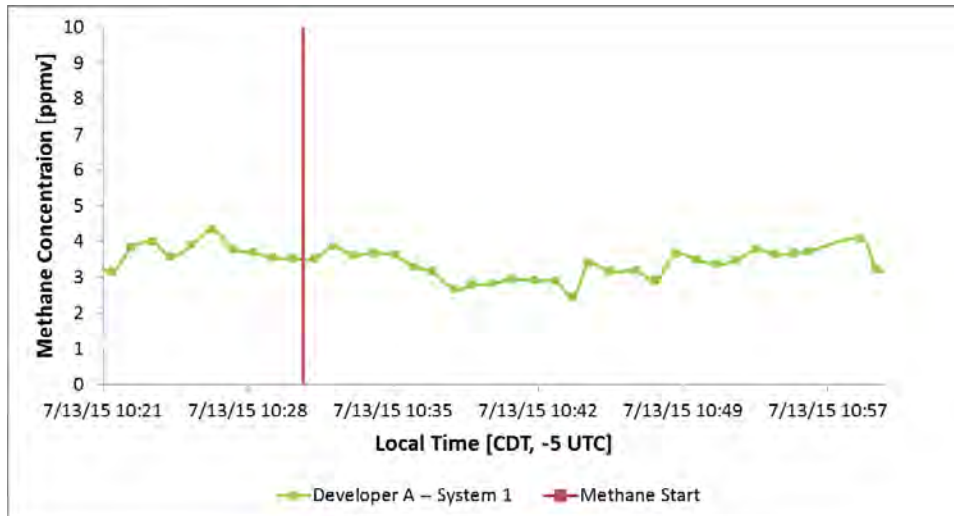


Figure A.10. Developer A Data Trace for a 2.5-scfm Leak from 130 ft of Distance



Figure A.11. Developer A Data Trace for a 5-scfm Leak from 30 ft of Distance



Figure A.12. Developer A Data Trace for a 5-scfm Leak from 50 ft of Distance

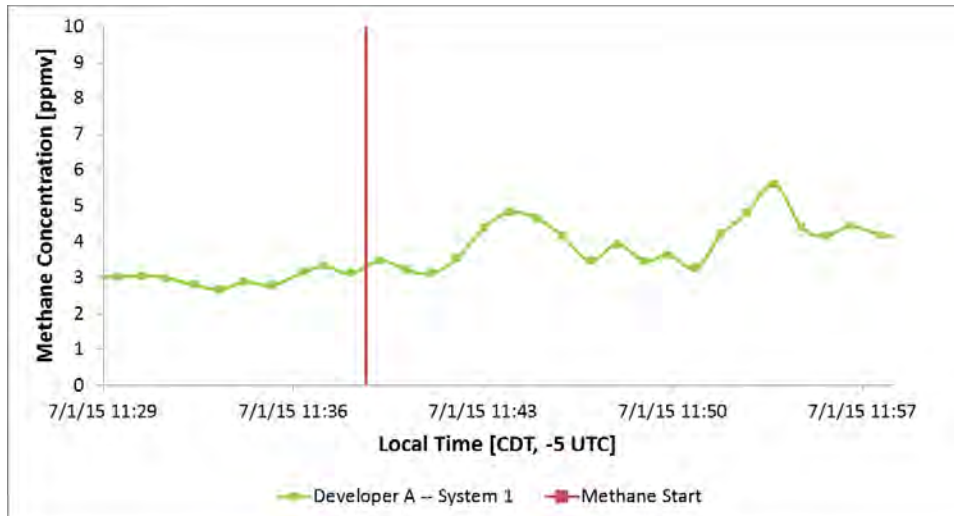


Figure A.13. Developer A Data Trace for a 5-scfm Leak from 70 ft of Distance



Figure A.14. Developer A Data Trace for a 5-scfm Leak from 82 ft of Distance

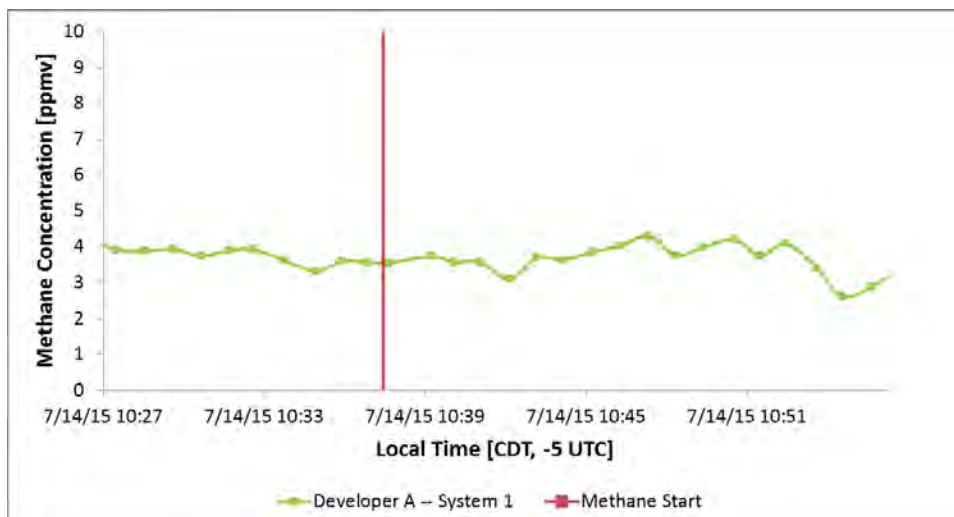


Figure A.15. Developer A Data Trace for a 5-scfm Leak from 130 ft of Distance

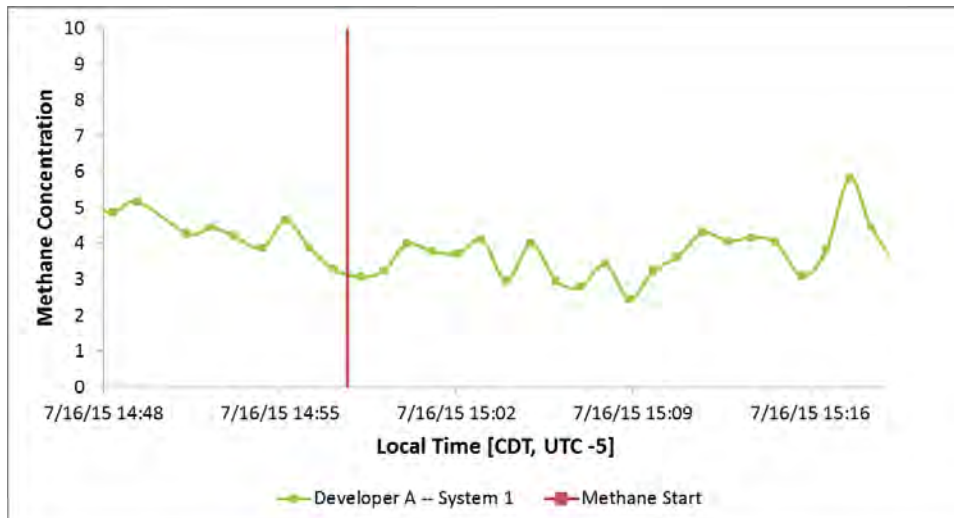


Figure A16. Developer A Data Trace for a 0.5-scfm Leak from 130 ft of Distance

APPENDIX B

OUTDOOR TESTING GRAPHS – DEVELOPER B

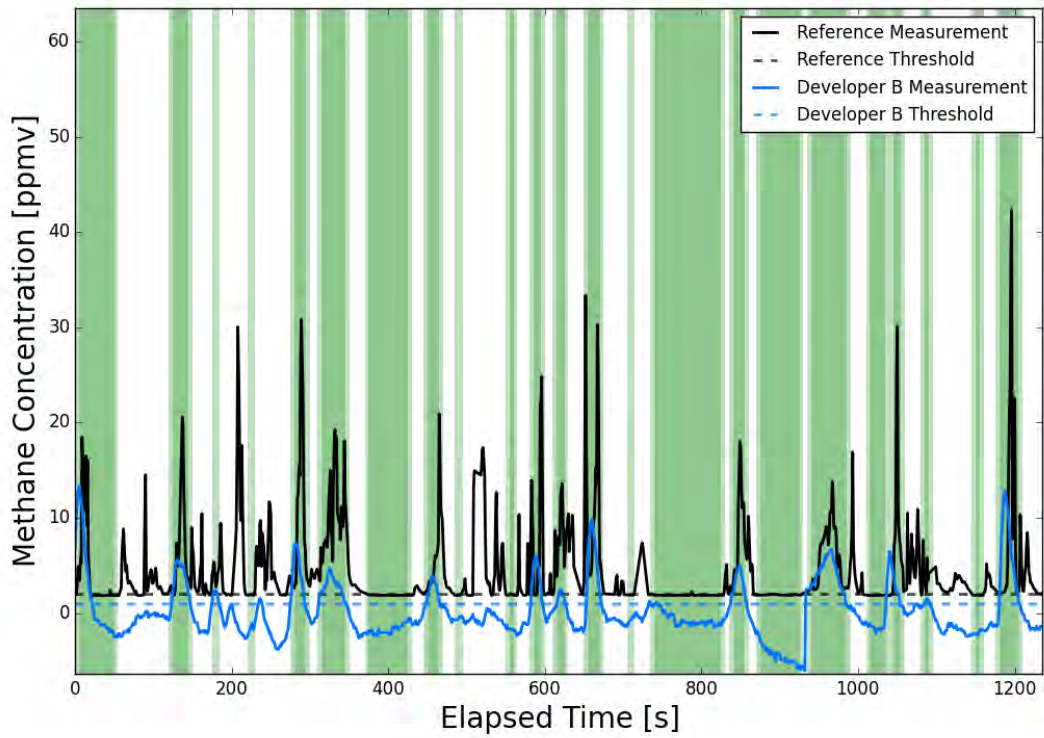


Figure B.1. Developer B Data Trace for a 1-scfm Leak from 30 ft of Distance

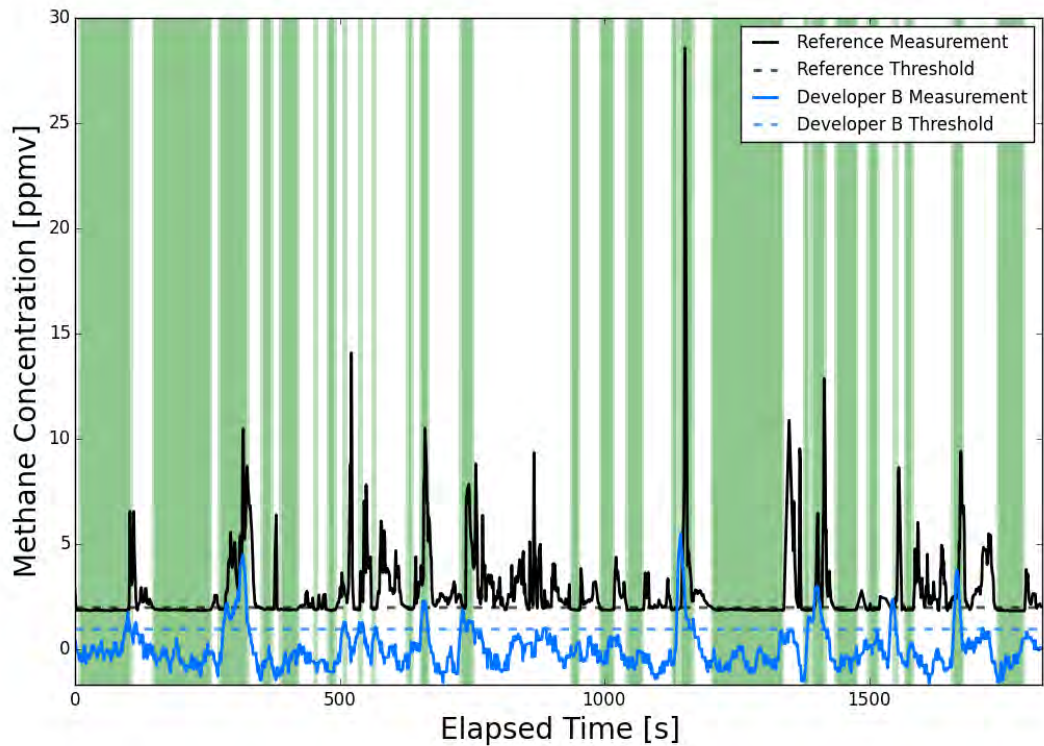


Figure B.2. Developer B Data Trace for a 1-scfm Leak from 70ft of Distance

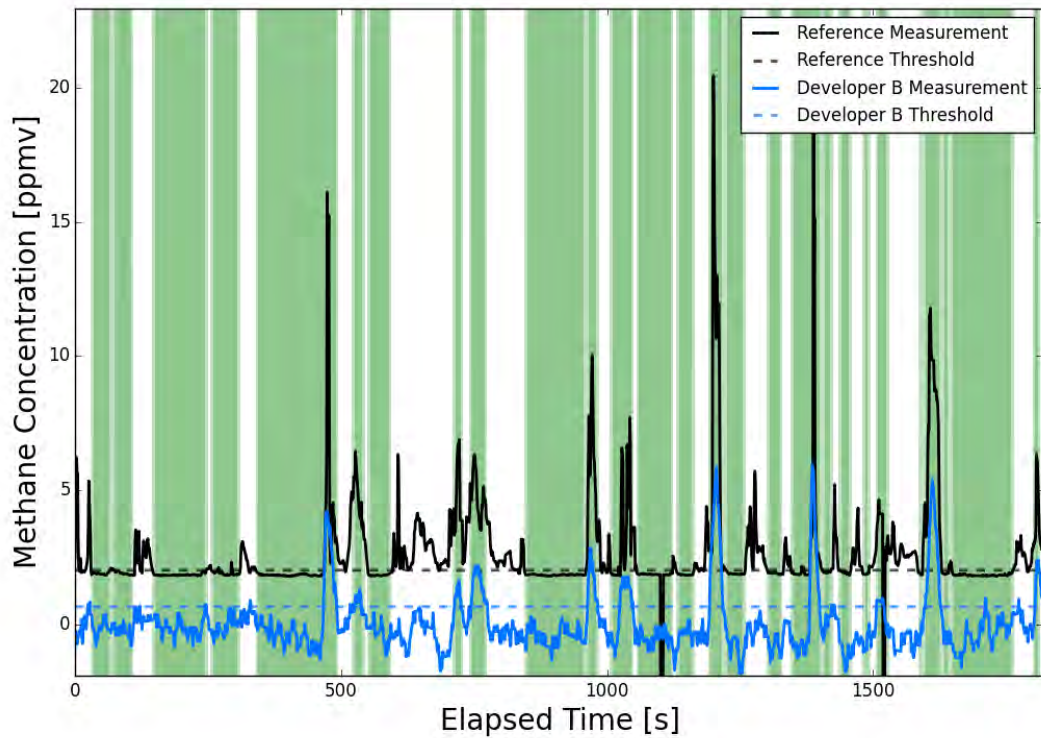


Figure B.3. Developer B Data Trace for a 1-scfm Leak from 82 ft of Distance

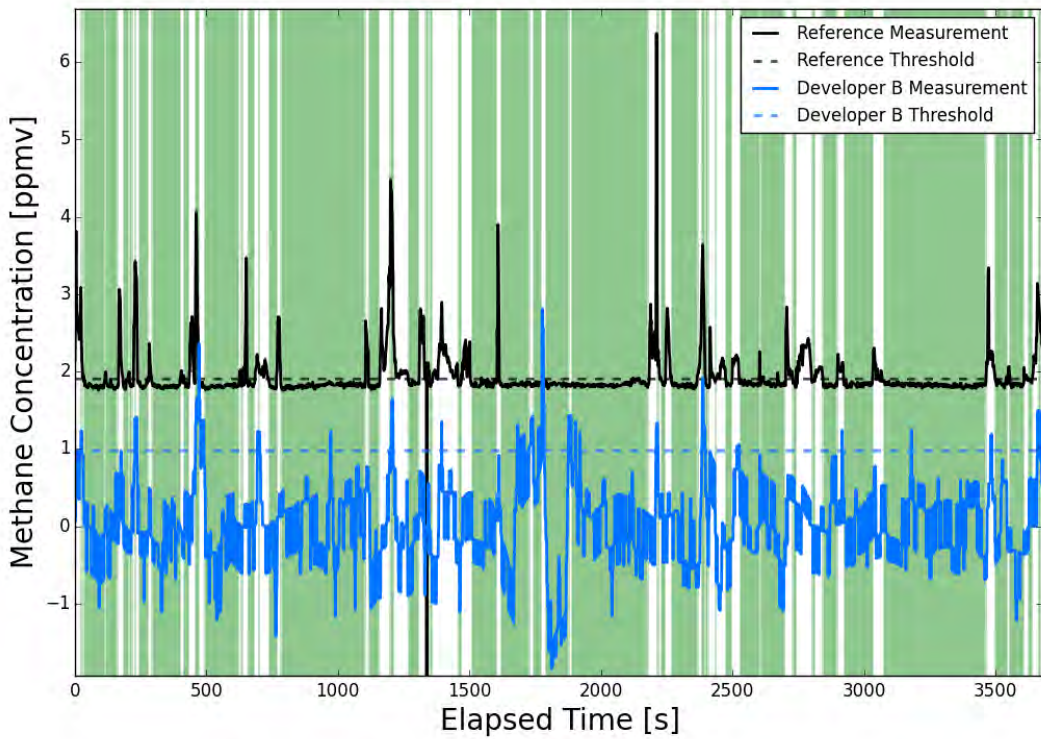


Figure B.4. Developer B Data Trace for a 1-scfm Leak from 130 ft of Distance

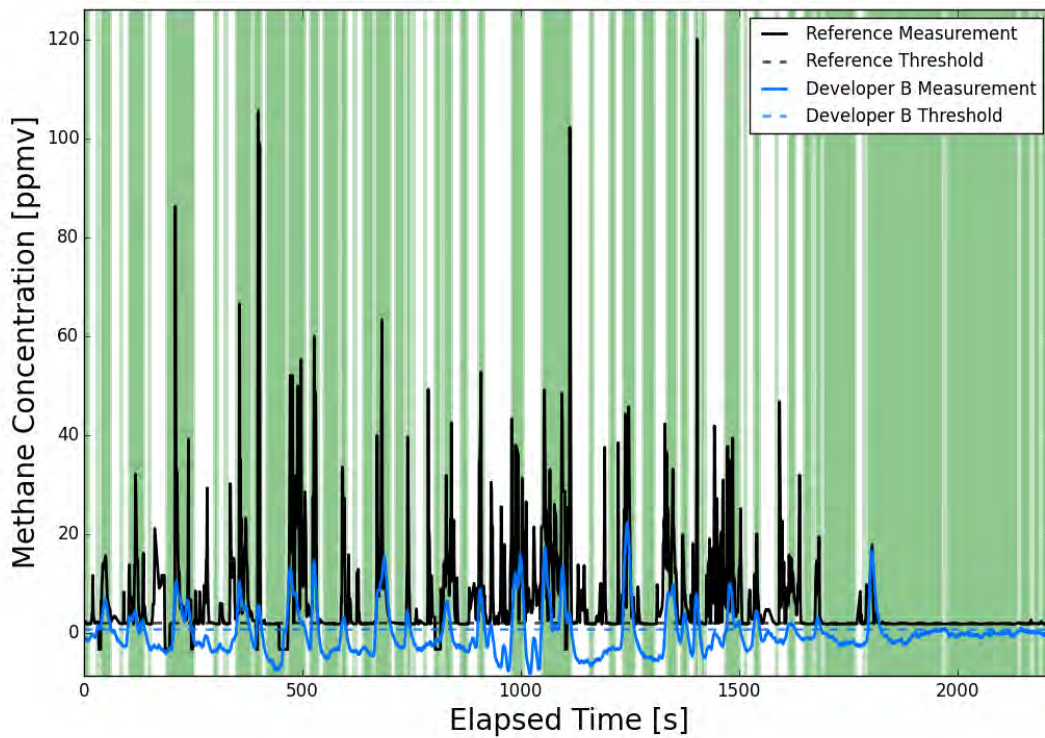


Figure B.5. Developer B Data Trace for a 2.5-scfm Leak from 30 ft of Distance

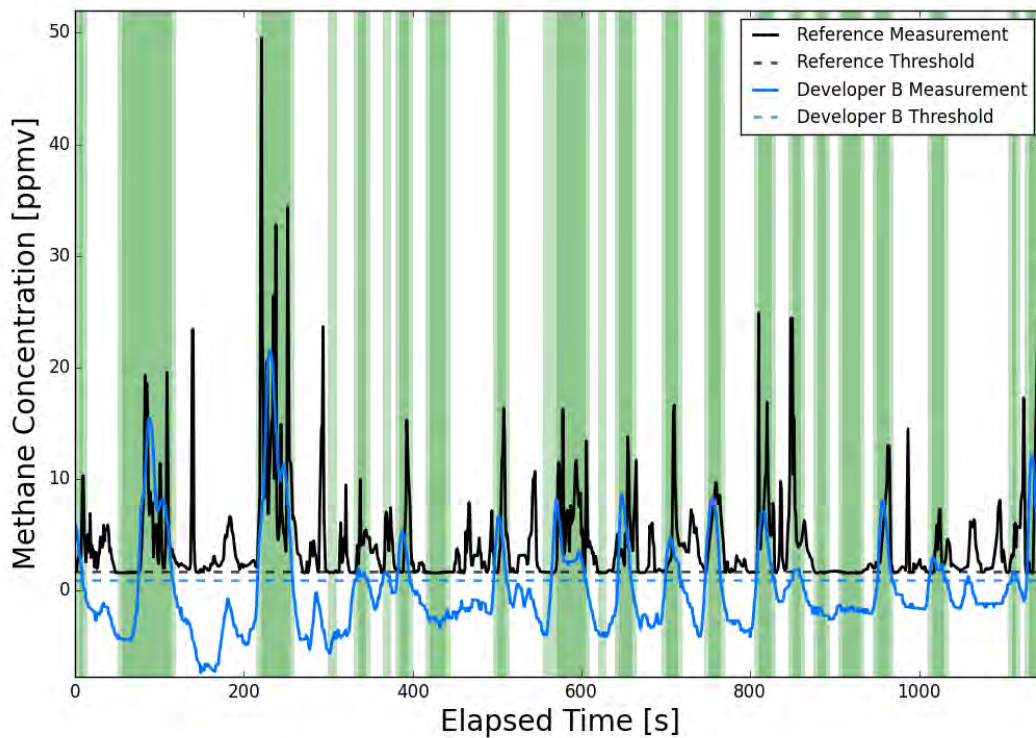


Figure B.6. Developer B Data Trace for a 2.5-scfm Leak from 50-ft of Distance

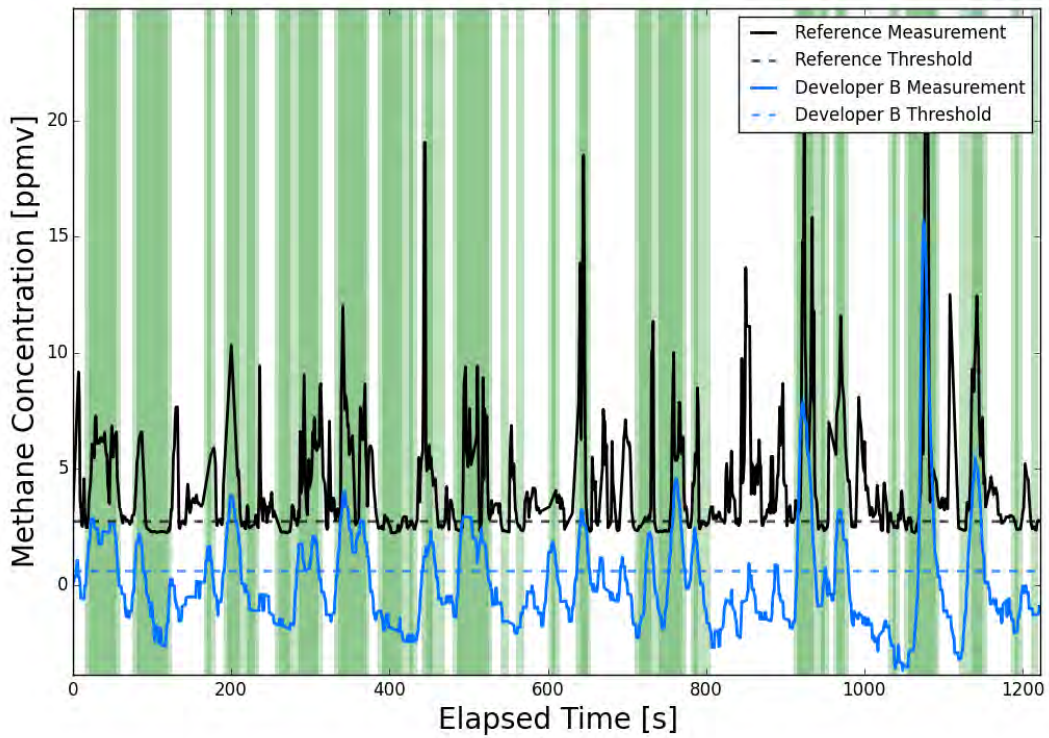


Figure B.7. Developer B Data Trace for a 2.5-scfm Leak from 70 ft of Distance

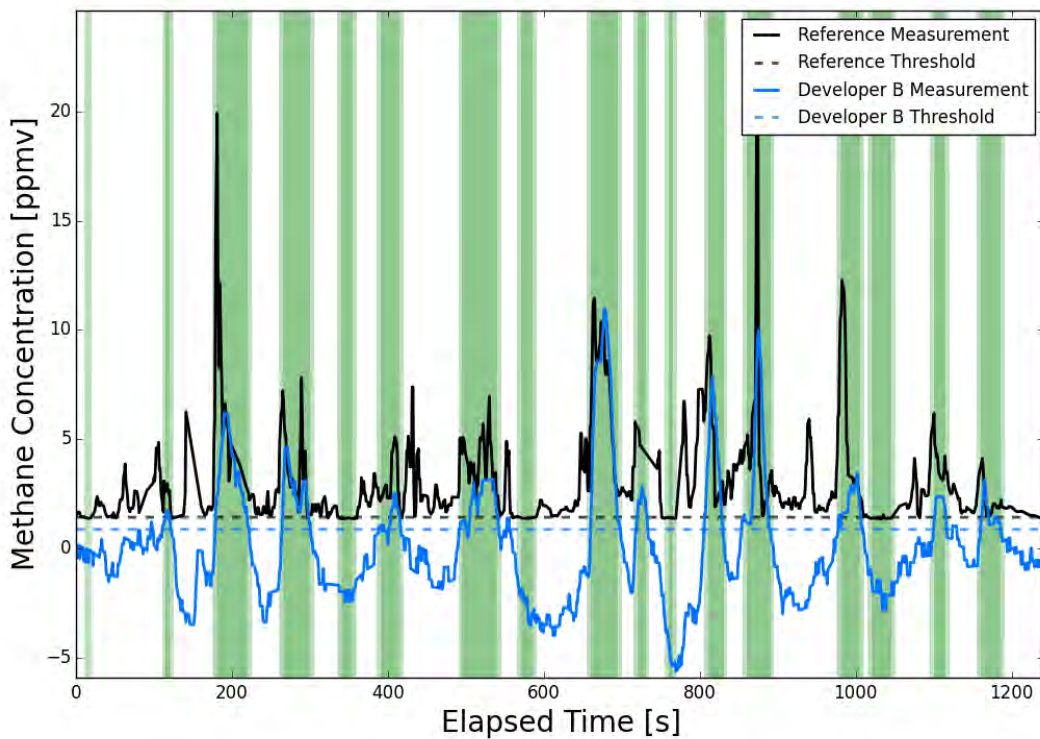


Figure B.8. Developer B Data Trace for a 2.5-scfm Leak from 82 ft of Distance

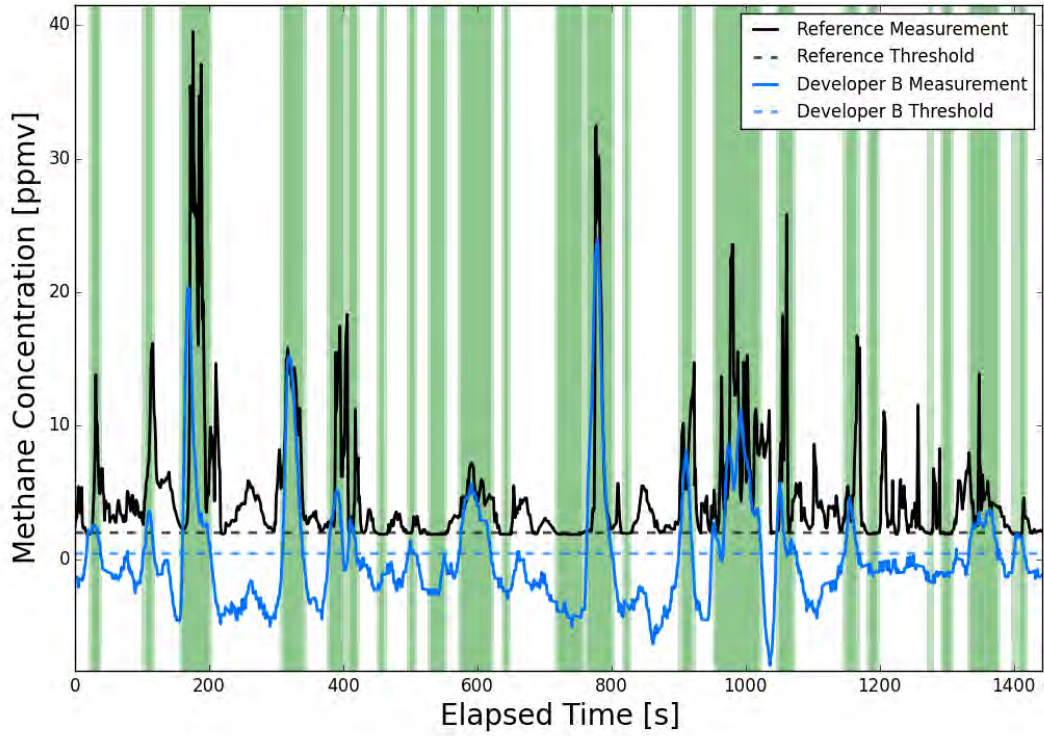


Figure B.9. Developer B Data Trace for a 5-scfm Leak from 30 ft of Distance

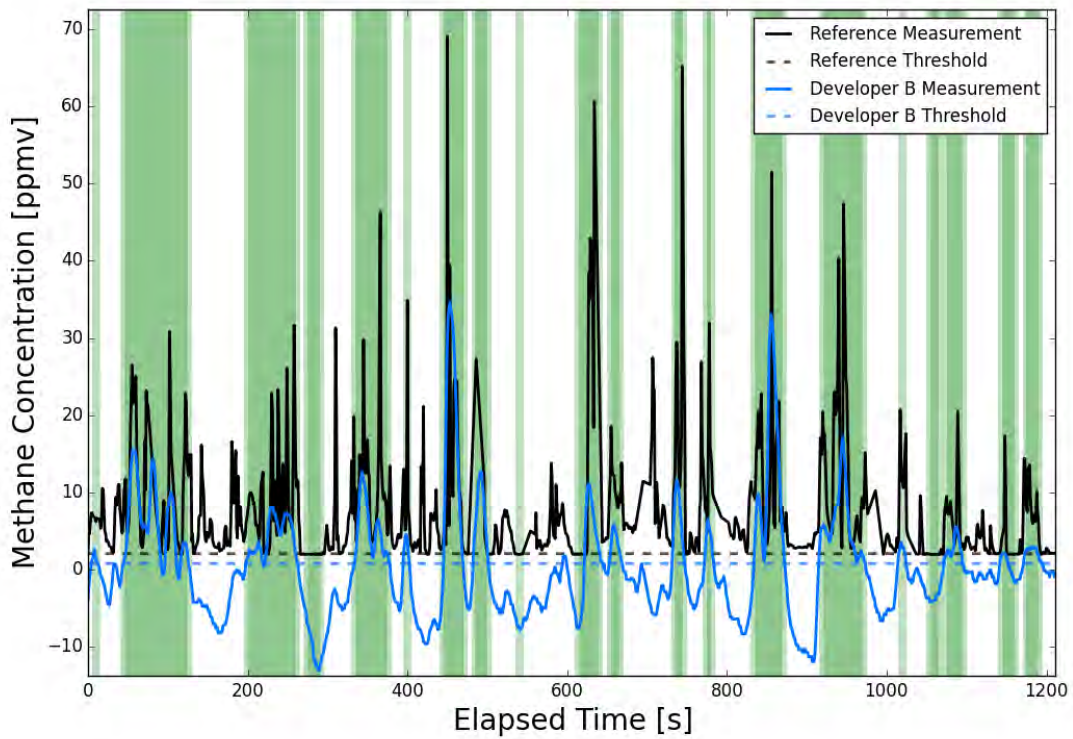


Figure B.10. Developer B Data Trace for a 5-scfm Leak from 50 ft of Distance

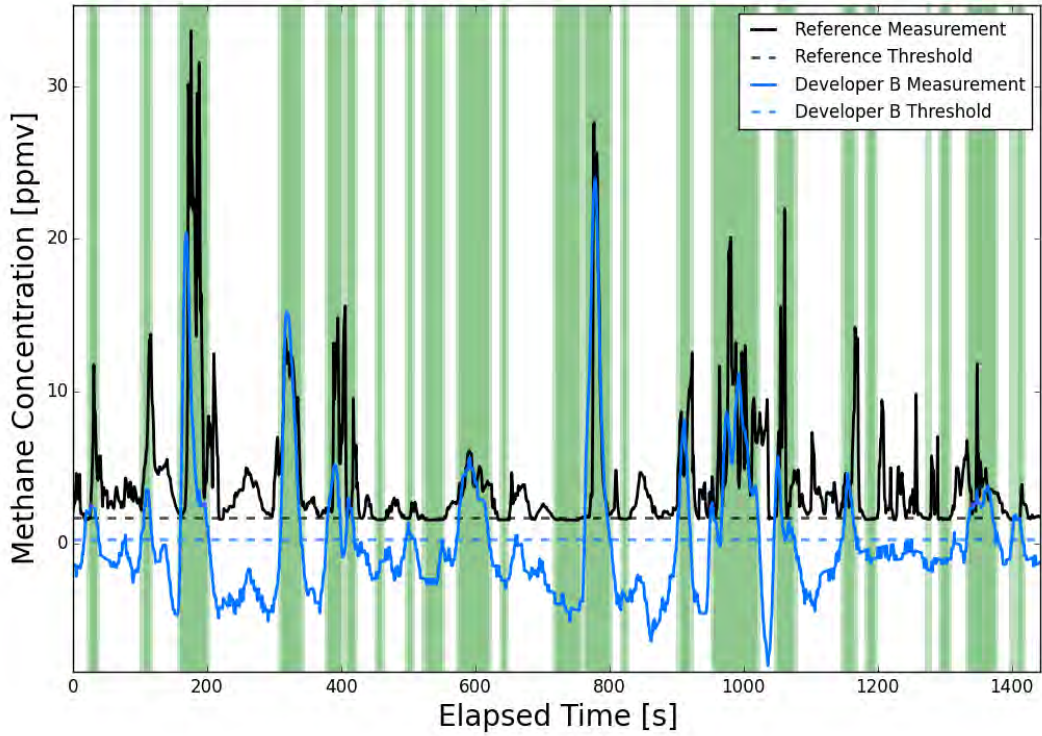


Figure B.11. Developer B Data Trace for a 5-scfm Leak from 70 ft of Distance

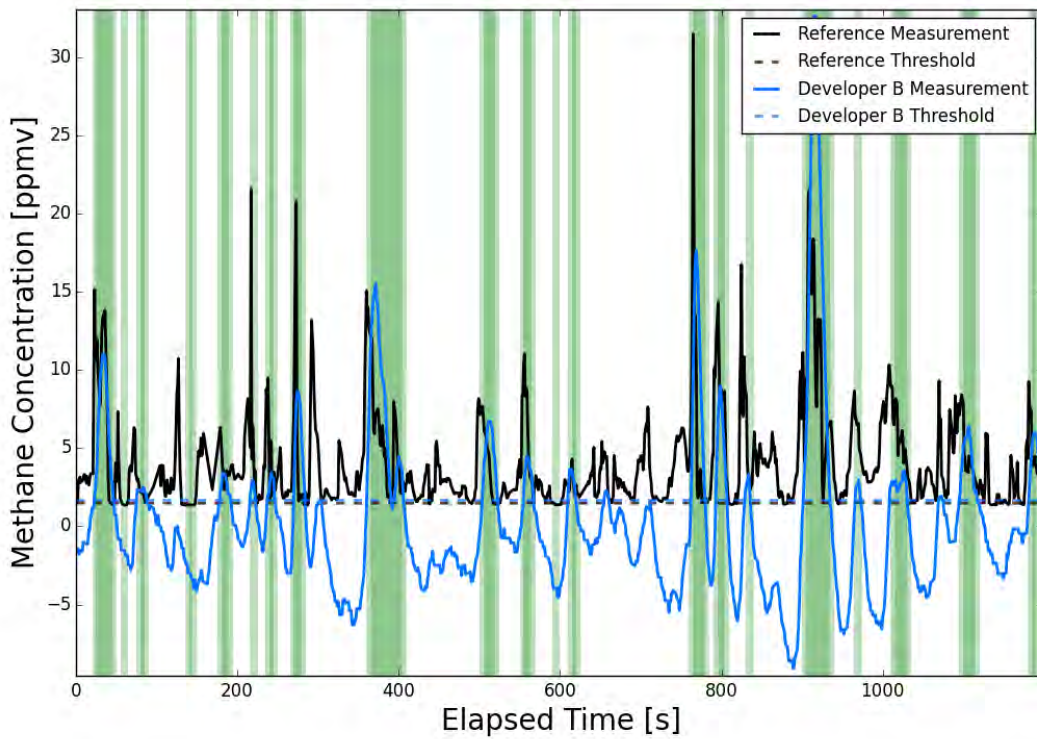


Figure B.12. Developer B Data Trace for a 5-scfm Leak from 82 ft of Distance

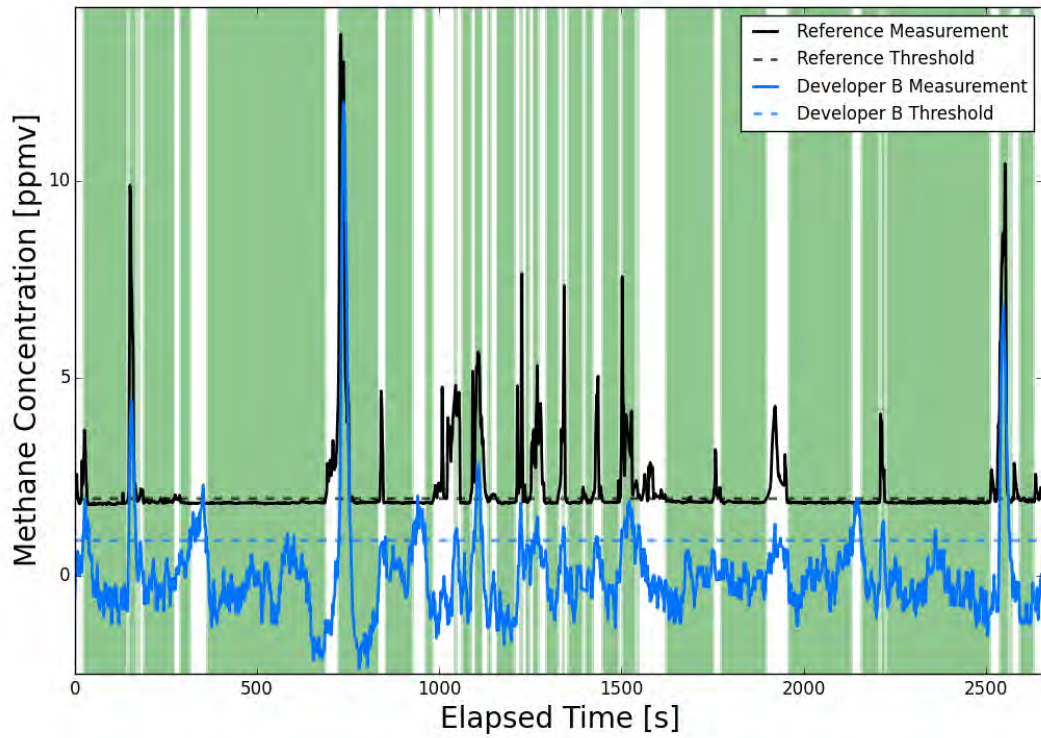


Figure B.13. Developer B Data Trace for a 5-scfm Leak from 130 ft of Distance

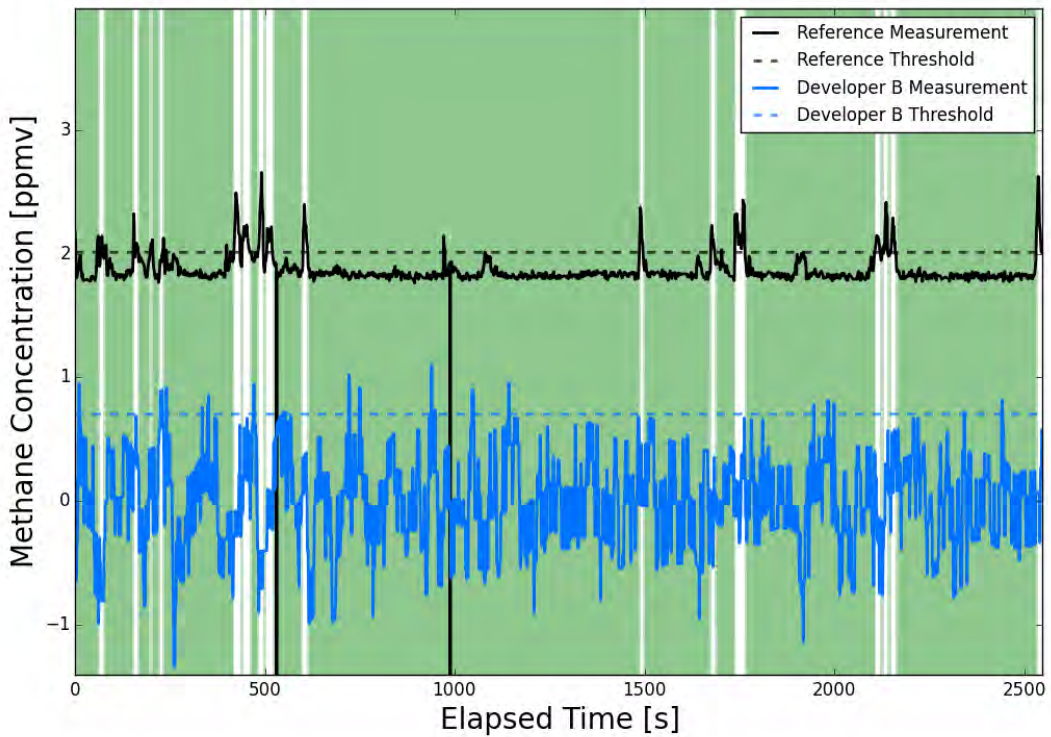


Figure B.14. Developer B Data Trace for a 0.5-scfm Leak from 130 ft of Distance

APPENDIX C
OUTDOOR TESTING GRAPHS – DEVELOPER C

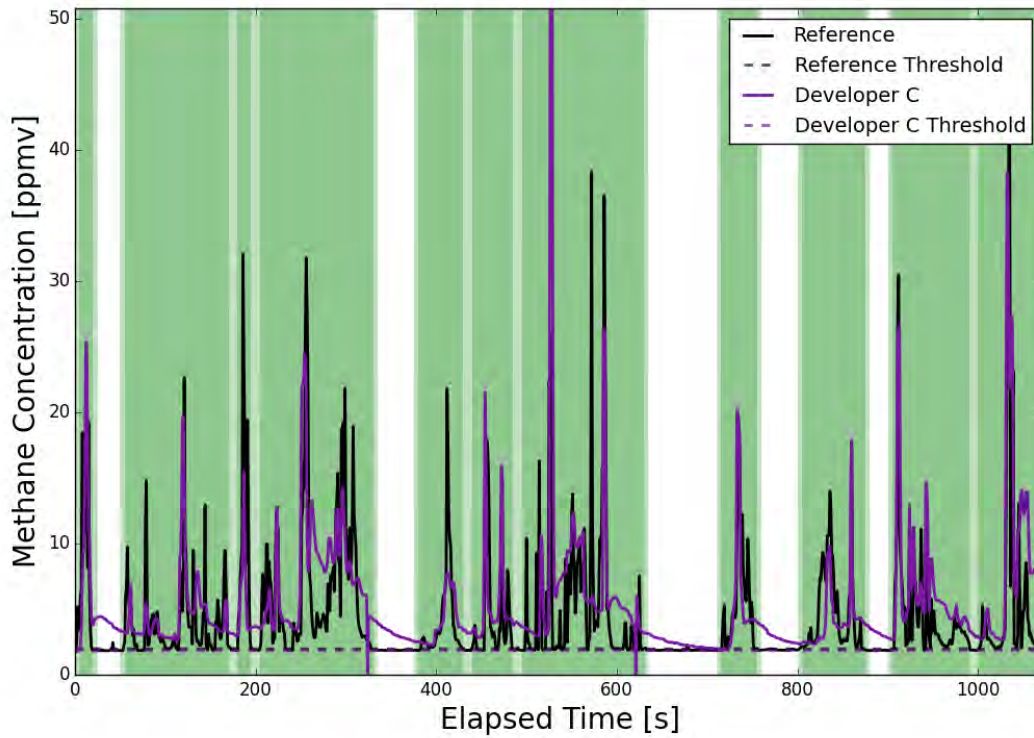


Figure C.1. Developer C Data Trace for a 1-scfm Leak from 30 ft of Distance

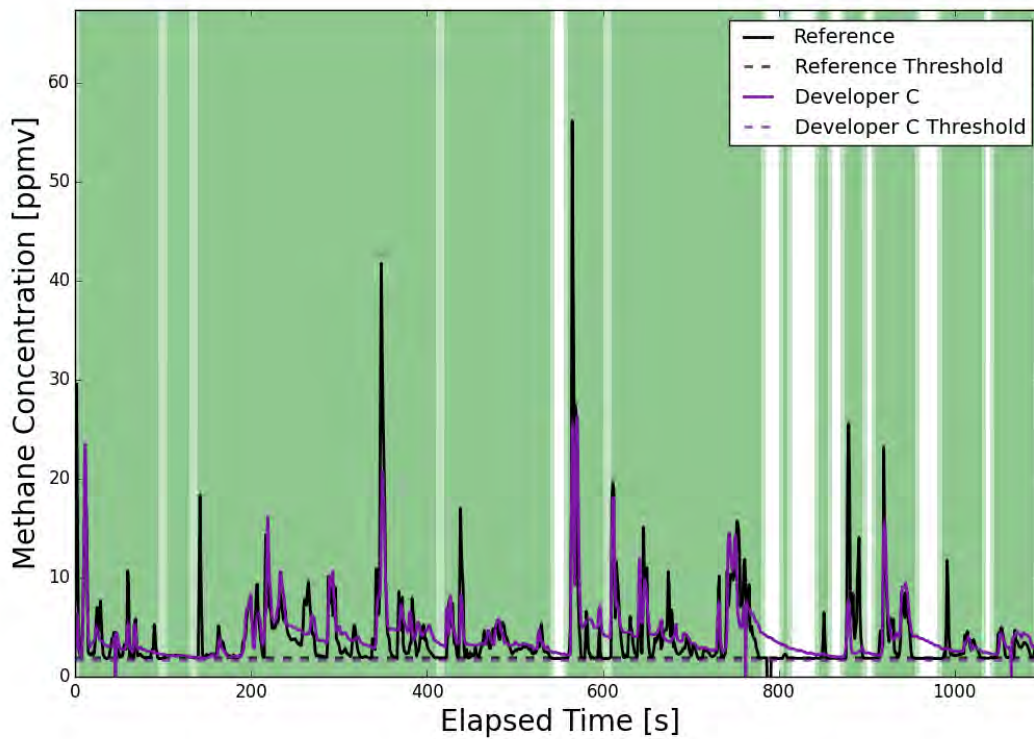


Figure C.2. Developer C Data Trace for a 1-scfm Leak from 50 ft of Distance

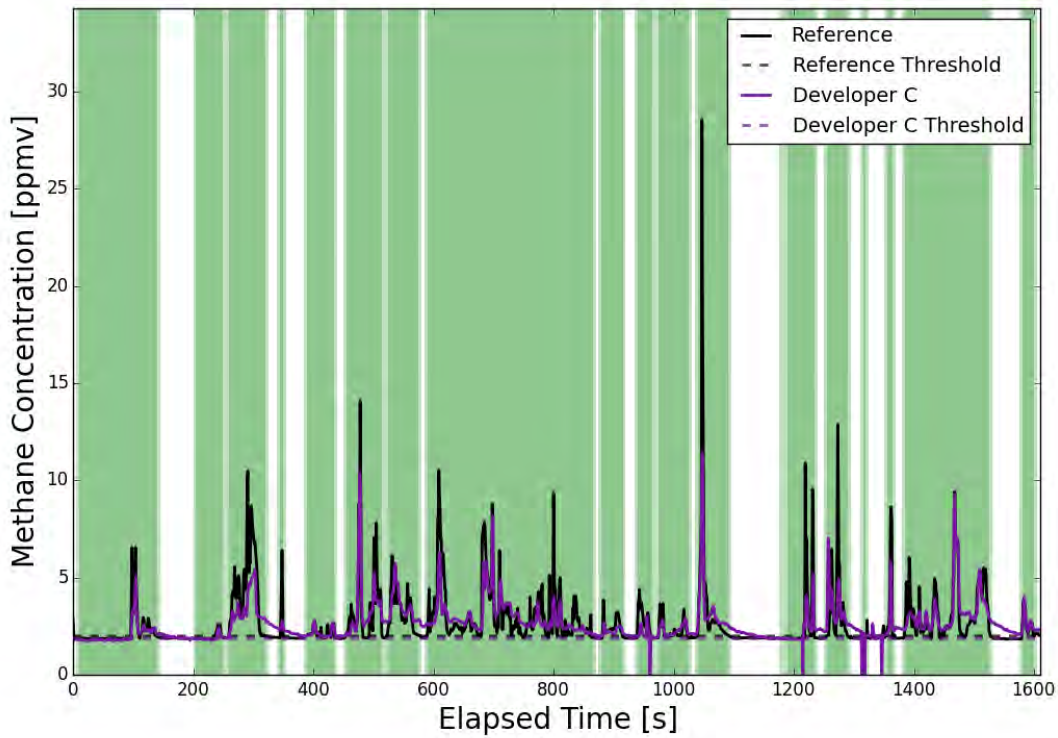


Figure C.3. Developer C Data Trace for a 1-scfm Leak from 70 ft of Distance

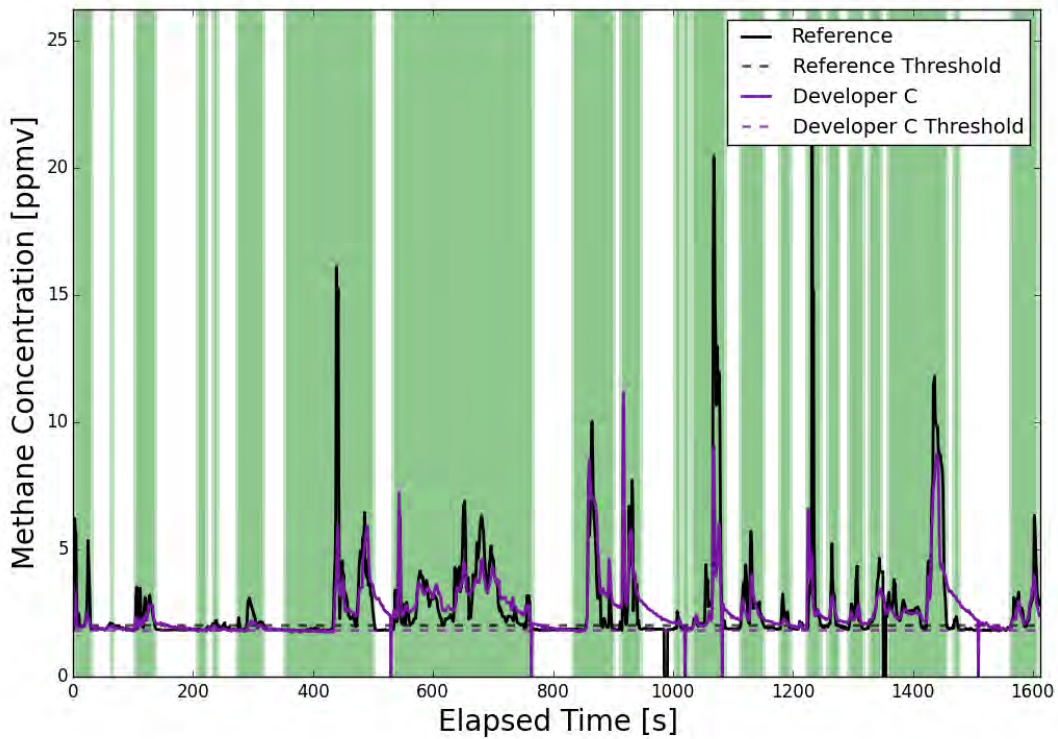


Figure C.4. Developer C Data Trace for a 1-scfm Leak from 82 ft of Distance

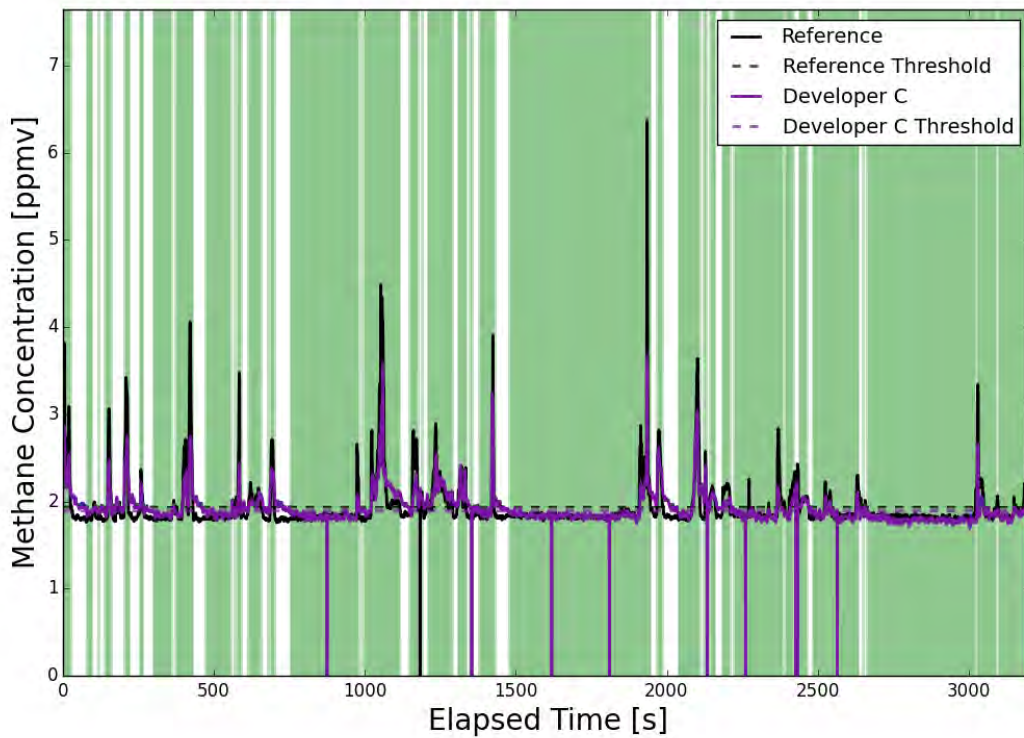


Figure C.5. Developer C Data Trace for a 1-scfm Leak from 130 ft of Distance

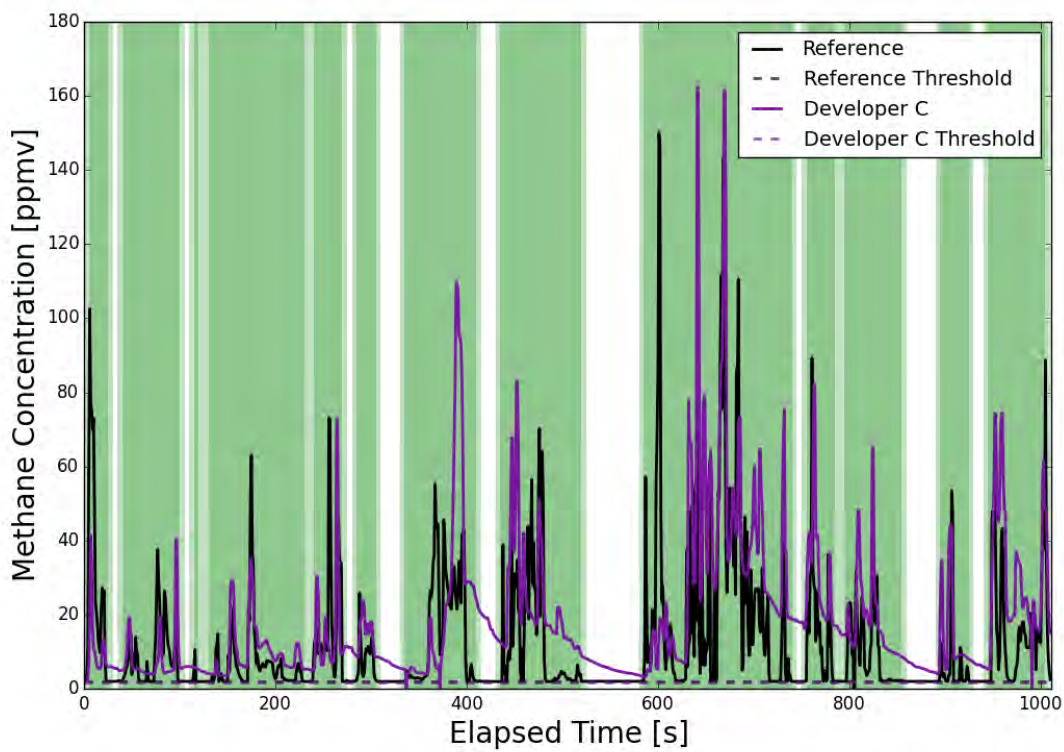


Figure C.6. Developer C Data Trace for a 2.5-scfm Leak from 30 ft of Distance

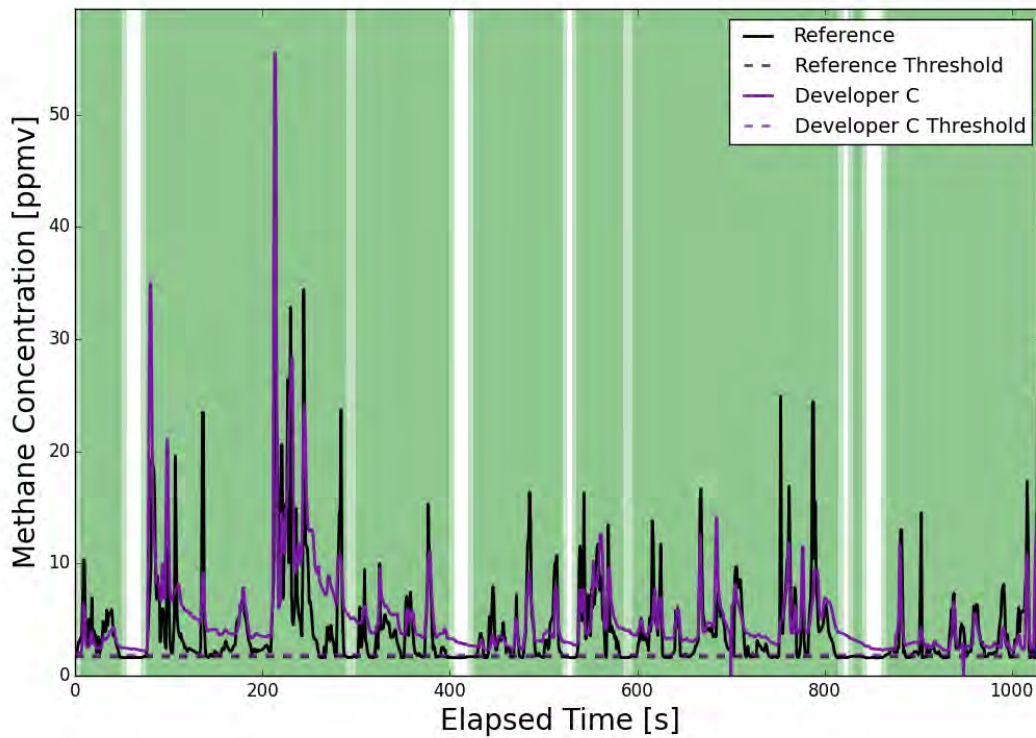


Figure C.7. Developer C Data Trace for a 2.5-scfm Leak from 50 ft of Distance

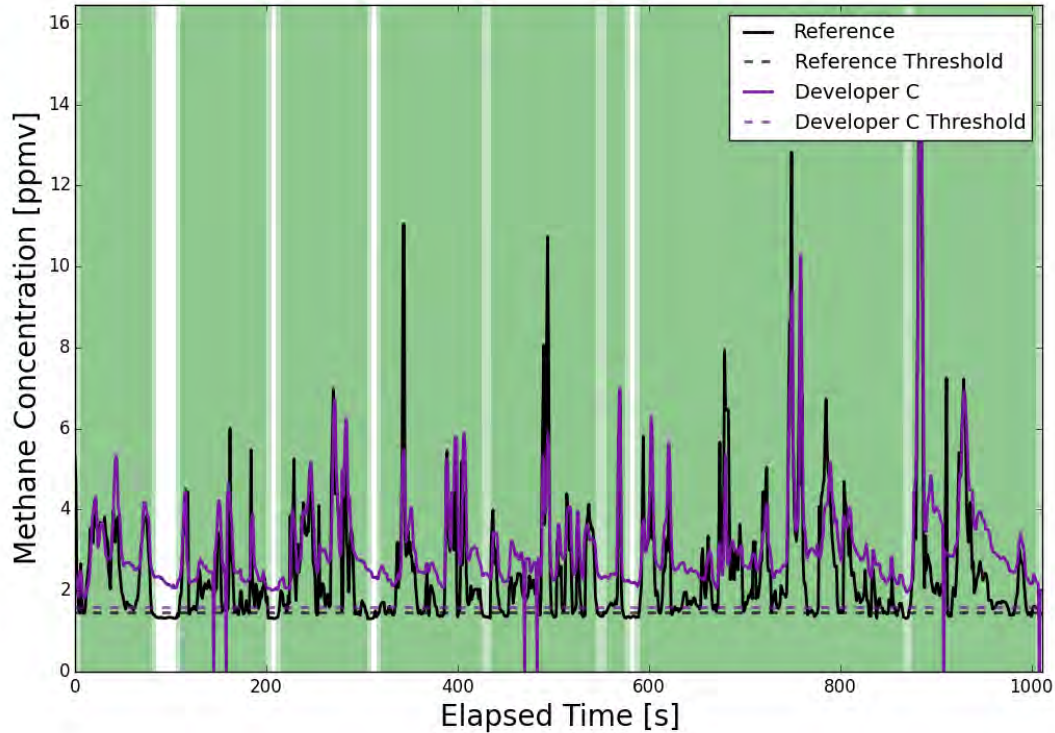


Figure C.8. Developer C Data Trace for a 2.5-scfm Leak from 70 ft of Distance

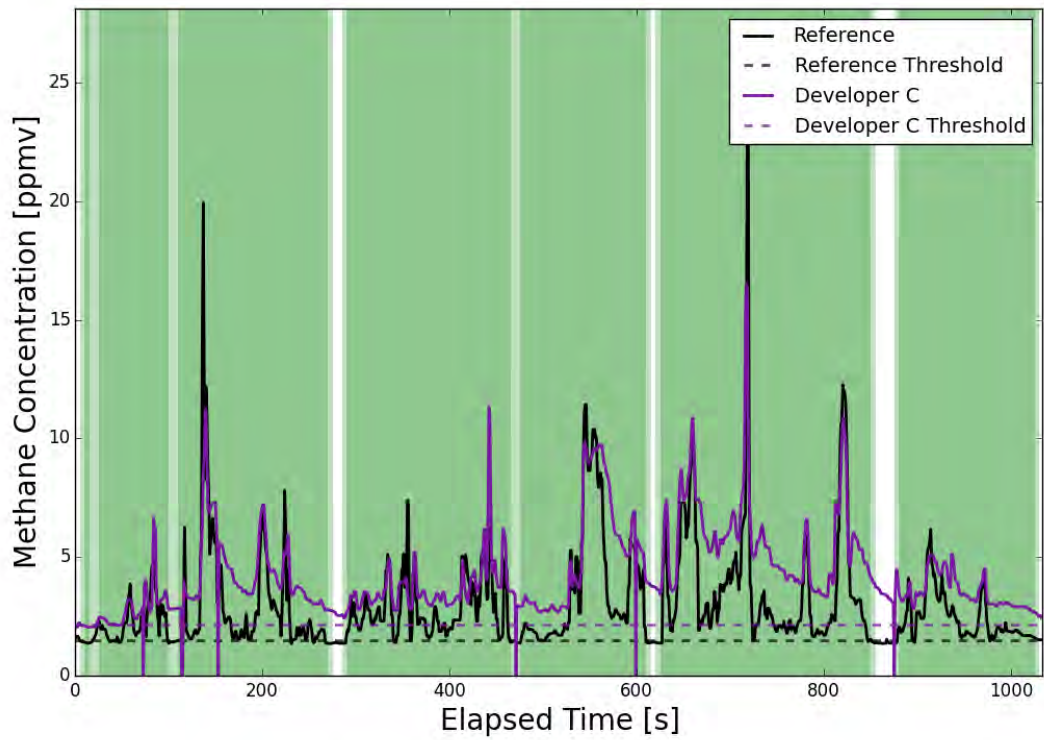


Figure C.9. Developer C Data Trace for a 2.5-scfm Leak from 82 ft of Distance

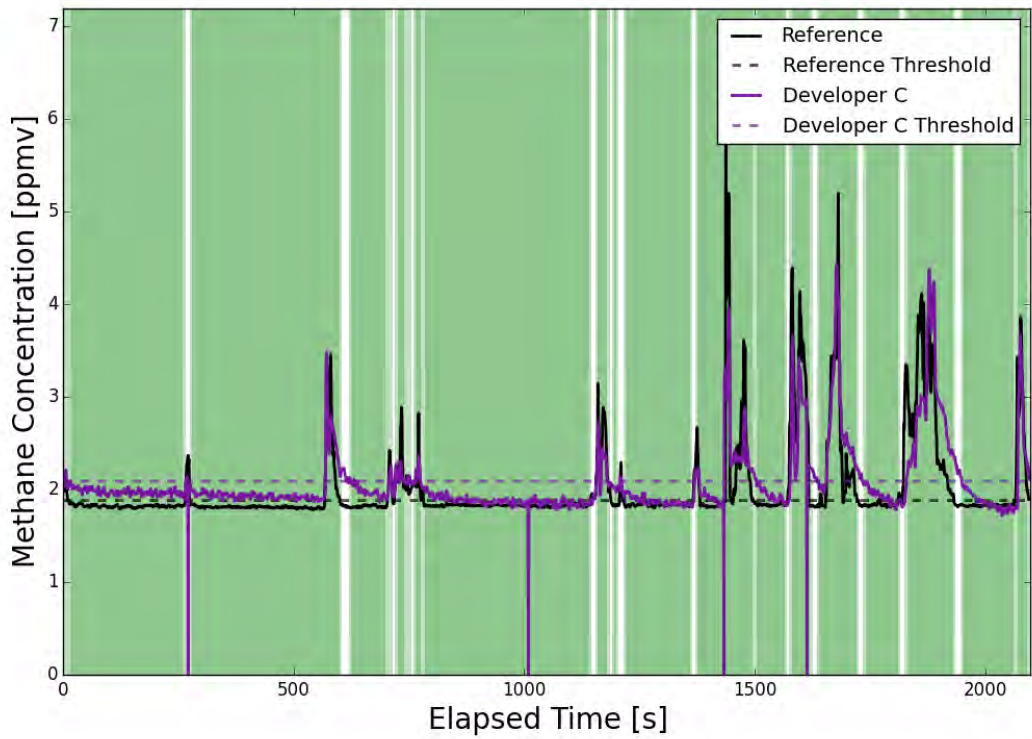


Figure C.10. Developer C Data Trace for a 2.5-scfm Leak from 130 ft of Distance

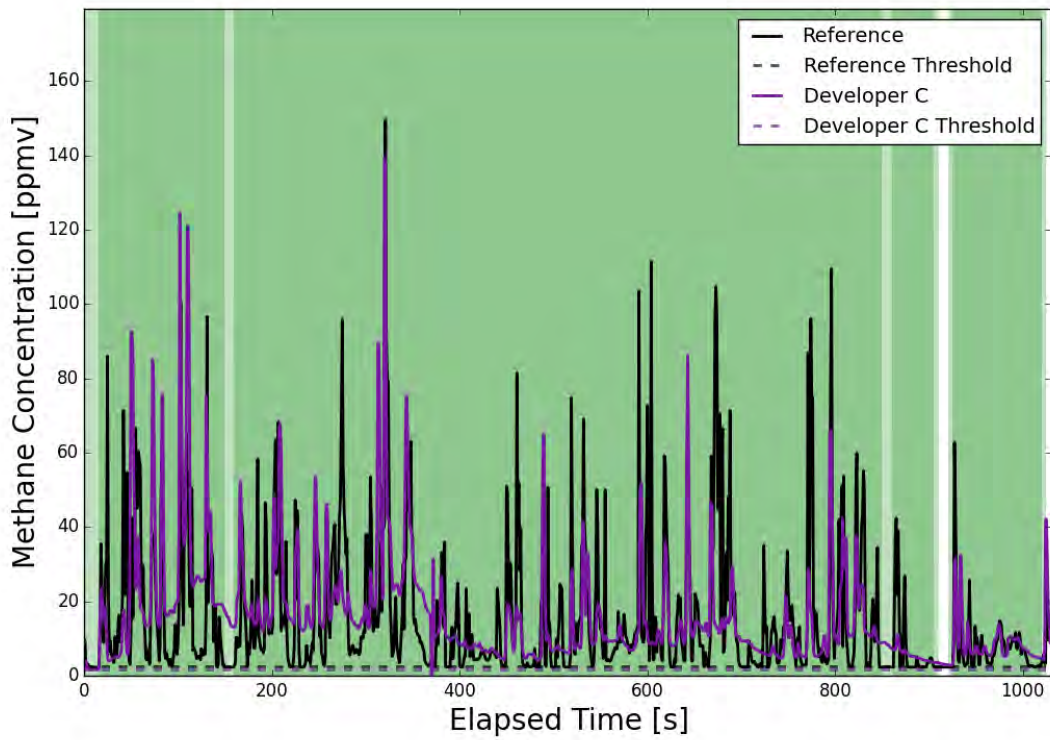


Figure C.11. Developer C Data Trace for a 5-scfm Leak from 30 ft of Distance

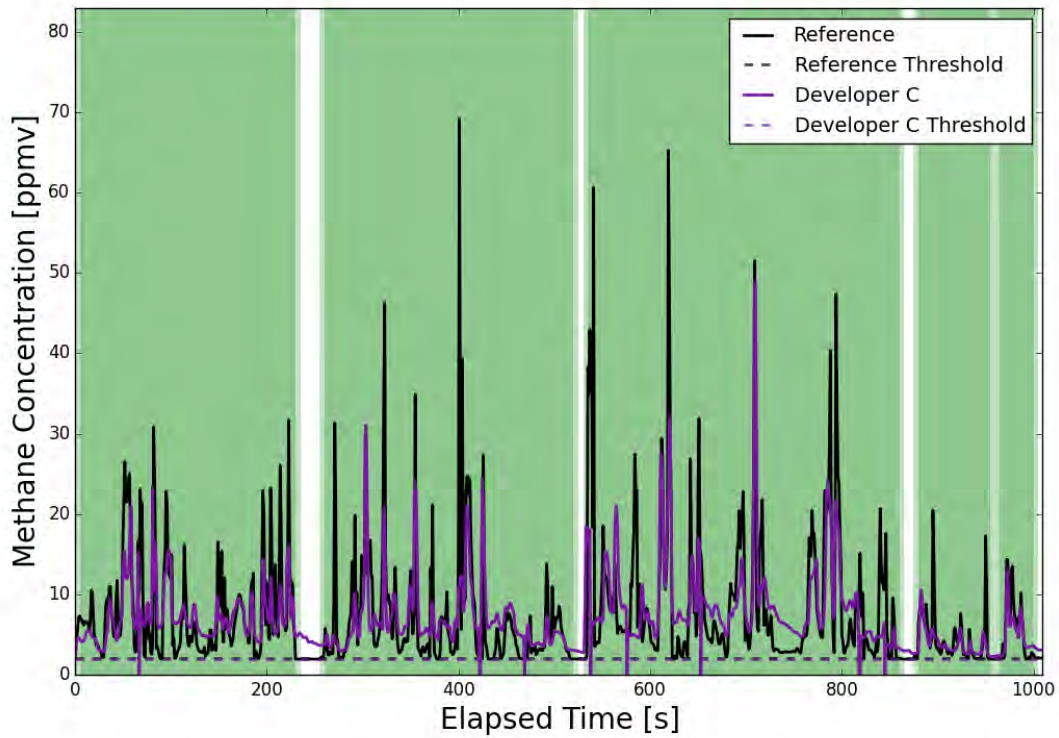


Figure C.12. Developer C Data Trace for a 5-scfm Leak from 50 ft of Distance

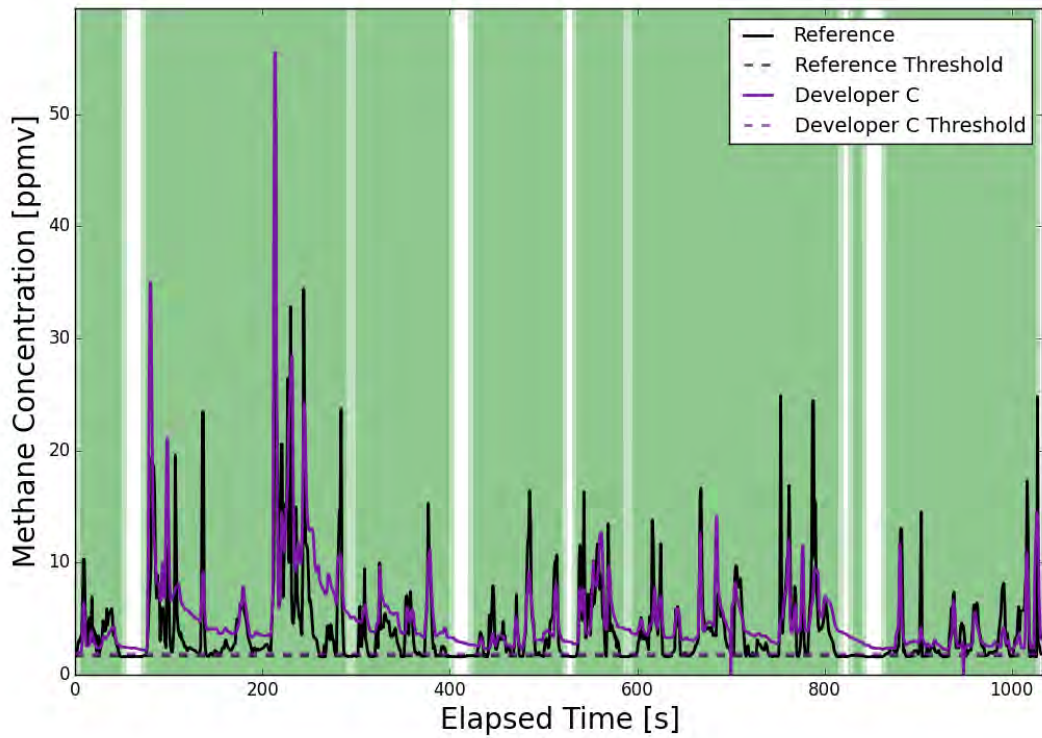


Figure C.13. Developer C Data Trace for a 5-scfm Leak from 70 ft of Distance

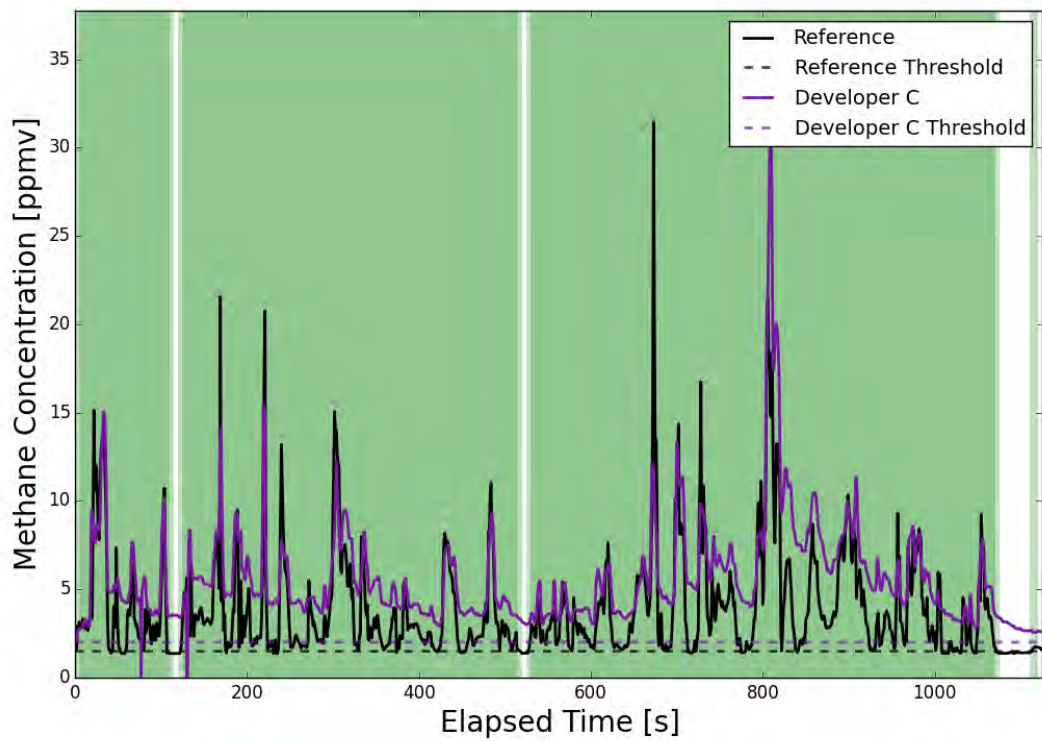


Figure C.14. Developer C Data Trace for a 5-scfm Leak from 82 ft of Distance

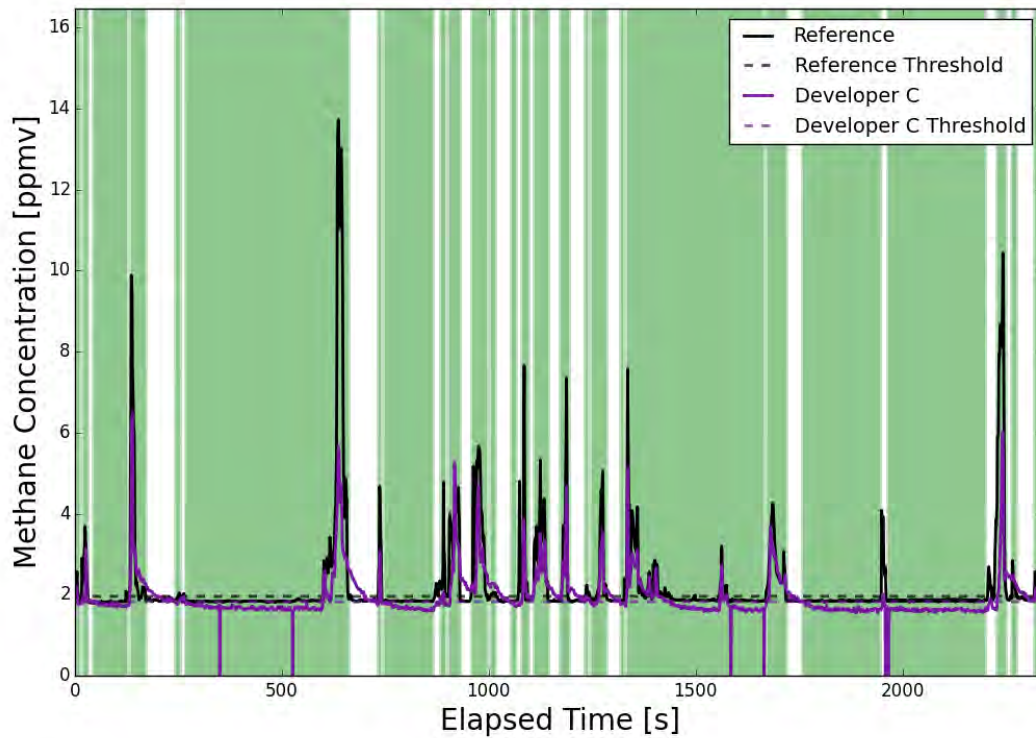


Figure C.15. Developer C Data Trace for a 5-scfm Leak from 130 ft of Distance

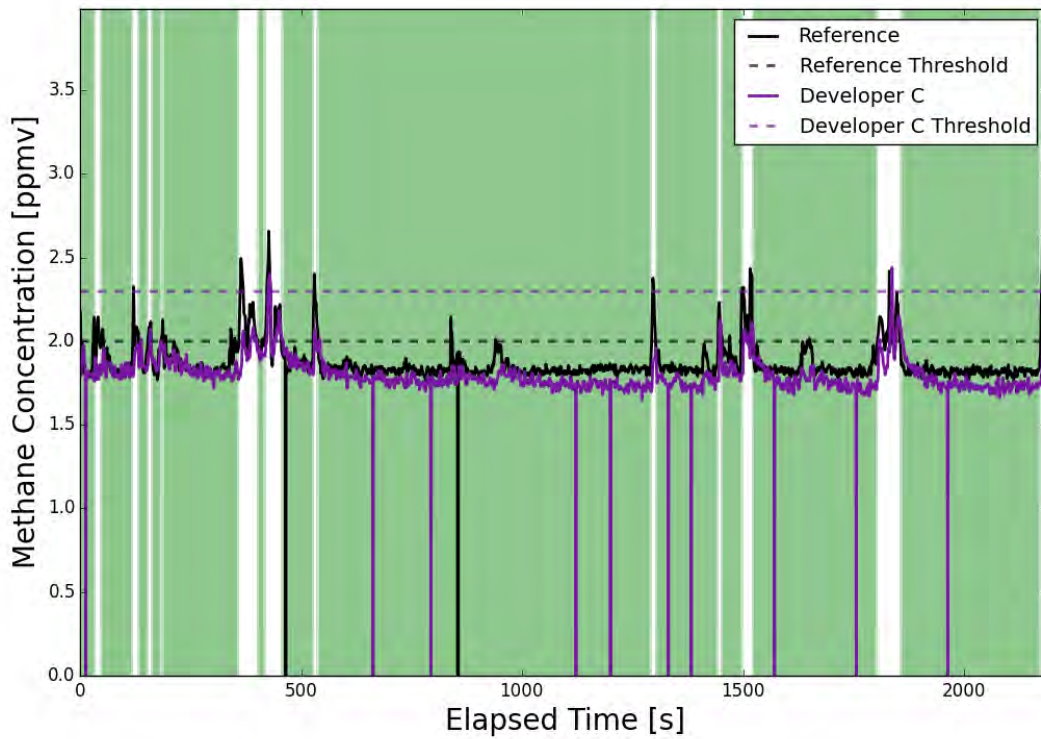


Figure C.16. Developer C Data Trace for a 0.5-scfm Leak from 130ft of Distance

APPENDIX D

OUTDOOR TESTING GRAPHS – DEVELOPER D

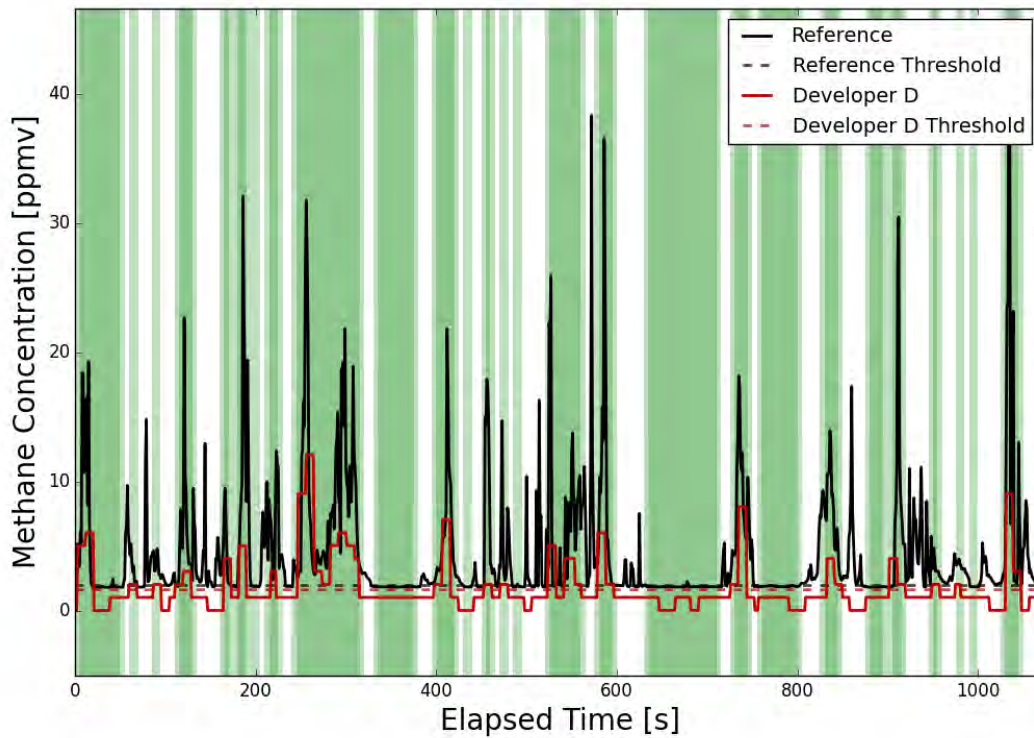


Figure D.1. Developer D Data Trace for a 1-scfm Leak from 30 ft of Distance

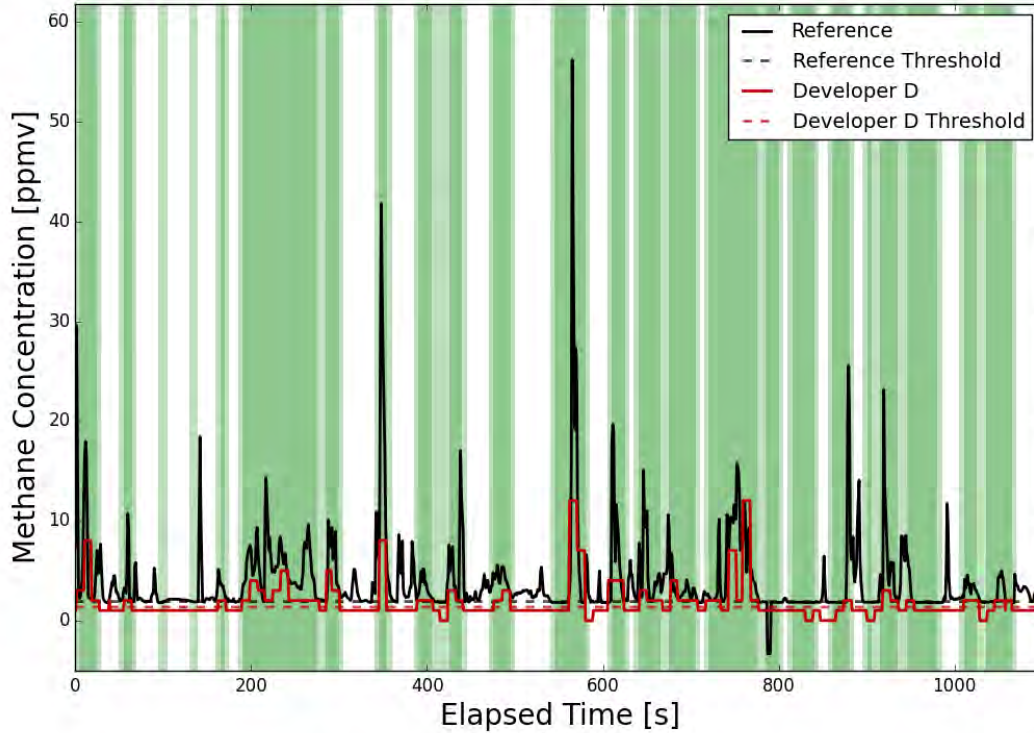


Figure D.2. Developer D Data Trace for a 1-scfm Leak from 50 ft of Distance

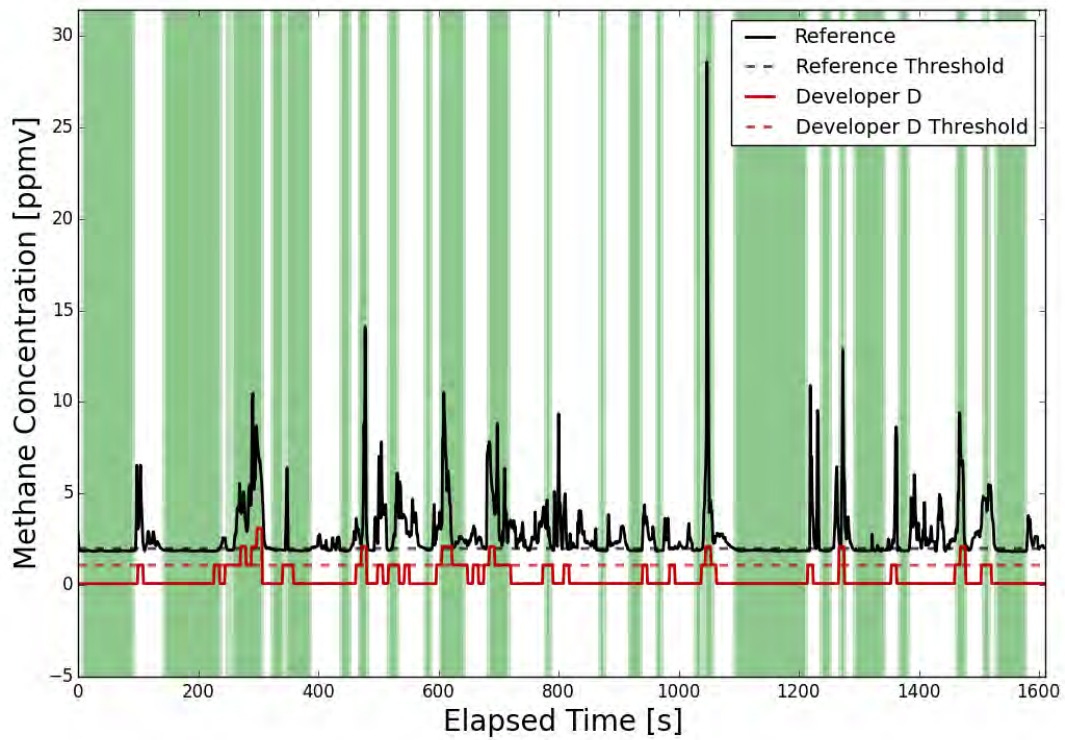


Figure D.3. Developer D Data Trace for a 1-scfm Leak from 70 ft of Distance

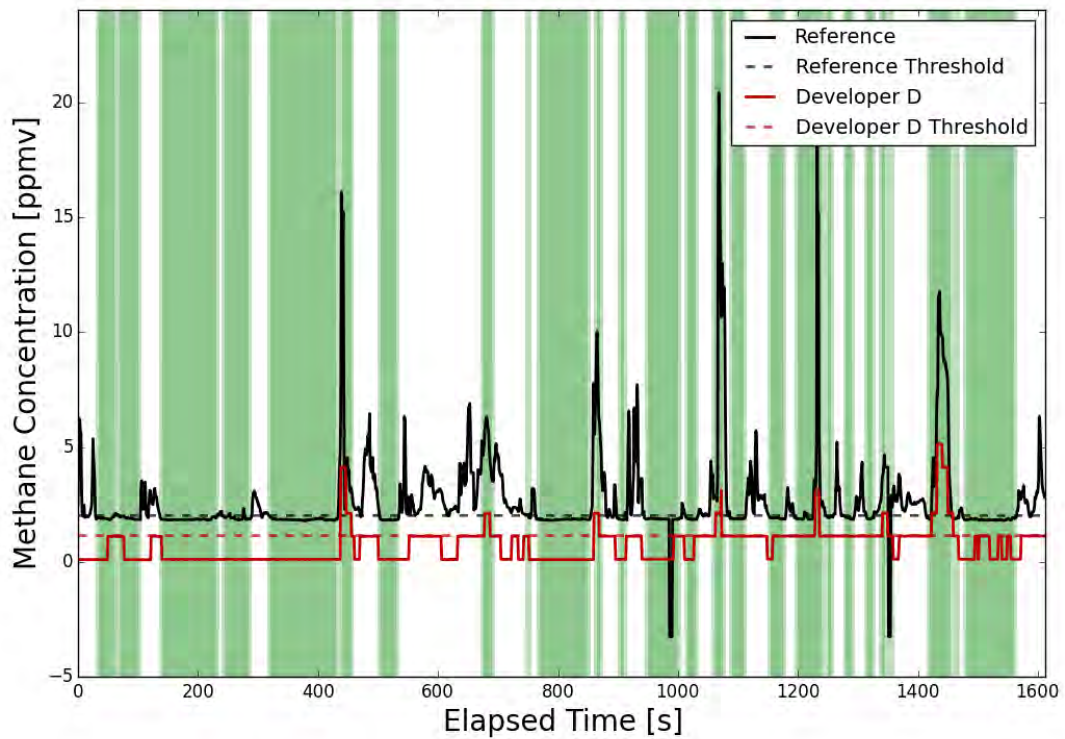


Figure D.4. Developer D Data Trace for a 1-scfm Leak from 82 ft of Distance

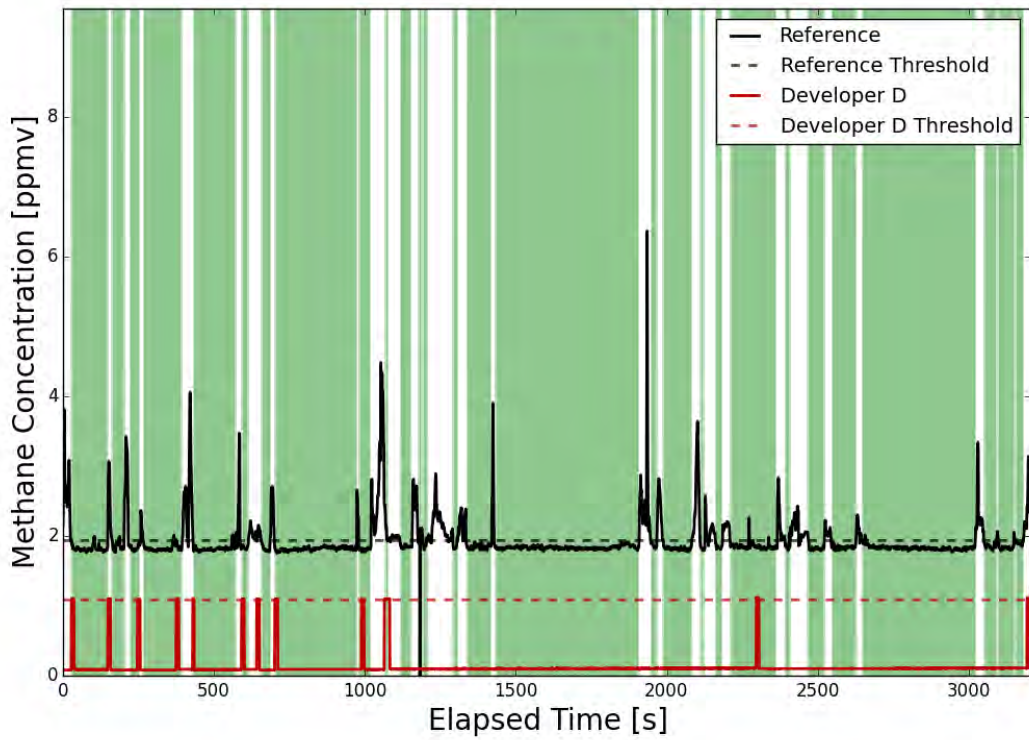


Figure D.5. Developer D Data Trace for a 1-scfm Leak from 130 ft of Distance

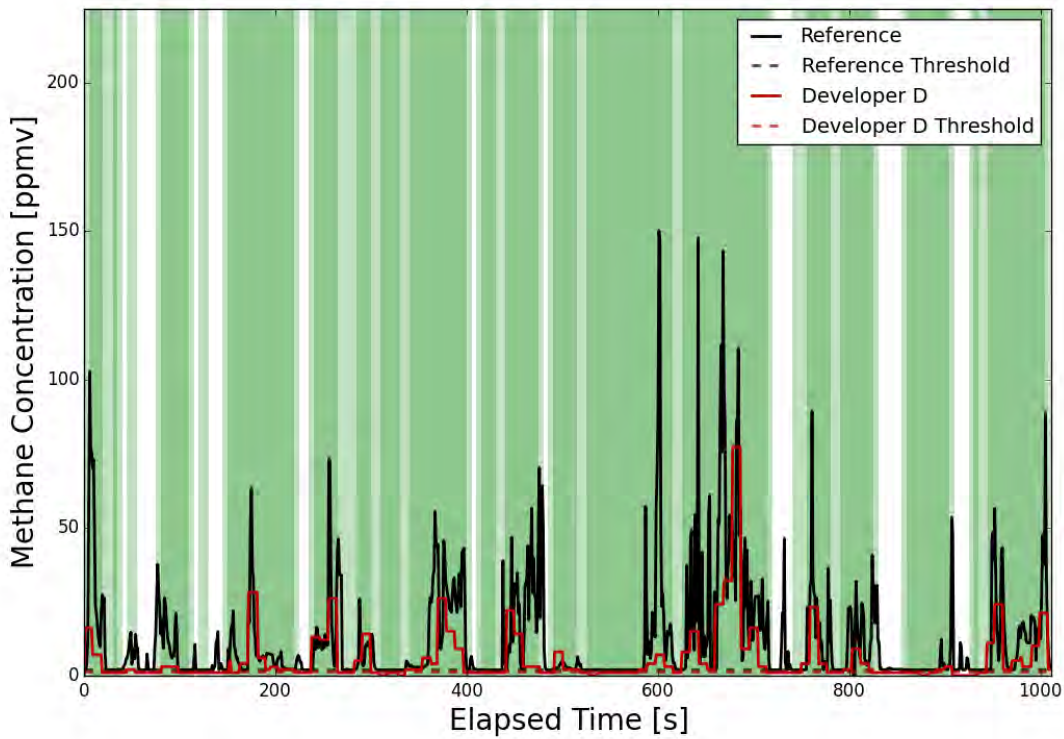


Figure D.6. Developer D Data Trace for a 2.5-scfm Leak from 30 ft of Distance

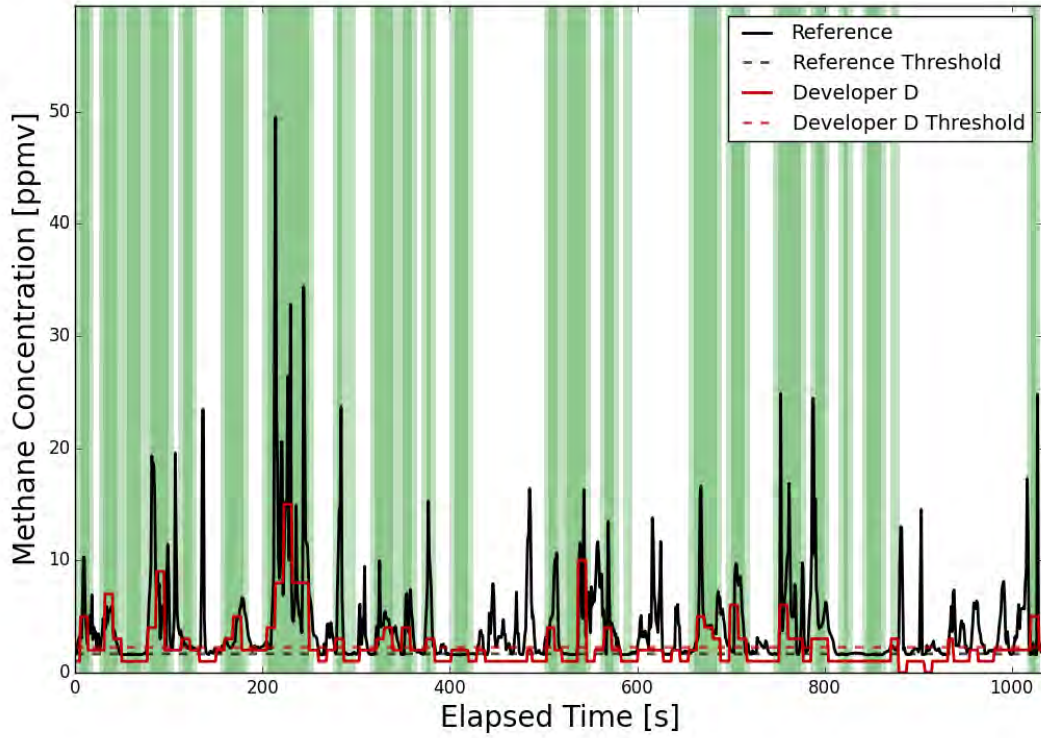


Figure D.8. Developer D Data Trace for a 2.5-scfm Leak from 50 ft of Distance

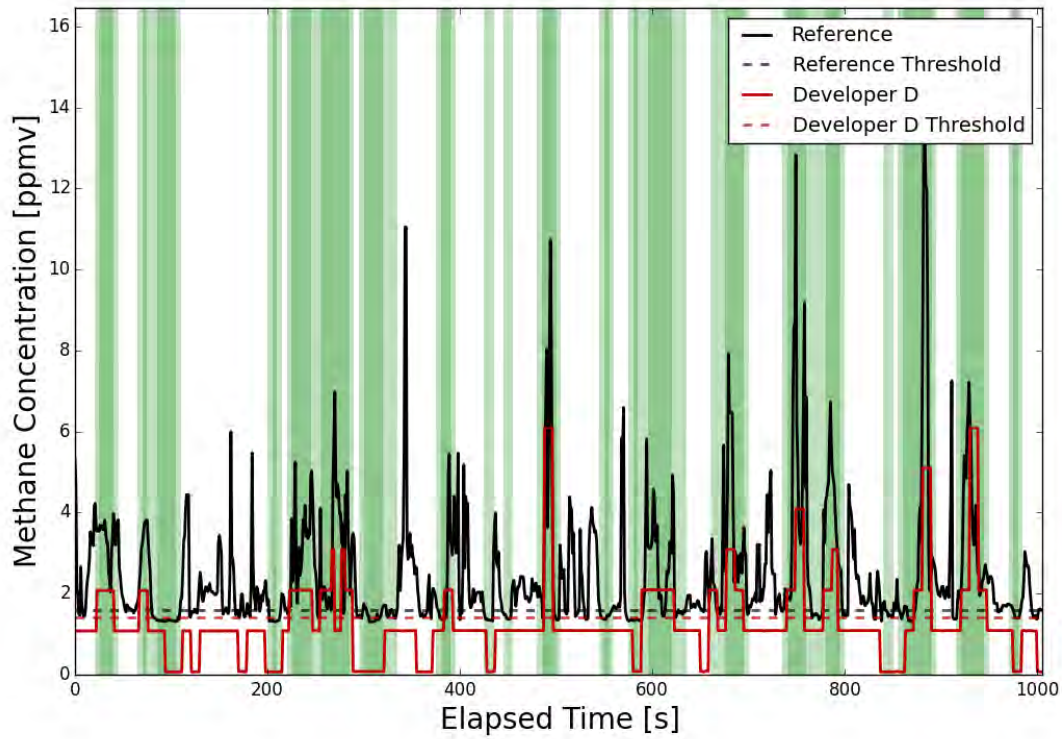


Figure D.9. Developer D Data Trace for a 2.5-scfm Leak from 70 ft of Distance

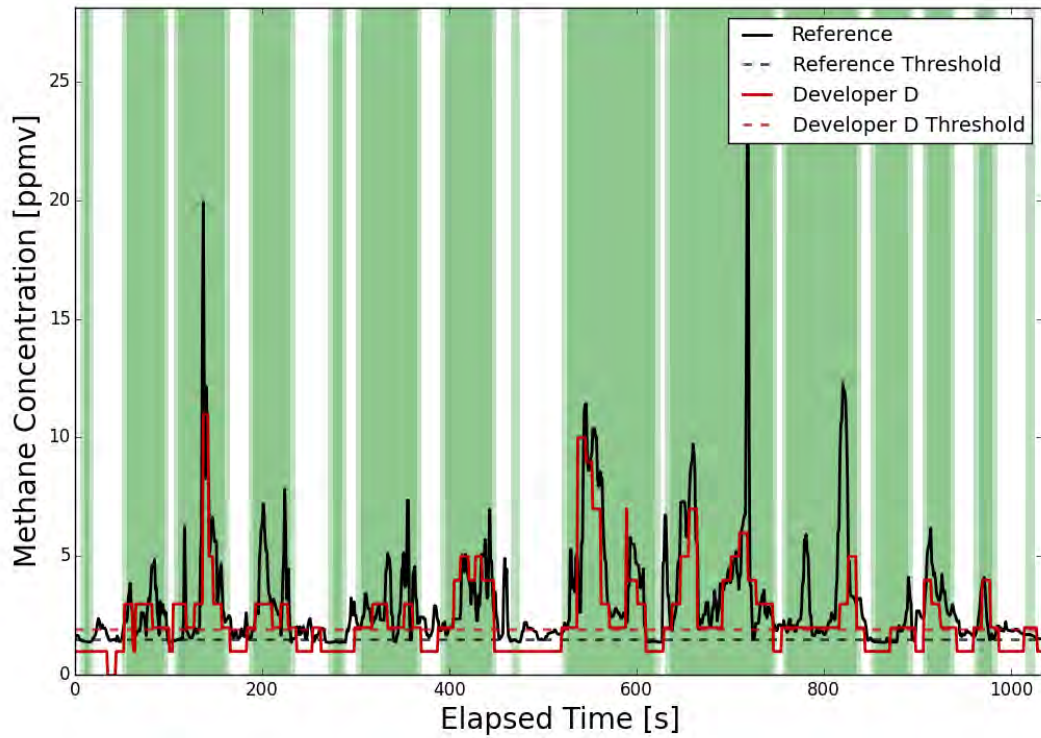


Figure D.10. Developer D Data Trace for a 2.5-scfm Leak from 82 ft of Distance

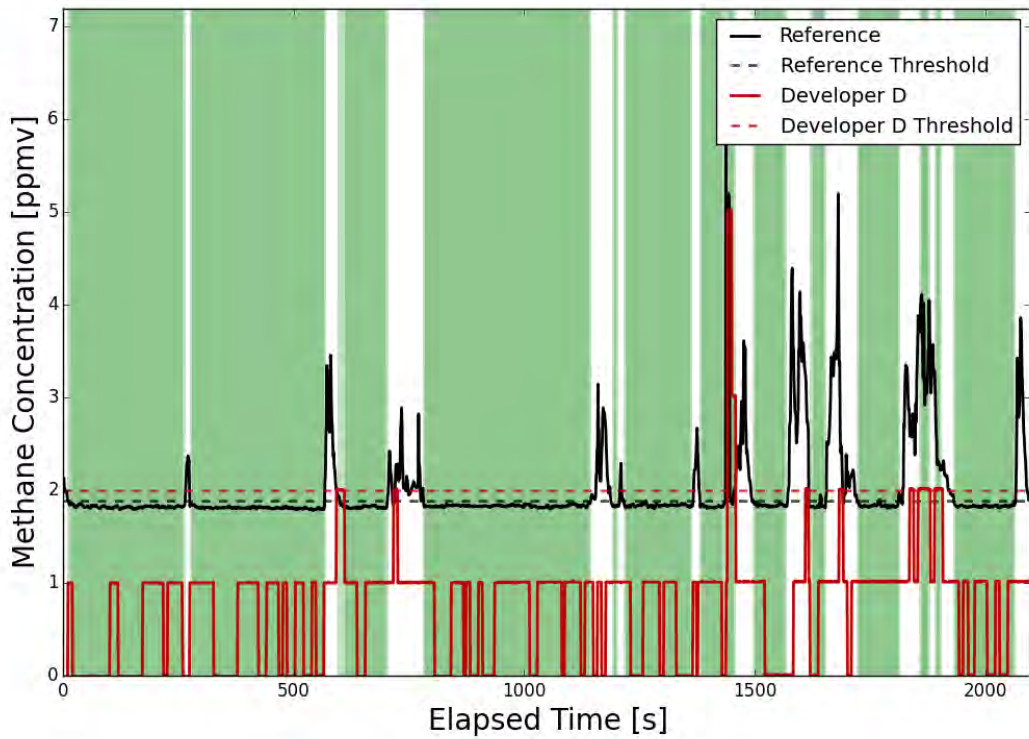


Figure D.11. Developer D Data Trace for a 2.5-scfm Leak from 130 ft of Distance

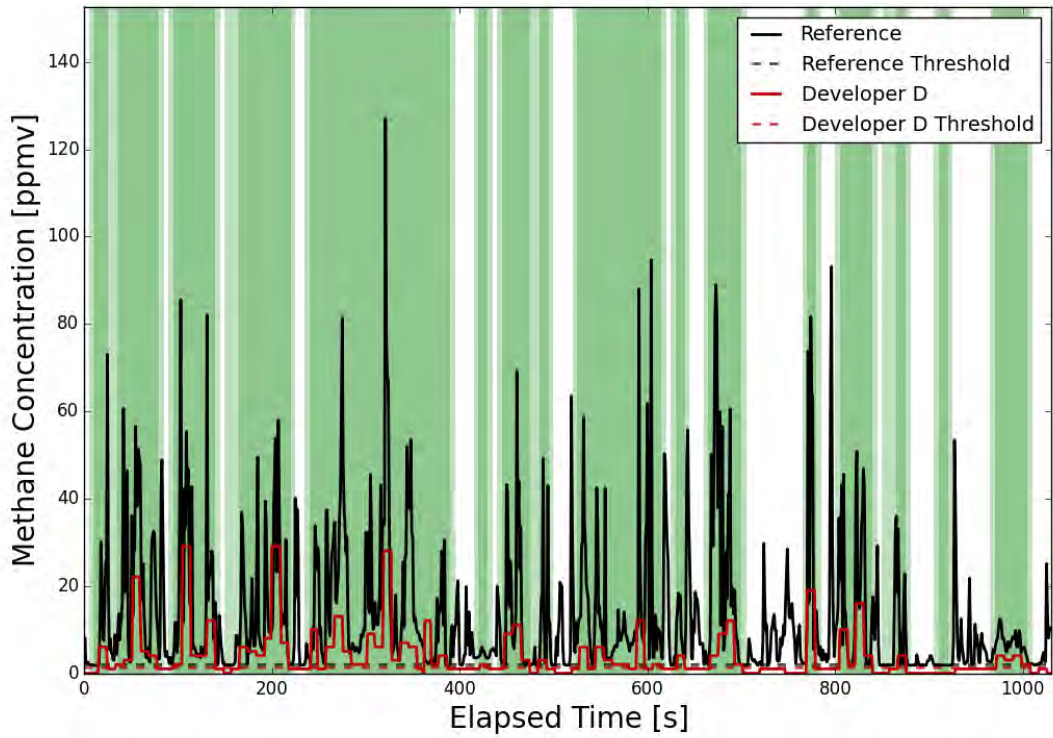


Figure D.12. Developer D Data Trace for a 5-scfm Leak from 30 ft of Distance

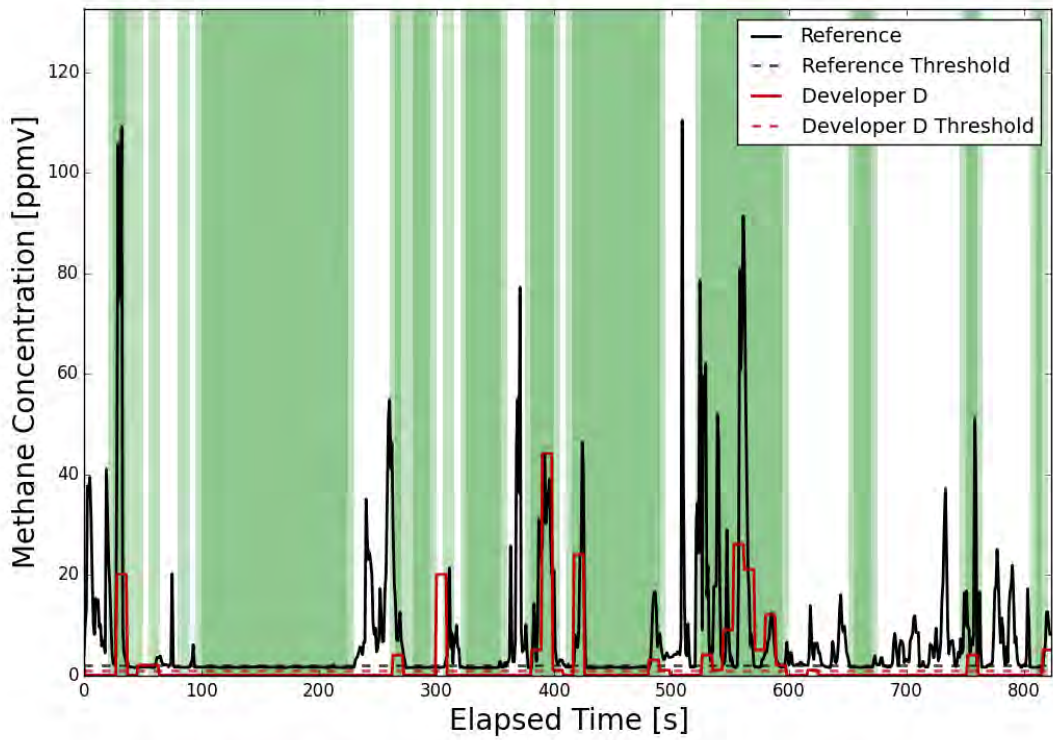


Figure D.13. Developer D Data Trace for a 5-scfm Leak from 70 ft of Distance

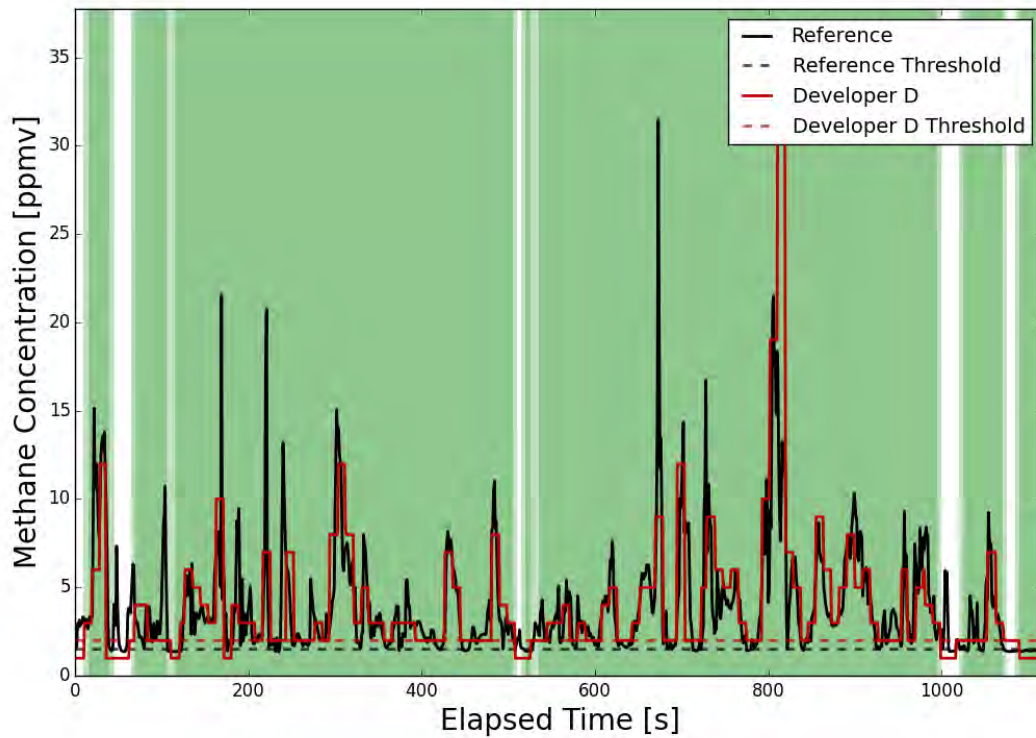


Figure D.14. Developer D Data Trace for a 5-scfm Leak from 82 ft of Distance

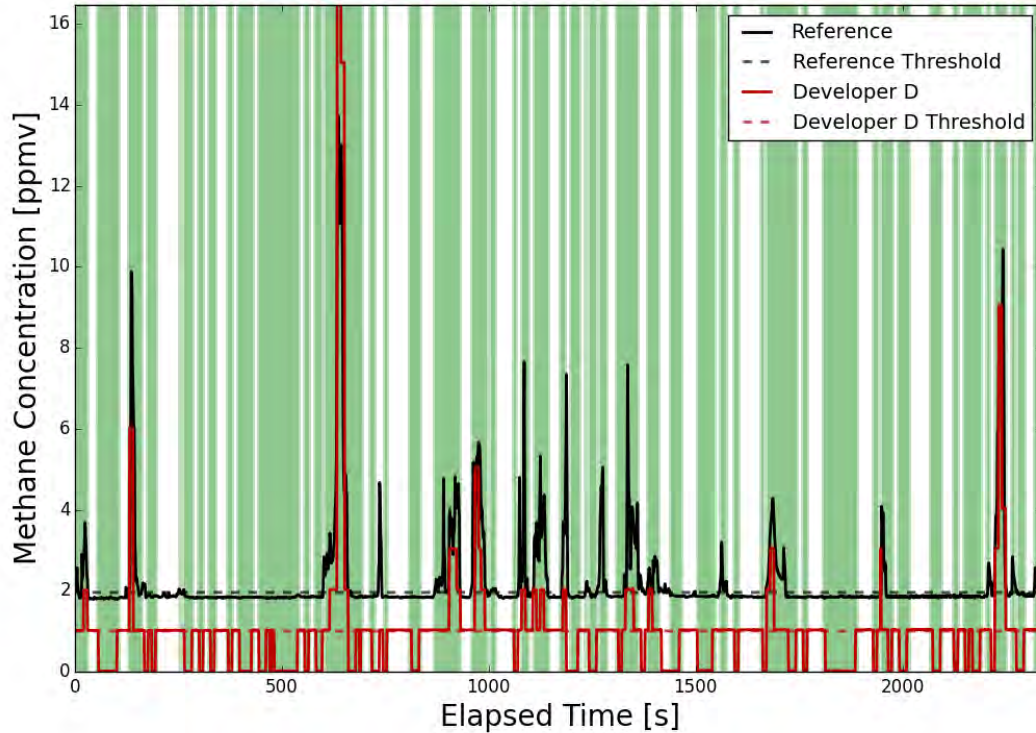


Figure D.15. Developer D Data Trace for a 5-scfm Leak from 130 ft of Distance

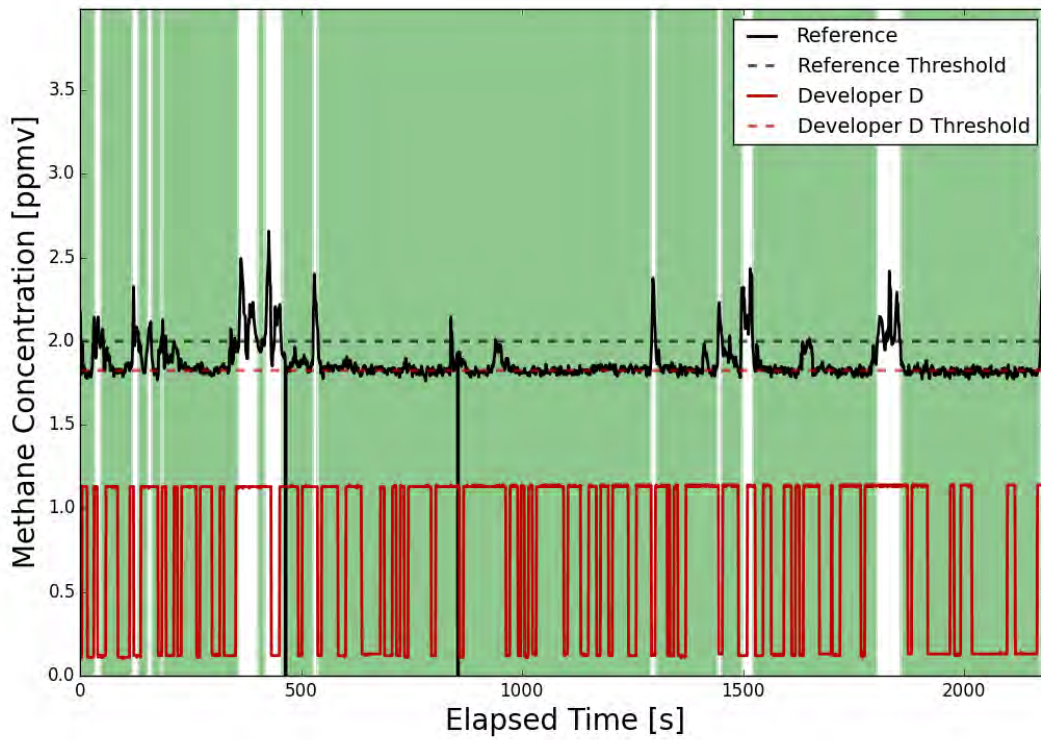


Figure D.16. Developer D Data Trace for a 0.5-scfm Leak from 130 ft of Distance